

ISSN 2217-8139 (Print)
ISSN 2334-0229 (Online)

UDK: 06.055.2:62-03+620.1+624.001.5(497.1)=861



2014.
GODINA
LVII



GRAĐEVINSKI MATERIJALI I KONSTRUKCIJE

3

BUILDING MATERIALS AND STRUCTURES

ČASOPIS ZA ISTRAŽIVANJA U OBLASTI MATERIJALA I KONSTRUKCIJA
JOURNAL FOR RESEARCH OF MATERIALS AND STRUCTURES



DRUŠTVO ZA ISPITIVANJE I ISTRAŽIVANJE MATERIJALA I KONSTRUKCIJA SRBIJE
SOCIETY FOR MATERIALS AND STRUCTURES TESTING OF SERBIA

Odlukom Skupštine ***Društva za ispitivanje materijala i konstrukcija***, održane 19. aprila 2011. godine u Beogradu, promenjeno je ime časopisa **Materijali i konstrukcije** i od sada će se časopis publikovati pod imenom **Građevinski materijali i konstrukcije**.

According to the decision of the Assembly of the ***Society for Testing Materials and Structures***, at the meeting held on 19 April 2011 in Belgrade the name of the Journal **Materijali i konstrukcije** (Materials and Structures) is changed into **Building Materials and Structures**.

Professor Radomir Folic
Editor-in-Chief

GRAĐEVINSKI MATERIJALI I KONSTRUKCIJE

BUILDING MATERIALS AND STRUCTURES

ČASOPIS ZA ISTRAŽIVANJA U OBLASTI MATERIJALA I KONSTRUKCIJA
JOURNAL FOR RESEARCH IN THE FIELD OF MATERIALS AND STRUCTURES

INTERNATIONAL EDITORIAL BOARD

Professor **Radomir Folić**, Editor in-Chief
Faculty of Technical Sciences, University of Novi Sad, Serbia
Fakultet tehničkih nauka, Univerzitet u Novom Sadu, Srbija
e-mail: folic@uns.ac.rs

Professor **Mirjana Malešev**, Deputy editor
Faculty of Technical Sciences, University of Novi Sad,
Serbia
Fakultet tehničkih nauka, Univerzitet u Novom Sadu, Srbija
e-mail: miram@uns.ac.rs

Dr **Ksenija Janković**
Institute for Testing Materials, Belgrade, Serbia
Institut za ispitivanje materijala, Beograd, Srbija

Dr **Jose Adam, ICITECH**
Department of Construction Engineering, Valencia,
Spain.

Professor **Radu Banchila**
Dep. of Civil Eng. „Politehnica“ University of
Timisoara, Romania

Professor **Dubravka Bjegović**
Civil Engineering Institute of Croatia, Zagreb, Croatia

Assoc. professor **Meri Cvetkovska**
Faculty of Civil Eng. University "St Kiril and Metodij",
Skopje, Macedonia

Professor **Michael Forde**
University of Edinburgh, Dep. of Environmental Eng.
UK

Dr **Vladimir Gocevski**
Hydro-Quebec, Motreal, Canda

Dr. Habil. **Miklos M. Ivanyi**
UVATERV, Budapest, Hungary

Professor **Asterios Liolios**
Democritus University of Thrace, Faculty of Civil
Eng., Greece

Predrag Popović
Wiss, Janney, Elstner Associates, Northbrook,
Illinois, USA.

Professor **Tom Schanz**
Ruhr University of Bochum, Germany

Professor **Valeriu Stoin**
Dep. of Civil Eng. „Poloitehnica“ University of
Timisoara, Romania

Acad. Professor **Miha Tomažević**, SNB and CEI,
Slovenian Academy of Sciences and Arts,

Professor **Mihailo Trifunac**, Civil Eng.
Department University of Southern California, Los
Angeles, USA

Lektori za srpski jezik: Dr **Miloš Zubac**, profesor

Proofreader: **Aleksandra Borojev**, profesor
Prof. **Jelisaveta Šafranj**, Ph D

Technical editor: **Stoja Todorovic**, e-mail: saska@imk.grf.bg.ac.rs

PUBLISHER

Society for Materials and Structures Testing of Serbia, 11000 Belgrade, Kneza Milosa 9
Telephone: 381 11/3242-589; e-mail: dimk@ptt.rs, veb sajt: www.dimk.rs

REVIEWERS: All papers were reviewed
COVER: Poplava u Obenovcu-Srbija, maja 2014
Flood in Obrenovac-Serbia, May 2014

Financial supports: Ministry of Scientific and Technological Development of the Republic of Serbia

DRUŠTVO ZA ISPITIVANJE I ISTRAŽIVANJE MATERIJALA I KONSTRUKCIJA SRBIJE
SOCIETY FOR MATERIALS AND STRUCTURES TESTING OF SERBIA

GRAĐEVINSKI MATERIJALI I KONSTRUKCIJE

BUILDING MATERIALS AND STRUCTURES

ČASOPIS ZA ISTRAŽIVANJA U OBLASTI MATERIJALA I KONSTRUKCIJA
JOURNAL FOR RESEARCH IN THE FIELD OF MATERIALS AND STRUCTURES

SADRŽAJ

Zdravko BONEV Stanislav DOSPEVSKI EVROKOD 8: UPOTREBA POVOLJNE FORMULACIJE ZA POBOLJŠANO I SIGURNO PROJEKTOVANJE Originalni naučni rad	3
Zvonko TOMANOVIĆ TESTIRANJE FENOMENA PUZANJA MEKE STIJENE Originalni naučni rad	21
Živojin PRAŠČEVIĆ Nataša PRAŠČEVIĆ PRIMENA MODIFIKOVANOG RASPLINUTOG TOPSIS METODA ZA VIŠEKRITERIJUMSKE ODLUKE U GRAĐEVINARSTVU Originalni naučni rad	43
Vesna BULATOVIĆ Vilma DUCMAN Miroslava RADEKA KARAKTERISTIKE TRANZITNE ZONE BETONA NA BAZI LAKOG AGREGATA Originalni naučni rad	63
Uputstvo autorima	78

CONTENTS

Zdravko BONEV Stanislav DOSPEVSKI EUROCODE 8: USE OF ADVANTAGEOUS FORMULATIONS FOR IMPROVED AND SAFE DESIGN Original scientific paper	3
Zvonko TOMANOVIĆ TESTING OF CREEP PHENOMENA ON SOFT ROCK Original scientific paper	21
Živojin PRASCEVIC Nataša PRASCEVIC APPLICATION OF MODIFIED FUZZY TOPSIS METHOD FOR MULTICRITERIA DECISIONS IN CIVIL ENGINEERING Original scientific paper	43
Vesna BULATOVIĆ Vilma DUCMAN Miroslava RADEKA CHARACTERISTICS OF LIGHTWEIGHT AGGREGATE CONCRETE INTERFACIAL TRANSITION ZONE Original scientific paper	63
Preview report	78

CIP - Katalogizacija u publikaciji
Narodna biblioteka Srbije, Beograd

620.1

GRAĐEVINSKI materijali i konstrukcije :
časopis za istraživanja u oblasti materijala
i konstrukcija = Building Materials and
Structures : journal for research of
materials and structures / editor-in-chief
Radomir Folić. - God. 54, br. 1 (2011)-
- Beograd (Kneza Miloša 9) : Društvo za
ispitivanje i istraživanje materijala i
konstrukcija Srbije, 2011- (Novi Beograd :
Hektor print). - 30 cm

Tromesečno. - Je nastavak: Materijali i
konstrukcije = ISSN 0543-0798
ISSN 2217-8139 = Građevinski materijali i
konstrukcije
COBISS.SR-ID 188695820



EUROCODE 8: USE OF ADVANTAGEOUS FORMULATIONS FOR IMPROVED AND SAFE DESIGN

EVROKOD 8: UPOTREBA POVOLJNE FORMULACIJE ZA POBOLJŠANO I SIGURNO PROJEKTOVANJE

Zdravko BONEV
Stanislav DOSPEVSKI

ORIGINALNI NAUČNI RAD
ORIGINAL SCIENTIFIC PAPER
UDK: 624.042.7:006.44EN

1 INTRODUCTION

In the recent years current design philosophies evidently are in the period of evolution. The general purpose considering seismic resistant design is to save human live and minimize human damages in engineering structures. The experience from the past earthquakes shows that sometimes design theory is not in compliance with the observed results. A lot of efforts have been directed towards achievement a good correlation between theoretical background and observation results. The use of structural mechanics principles contributes more or less towards improving the precision of computational procedures. This is good background for implementation of performance-based seismic design. More adequate approaches and better numerical simulation in the field of seismic action and efficient dynamic models of structures are developed.

EN 1998-1 provisions are great contributes towards very good agreement between theory and practice. Implementation of capacity design principles is the milestone for better predictability of the plastic mechanisms when structures are subjected to seismic ground motion. Structures are designed using performance based seismic design methodology, which allows for better identification of structural performance. European standard proposes very good balance between reliability of the methods and simplicity of their use. EN 1998-1, [9] provides better protection of human life and civil engineering structures as well.

Figure 1 illustrates the main concept in development strategy for decreasing the gap between theory and practice. At first, design theory should become more precise, using fewer assumptions and more refined methods, which are capable to capture the most important features of seismic performance of structures. The "old" generation of BG design codes (solid line) is replaced with a new expanded figure (dashed line) showing new advantageous level of the design theory. On the other hand construction methodology is also expanded, moving from old (solid line) to new (dashed line) position. The existing gap between figures denoted by solid lines and dashed lines illustrates the potential distinctions that may appear between theory and practice. Expansion of design methods in EN 1998-1 is achieved by implementation of more science into the design procedures, for instance nonlinear seismic performance, probabilistic methods in defining the limit states, use of more sophisticated models for seismic action. Performance requirements and detailing rules of EN 1998-1 (dashed line) can be pointed out as a matter of new civil engineering practice.

As a result of comparison it is evident that the gap between dashed line figures is going to be smaller than the gap between solid line figures. The basic idea of EN 1998-1 is to implement more scientific developments into the new theoretical background and to carry out corresponding changes in practical regulations which are in conformity with the new design principles. For example considerable attention is paid to ductility as a basic tool for energy dissipation and design load reduction. Special detailing rules are proposed to ensure ductility in the practice as a property of structural critical zones and connections.

Professor Zdravko Bonev, PhD, University of Architecture, Civil Engineering and Geodesy, Department of Structural Mechanics, 1 Hristo Smirnenski Blvd, Sofia, Bulgaria, e-mail: zbp_uacg@abv.bg
Stanislav Dospevski, PhD Civil Engineer, University of Architecture, Civil Engineering and Geodesy, Department of Structural Mechanics, 1 Hristo Smirnenski Blvd, Sofia, Bulgaria, e-mail: stdospevsky@abv.bg

The subject of the paper is closely related to the “open topics”, which are the subject of the National Annex and Nationally determined parameters for Bulgaria. The main goal of the paper is to share the experience of the team, involved to carry out the work related to Part 6: Masts, Chimneys and Towers and Part 3: Repairing and Strengthening of Reinforced Concrete and Masonry Structures.

2 SELECTED TOPICS OPENED FOR DISCUSSION

2.1 Topic 1: Accounting for spatial variability of seismic action

For a number of structures seismic ground accelerations are assumed to be uniformly distributed at the base of the structure similarly to “shaking table effect”. For irregular or long in plan structures like storages, bridges and tubes uniform distribution of the ground accelerations or displacements is no longer applied. EN 1998-1

states that spatial variability of the seismic action should be accounted for. For tall and slender structures spatial variability of the seismic action on input also should be taken into consideration. There are mainly two models which are currently in use to do this. First model implies the ground acceleration distribution at the base to follow the shape of the “standing wave function”, typical for shear waves and surface waves of Love. The second model proposes to enter as seismic input into the structure both translational components of ground accelerations and rotational components of the ground accelerations.

Model 1: ground accelerations which follow the shape of standing wave function

(References [3], [4], [7], [8], [15], [18], [19], [20] and [21])

In this case seismic input is represented by horizontal ground accelerations, which are evidently, non-uniformly distributed. Figure 2 shows simple ground

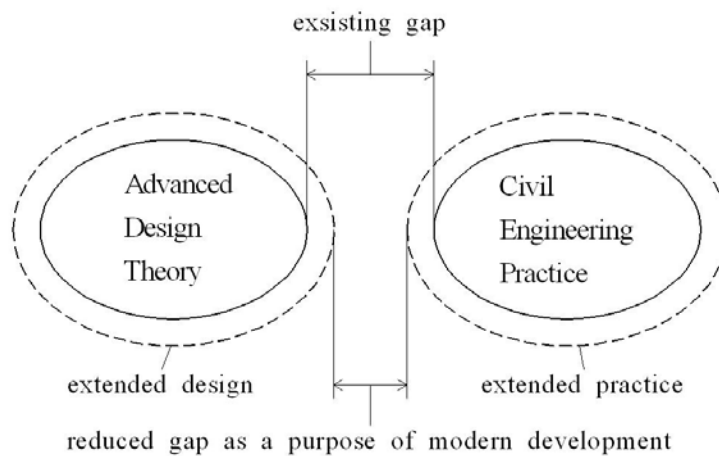


Figure 1. General strategy for compliance between design methods and engineering practice

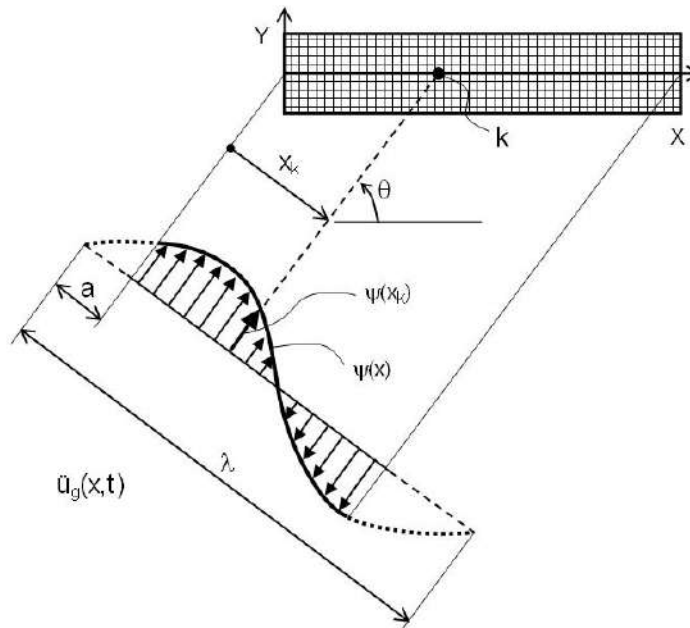


Figure 2. Long in plan structure (horizontal plane XY) subjected to standing wave (shear wave)

motion being consistent of accelerations which are non-uniformly distributed. A bridge structure is subjected to this seismic input. The transferred motion of all masses attached to the deck structure, is the same as the motion of the base. Figure 2. shows that the ground accelerations given in it provoke domination of torsional response over the translation-based solution.

Figure 3 shows long in plan structure subjected to horizontal accelerations at the base which are non-uniformly distributed. The most widely used model of seismic action requires however uniform distribution of the ground accelerations. This idea can be achieved by separation of the long in plan building into separate parts, which behave as dynamically independent units. Ground acceleration function is also separated (dashed line) and each line part-by-part becomes easier to be approximated with uniform line. Having the seismic joints the spatial effect of seismic loading now is reduced. Some recent investigations show that dynamic independence of the separate units remains questionable because they interact through soil.

Model 2: using rotational components of the seismic ground motion (References [2], [10] and [22])

This model is provided in [10]. Numerical response evaluation using [10]-regulations and approach is given in [2]. The existing model of seismic action, having three translational components, is extended by adding the rota-

tion components of the ground accelerations as shown in Figure 4. The corresponding rotational SDOF system defining rotational motion is shown in the same figure. Thus, the full set of ground acceleration components contains six components – three translational and three rotational components (Fig. 4).

The elastic response spectra according to [9] of Types 1 and 2 are shown in Figure 5 and they are related to translational accelerations measured on the free field.

The definition of the rotational components of the ground motion using response spectra facilities is carried out in [10]. Following the pattern in Part 6 three rotational spectra are introduced: first two spectra, defined by equation (1) are related with surface waves of Rayleigh and imply rotational motion around both horizontal directions. Third rotational spectrum in (1) is related to rotational motion around the vertical axis and appears to be a result of the surface waves of Love.

$$\begin{aligned}
 S_x^\theta &= 1,7\pi \frac{S_e(T)}{V_s T} \\
 S_y^\theta &= 1,7\pi \frac{S_e(T)}{V_s T} \\
 S_z^\theta &= 2,0\pi \frac{S_e(T)}{V_s T}
 \end{aligned}
 \tag{1}$$

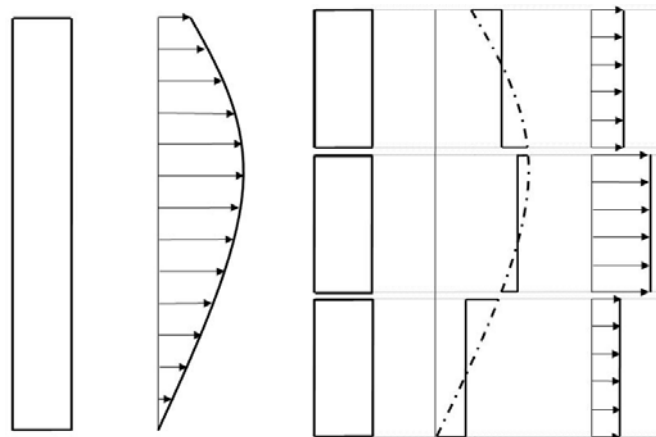


Figure 3. Nonuniform distribution of horizontal ground accelerations at the base of the building. Use of seismic joints to mitigate the effect of torsional ground acceleration input

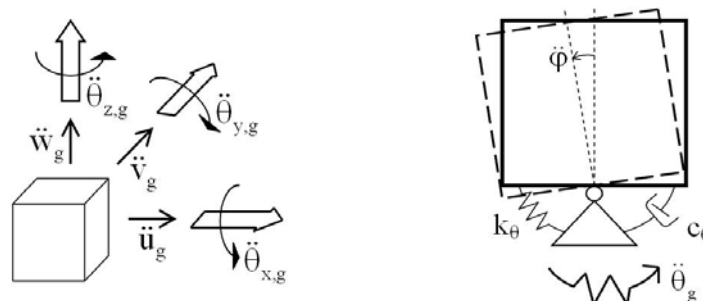


Figure 4. Full set of acceleration components at a point. Definition of acceleration spectrum through single rotational degree of freedom system

It is seen that all rotational spectra are expressed in terms of the elastic response spectrum, plotted in Figure 5. All spectra in Equations (1) are parametrically dependent on shear wave velocity V_s and on the current period of free undamped vibrations T . When the period T tends to zero, all formulae in (1) produce infinitely large rotational accelerations. This tendency was observed and studied by M. D. Trifunac and Lee considering records of rotational accelerations for specific earthquakes.

The plot of the rotational response spectra according to [10] and in conformity with Equations (1) are represented in Figure 6. Looking at both types of rotational spectra as a result of surface waves (Rayleigh and Love waves) as a tendency it can be seen that high frequency (small periods) response goes to infinity and or may become quite large for all ground types. Stiff soils (Ground types A and B) show narrow spectral amplification band, whereas soft soils (Ground types C and D) have more wide spectral amplification band. It can be expected that only stiff structures (with small fundamental period) can be affected essentially by rotational accelerations. On the other hand, spectral accelerations in large period range (T larger than 1.0 s for instance) are very small and their contribution can be neglected.

For MDOF systems response spectrum method is also applicable. To do this the application of this method including translational components only should be extended by implementation of rotational components, too, see Figure 6.

Application of the response spectrum method to tower structure is discussed in the following issue. Numerical model is prepared on the basis of finite elements – 3D or SHELL elements, as shown in Figure 7. The numerical model, composed by SHELL elements allows for calculation of cross section shape deformations, but the number of dynamic degrees of freedom is increased very much (Figure 7).

The transferred translational and rotational motion is presented in Figure 8. Translational motion is characterized by constant distribution of transferred accelerations in elevation. Rotational motion is characterized by linear distribution of the transferred motion induced by rotational accelerations of the base.

Translational and rotational transferred motions are considered and discussed below in order to determine the design seismic forces and the most important parameters for further calculations.

Because of the nature of response spectrum method, two separate and independent analyses are carried out. First one deals with the action effect, obtained only as a

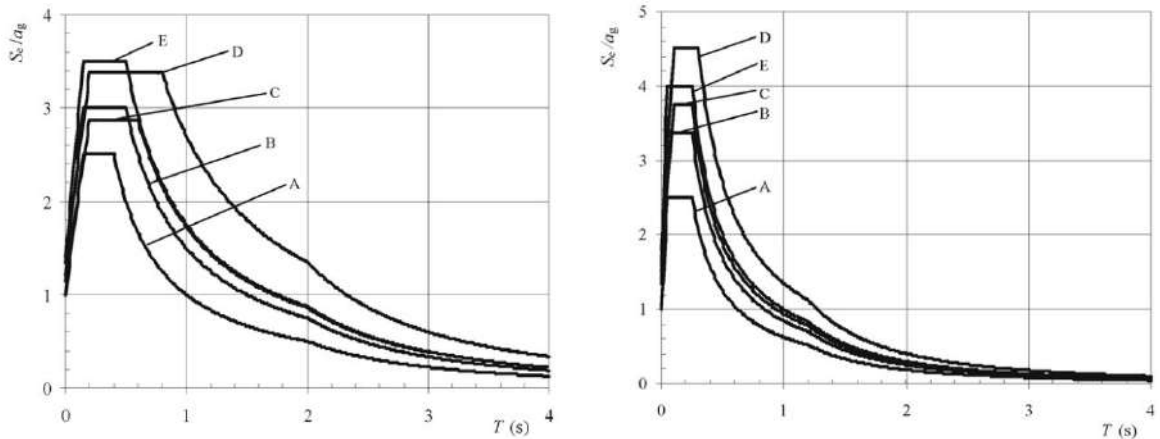


Figure 5. Elastic response spectrum: Type 1 (left) and Type 2 (right)

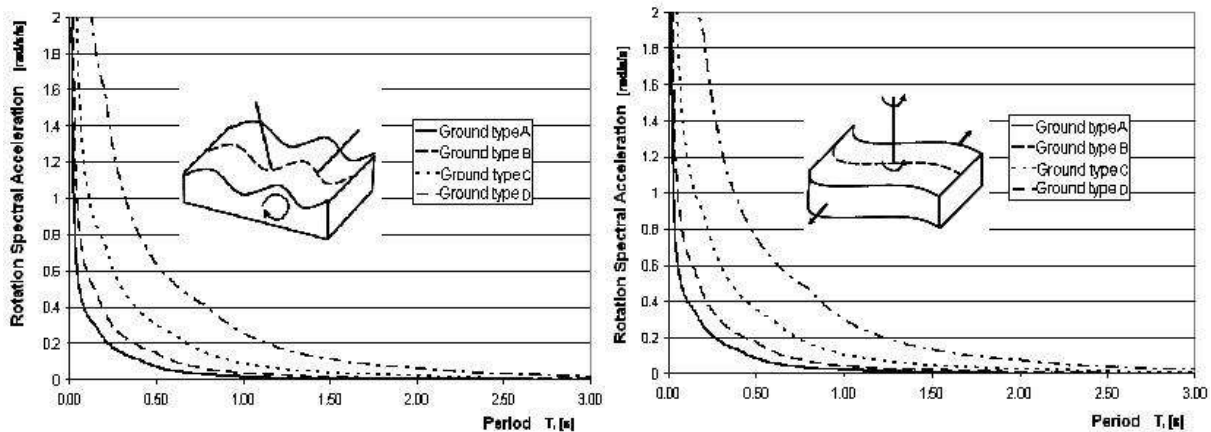


Figure 6. Elastic response spectra for rotational accelerations: spectra, obtained as a result of Rayleigh waves (left) and spectra obtained on the basis of Love waves (right)

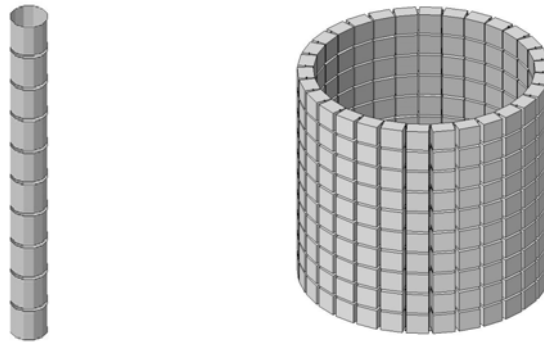


Figure 7. 3D frame elements and shell elements used to compose the dynamic model of a tower. Shell elements allow for catching cross section deformations

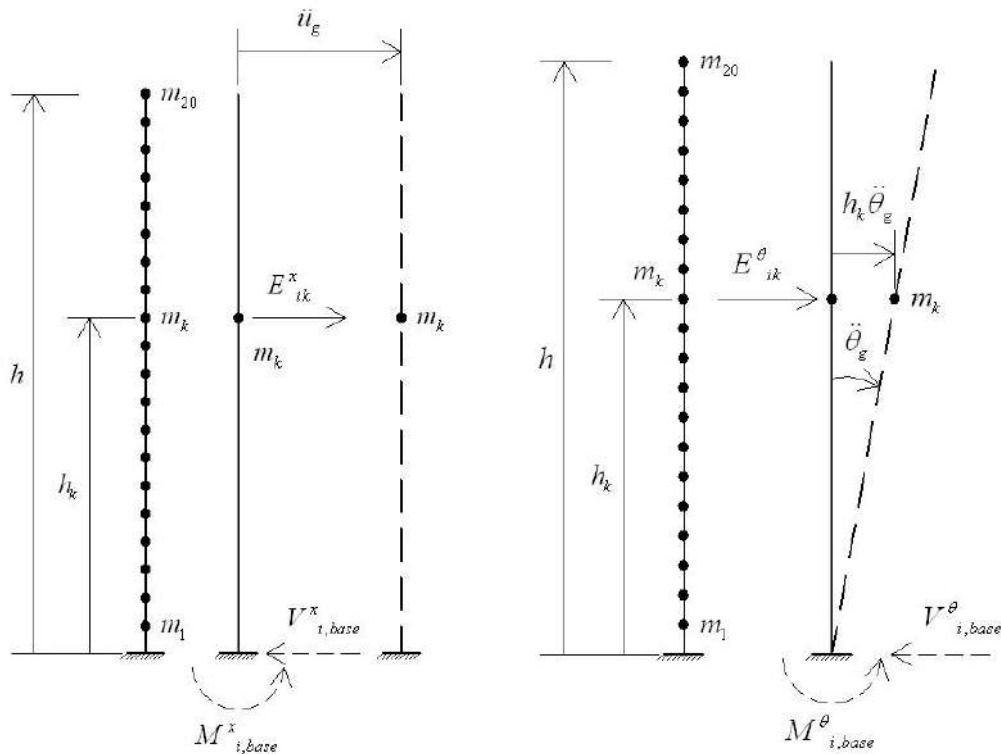


Figure 8. Transferred motion of the ground and its distribution in elevation (left – translational ground motion, right – rotational ground motion as a result of surface waves)

result of the translational component. This kind of analysis is traditional type of analysis well known from seismic resistant design courses. The second analysis deals with the structure subjected to rotational component only. By making use of component combination rule action effects from both analyses can be combined to account for that components are acting simultaneously.

Details concerning all calculations and notations are given in Appendix A. Only final results and simple numerical example are discussed herein.

A simple cantilever structure – tower is shown as a plane structure in Figure 8. The structure is subjected to horizontal ground motion, denoted by superscript X and rotational ground motion, denoted by superscript θ . Both

components are acting simultaneously so coupled effect in all responses should be accounted for. The dynamic model has twenty masses and twenty degrees of freedom.

structure is subjected to translational ground acceleration components only

The solution of this problem can be found elsewhere in current courses on structural dynamics and earthquake engineering. The only modal values of base shear force $V_{i,base}^x$ (Equation (2)) and base flexural moment $M_{i,base}^x$ (Equation (3)) are considered. All quantities entering in both equations are explained and discussed in Appendix A.

$$V_{i,base}^x = (\Gamma_i^x)^2 m_i^* S_e(T_i) \quad (2)$$

$$M_{i,base}^x = \Gamma_i^x \Gamma_i^\theta m_i^* h S_e(T_i) \quad (3)$$

Since modal correlation exists between two modal peaks of each modal pair, this is taken into account by correlation coefficients of Der Kiureghian (Appendix A). Thus the peak values of the base shear force and base flexural moment are determined after application of CQC as modal combination rule.

$$V_{base}^x = \sqrt{\sum_i \sum_j \rho_{ij} V_{i,base}^x V_{j,base}^x} \quad (4)$$

$$M_{base}^x = \sqrt{\sum_i \sum_j \rho_{ij} M_{i,base}^x M_{j,base}^x} \quad (5)$$

It is worth noting that the value of $V_{i,base}^x$ obviously always remains positive (see Equation (2)), whereas $M_{i,base}^x$ may have either positive or negative value (see Equation (3)).

structure is subjected to rotational ground acceleration components only

The solution of this problem should be found in conformity with response spectrum method and theory. Only modal values of base shear force $V_{i,base}^\theta$ (Equation (6)) and base flexural moment $M_{i,base}^\theta$ (Equation (7)) are considered. All quantities entering in both equations are explained and discussed in Appendix A.

$$V_{i,base}^\theta = \Gamma_i^x \Gamma_i^\theta m_i^* h S_e(T_i) \quad (6)$$

$$M_{i,base}^\theta = (\Gamma_i^\theta)^2 m_i^* h^2 S_e(T_i) \quad (7)$$

It is worth noting that the value of $V_{i,base}^\theta$ may have positive or negative sign (see Equation (6)). The value of $M_{i,base}^\theta$ ever remains positive.

The need for modal combination arises because a correlation can be found between each arbitrary pair of modal peaks. This is carried out using correlation coefficients of Der Kiureghian (Appendix A). Thus the peak values of the base shear force and base flexural moment are determined after application of CQC as modal combination rule.

$$V_{base}^\theta = \sqrt{\sum_i \sum_j \rho_{ij} V_{i,base}^\theta V_{j,base}^\theta} \quad (8)$$

$$M_{base}^\theta = \sqrt{\sum_i \sum_j \rho_{ij} M_{i,base}^\theta M_{j,base}^\theta} \quad (9)$$

peak action effects as a result of simultaneous action of both components of the ground accelerations

Now the fact that both components of the seismic ground motion (accelerations) are acting simultaneously, should be taken into account. It was proven that the cross correlation factors for translational and rotational acceleration records are zero. This shows that no correlation between translational and rotational component exists and peak values of base shear force $\max V_{base}$ and flexural moment $\max M_{base}$ when both components of the seismic ground motion are acting simultaneously, can be found using SRSS as component combination rule.

$$\max V_{base} = \sqrt{(V_{base}^x)^2 + (V_{base}^\theta)^2} \quad (10)$$

$$\max M_{base} = \sqrt{(M_{base}^x)^2 + (M_{base}^\theta)^2} \quad (11)$$

Note that Equations (9) and (10) are using information after the peak responses due to each of the ground motion component have already been determined.

effective mass ratios

Effective mass ratios point out whether the number of modes taken into account into the analysis is sufficient from the viewpoint of accuracy. For translational motion this problem is already settled and used for a number of years. Calculations are performed using the result provided with Equation (12).

For rotational ground motion new definitions for the total mass M_{Tot}^θ and for the modal participation factor Γ_i^θ are implemented (see Appendix A) correspondingly. Calculation of the effective mass ratio is performed using the result (13):

$$\alpha^x = \frac{\sum_{i=1}^N m_i^* (\Gamma_i^x)^2}{M_{Tot}^x} = 0,90 \div 0,95 \quad (12)$$

$$\alpha^\theta = \frac{\sum_{i=1}^N m_i^* (\Gamma_i^\theta)^2}{M_{Tot}^\theta} = 0,90 \div 0,95 \quad (13)$$

Information about all quantities entering in Equations (12) and (13) is provided in Appendix A.

Figure 9 illustrates the relationship "effective mass ratio versus number of modes, included in the analysis". Solid line represents the case of horizontal motion only (Equation (12)), whereas dashed line shows the variation of effective mass ratio in case of rotational motion of the base. It is seen that in the case of translational component only 3 modes are sufficient to achieve at least 90% accuracy. In the case of rotational component (dashed line) only one mode is sufficient to achieve 97% accuracy. This can be explained by the fact, that the shape of the rotational transferred motion

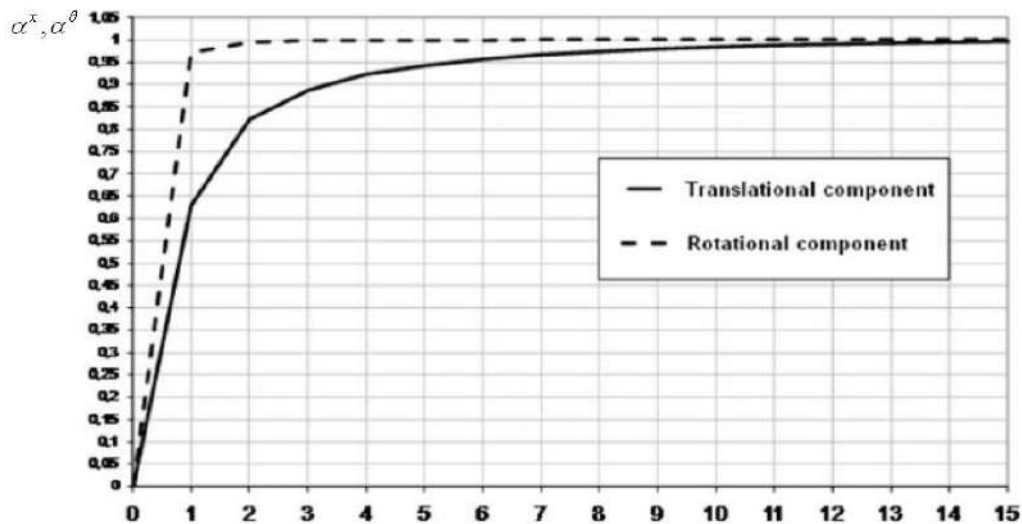


Figure 9. Sufficiency of the number of modes implying translational only (solid line) and rotational motion only (dashed line)

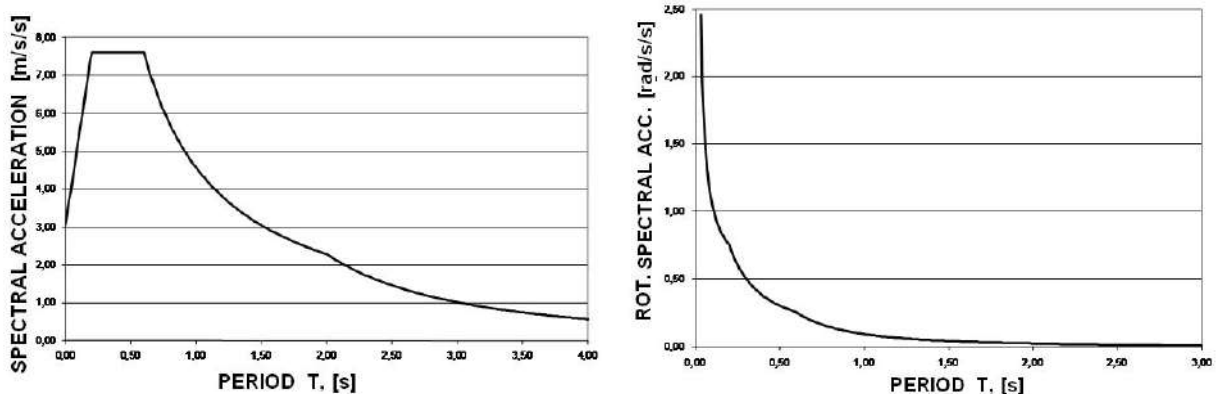


Figure 10. Elastic acceleration spectra: for translational motion (left) and for rotational motion - Rayleigh waves (right)

(see Figure 8) can be approximated accurate enough using only first (fundamental) mode of natural vibrations. It means that for tall and slender structures like towers the only one mode of natural vibrations is sufficient to reproduce the effect of base rotation. High mode responses are unaffected by the rotational motion of the base.

Numerical example

EN 1998-6 requires structures higher than 80 meters to be examined to both translational and rotational components of the ground motion. Supplemental condition is $a_g S > 0,25g$ (a_g is the design ground acceleration, S is the soil coefficient and g is the acceleration of gravity). In the considered example the response of an existing tower is studied for which the height is 60 m (less than 80 m) and $a_g S = 0,27g > 0,25g$. Damping ratio as a percentage of the critical is $\xi = 5\%$. Elastic response spectrum and Bulgarian National parameters are used to calculate and plot the spectra, needed for calculations and representing the seismic input. Figure 10 illustrates

graphically these data. Ground type C is used in calculations.

Figure 11 shows graphically the relationship “base moment - included number of modes”. Solid line represents the case in which both components horizontal and rotational are acting simultaneously. Dashed line shows the variation of the base moment when only horizontal component of the seismic action is considered. It is seen that, as expected, three modes are sufficient to obtain both lines. Obviously, high frequency response has no essential contribution over the base moment value. It is seen also, that taking into account horizontal and rotational components of the ground motion produces larger response than the response including only translational component. Dashed area gives impression about the distinction between two seismic action models. Difference is 11%, which is not on the side of safety when rotational component of ground accelerations is omitted.

It is shown (figure 9) that fundamental period is the most important parameter which forms the response due to rotational component. EN 1998-1 has a requirement for sufficient stiffness aiming to ensure limitations for the displacements. As a result the fundamental period is

going to be small (around zero) which leads to large rotational component contribution (see Figure 6). In the period (0. - 1.0 s) large contribution of rotational component is expected because structures should be designed to be stiff enough. This zone may generate amplification of the response because of the large influence of rotational component. The opposite opportunity is when structures have insufficient stiffness and are flexible. In this case it is expected the displacements to grow up and exceed the prescribed limits. Within the large period range (2.0 – 3.5 s) the horizontal component is expected to contain long period component which may lead to response amplification.

Within the period range (1.0 s - 2,0 s) large dynamic amplification is unlikely to expect. Figure 12 shows properly the three zones. The large amplification effect of first and third zones can be reduced by using viscous dampers and seismic protection technics. The amplification effect of the first zone can be reduced by high frequency component of the viscous damping. The amplification effect of long period zone can be reduced by low frequency component of the viscous damping.

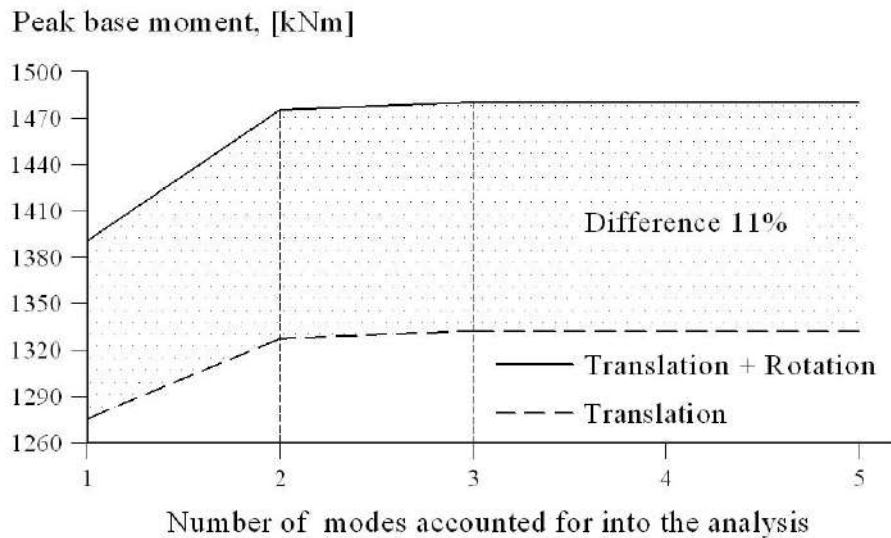


Figure 11. Peak responses for the base moment: including translational and rotational components simultaneously (solid line) and translational component of the ground acceleration acting alone (dashed line)

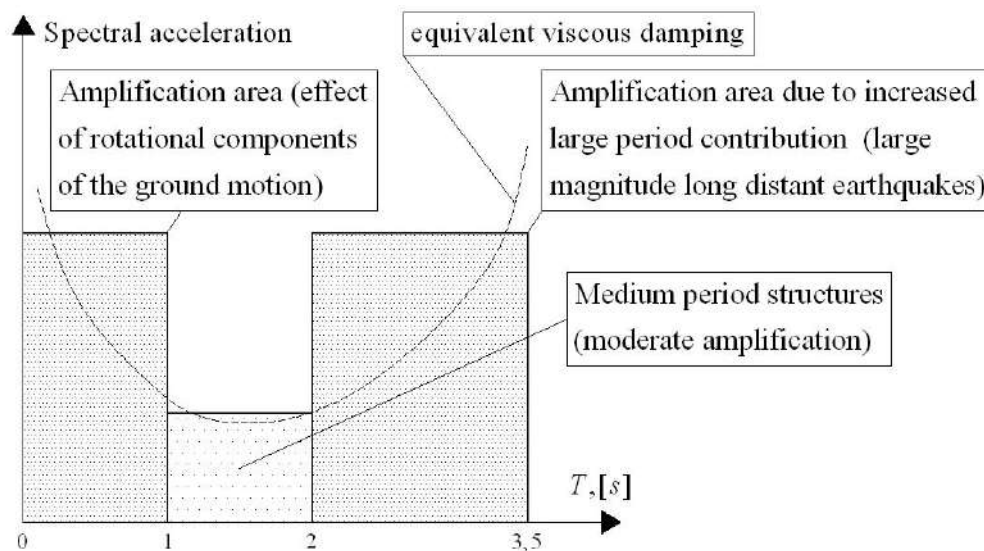


Figure 12. Suggestion for mitigation of amplification by making use of added damping being implemented as equivalent viscous damping

2.2 **Topic 2: Performance based seismic design and need verification for strengthening of existing structures** (References [5], [11], [12], [14], [16], [17] and EN 1998-3)

Part 3 (EN 1998-3) is very ambitious attempt to create new regulations for design of strengthened structures. It is compulsory to proof two important issues: 1) the need for strengthening, and 2) the benefit of strengthening. The study discussed in the paper proposes numerical technique, which allows for proving the need and the benefit of strengthening. Both proofs are carried out on the basis of adequate numerical models, which are capable of catching inelastic behaviour and effects of it. Another important factor – the cost of the strengthening and economic viability. The question that is able to afford strengthening is dependent on governmental priorities and should be settled by governmental institutions. In this topic 2 only the need and benefit are considered.

Capacity design principles and rules are widely used in [9] to improve the seismic performance of existing buildings designed in conformity with old generation of codes. This can be done by doing the following 1) improvement of the energy dissipation capability and ductile performance; 2) improvement of the predictability of the plastic and failure mechanisms. Energy dissipation and ductile behaviour lead to reduction of design seismic forces. Prediction of the plastic and failure mechanisms is a great advantage from the viewpoint of methodology. The basic idea is to control structural performance by more adequate regulations and more proper design philosophy.

For new designed structures the use of capacity design rules, performance requirements and detailing rules of [9] contribute towards achievement of global plastic mechanism (Figure 14). Capacity design philosophy allows for the plastic mechanism to be predicted and implemented in calculations. Advantages such as good energy dissipation distribution in elevation, elastic and strong columns and dissipative beams contribute towards good performance for local and global ductility. Another advantage of new design principles is that the influence of $P-\Delta$ effect is limited because there is no storey with strongly dominating interstorey drift over the other drifts.

The performance based evaluation procedure implies the use of two types of capacity spectra: actual capacity spectrum (ACS) and target capacity spectrum (TCS). Seismic demands of the action effects are easy obtained as a result of design seismic loading. The algorithm proposes comparison of seismic demands before and after strengthening. The analysis results are easy to be interpreted and provide argumentation for strengthening and benefit of it. Comparable analysis of the results before and after strengthening is a good basis for making conclusions by design engineers.

Some basic terms and formulations are discussed below.

actual capacity spectra (ACS)

Actual capacity spectrum corresponds to a certain structure, which is designed according to EN 1998-1 or according to some other seismic resistant design code. Actual capacity spectra however can be determined also for structures which are designed without proper design criteria and performance requirements. At first base shear force – roof displacement diagram (pushover curve) is calculated, then on the basis of simple modifications actual capacity spectrum (ACS) is obtained. This spectrum is a plot of “first floor acceleration against modified displacement”. Modified displacement u^* is related to the unique displacement of equivalent single degree of freedom (ESDOF) system. “Zero length” plastic hinge concept is applied. Details concerning plastic hinge parameters are not discussed in the paper. As a matter of fact, it is clear that actual capacity spectrum is obtained on structural data.

Figure 13a illustrates one three storey three bays reinforced or steel frame. It is loaded statically with monotonically increased vertical loads first and after ending of the process a new loading case with monotonically increased horizontal loads is initiated. Action effects are obtained as a sum of the action effects from both subsequent loading cases. Lateral loads are applied at the storey levels and their increase continues till the base shear capacity is reached.

The typical force-deformation curve is shown in Figure 13b. As a matter of fact further theoretical development is performed using idealized bi-linear relationship. This line is obtained on the basis of actual relationship “base shear force – roof displacement” using energy balance principle recommended [9]. However this solution is not a unique one and it should be taken into account that it becomes a source of numerical error.

Figures 14 and 15 illustrate global (G) and “soft first storey” (F) mechanisms which propose different disposition of the plastic hinges. In first case plastic hinges are located at the end of the beams when loading procedure is still not terminated. Dissipated energy has relatively uniform distribution in elevation; in the second case dissipated energy is concentrated only in the first storey. This implies that failure mode is a product of inelastic deformations of the first storey only.

In old generation of codes capacity design principles do not take place in seismic resistance calculations. The prediction of the plastic mechanism in the process of design is impossible. In many cases plastic mechanism may surprise the design engineer and may have unexpected shape. Among all feasible mechanisms the most dangerous and unacceptable is the mechanism “soft first storey” (F - mechanism). For the sake of safety this mechanism is used in checking procedure, see Figure 15. This approach is applied when existing building is studied and capacity design rules are not used.

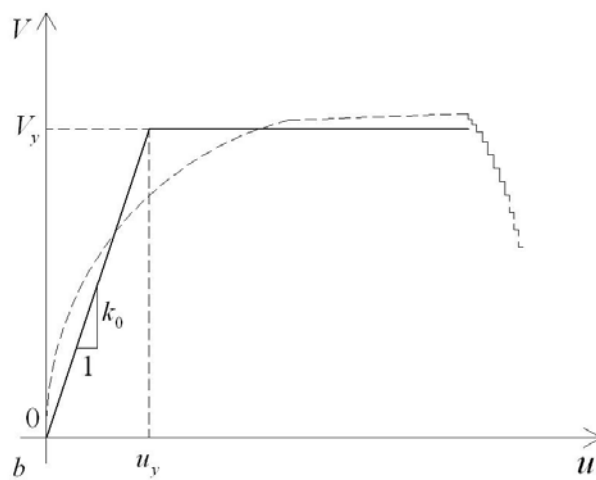
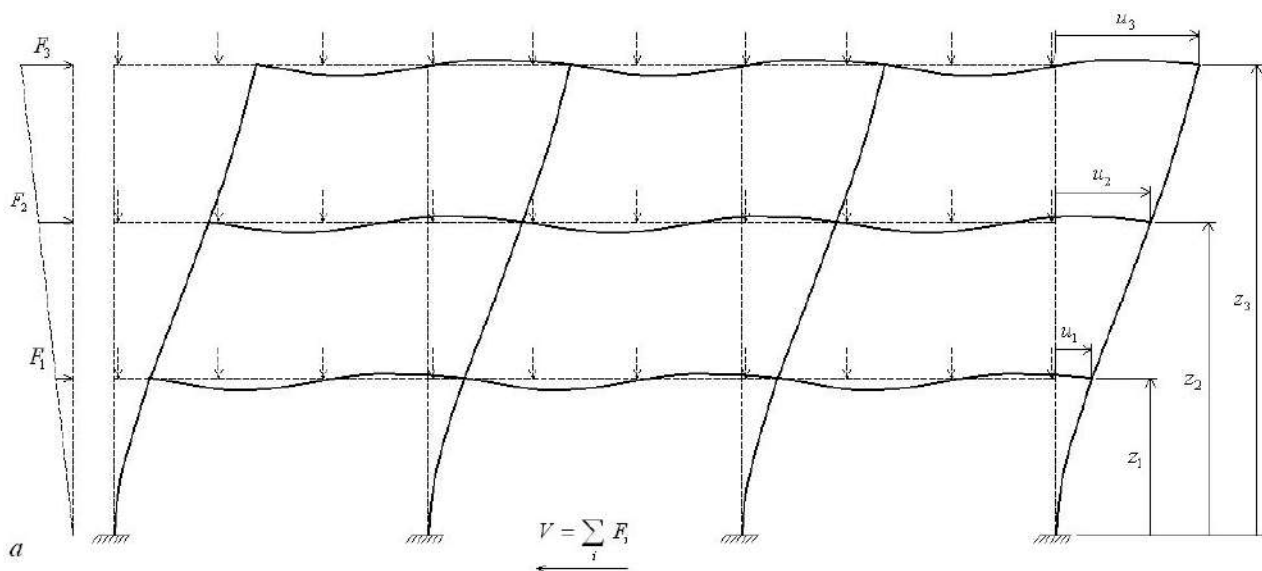


Figure 13. Determination of actual capacity spectrum:
 a – loading patterns for vertical and horizontal forces used in static pushover analysis;
 b – pushover curves: actual (dashed line) obtained through computations and idealized (solid line)
 bi - linear curve suggested in theoretical development.

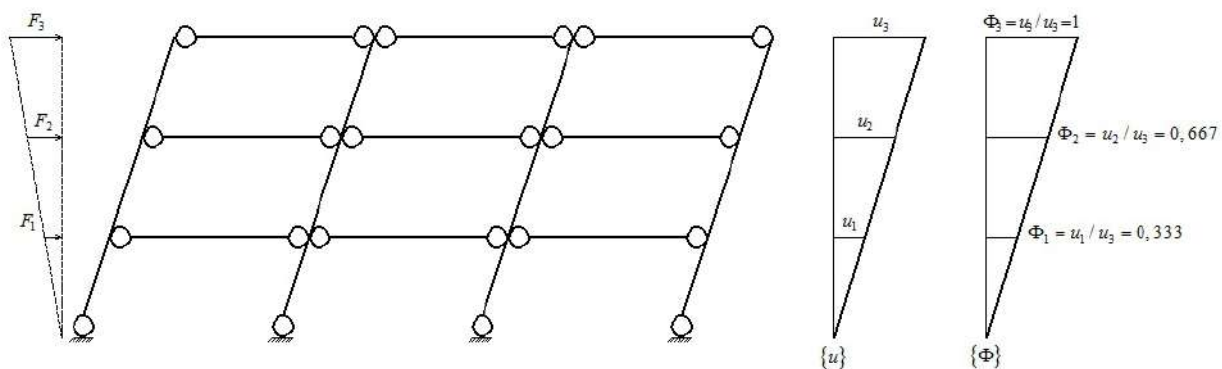


Figure 14. Global (G) plastic mechanism

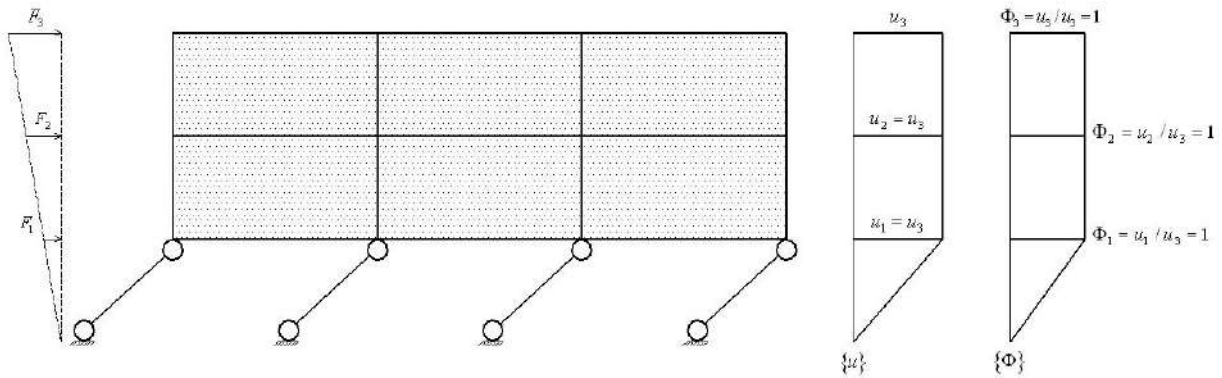


Figure 15. Soft first storey (F) plastic mechanism (local mechanism)

Appendix B contains information about transformation of MDOF structure and its system of differential equations into ESDOF (equivalent single degree of freedom system) equation (see Figure 13a) assuming G mechanism from Figure 14. The same transform for F - mechanism in Figure 15 mathematically seems to be a particular case of the more general case of G mechanism provided in Annex B. The introduction of G and F mechanisms implies the following explanations.

F – mechanism

The vector of dimensionless lateral displacements for F - mechanism takes very simple form containing only unity components:

$$\{\Phi\} = \begin{Bmatrix} 1 \\ 1 \\ 1 \end{Bmatrix} \quad (14)$$

Following Appendix B and taking into account Eq. (14) the quantities mentioned there can be calculated to give

mass of the ESDOF system:

$$m^* = \{\Phi\}^T [m] \{\Phi\} = \sum_{i=1}^3 m_i \Phi_i = m \quad (15)$$

mass parameter

$$\hat{m} = \{\Phi\}^T [m] \{\Phi\} = \sum_{i=1}^3 m_i \Phi_i^2 = m \quad (16)$$

$$\text{participation factor } \hat{\Gamma} = 1 \quad (17)$$

resisting force of the ESDOF system

$$f^* = \{\Phi\}^T \{f\} = \sum_{i=1}^3 f_i \Phi_i = V \quad (18)$$

equation of the motion of ESDOF system:

$$\ddot{u}(t) + \frac{V}{m} = -\ddot{u}_g \quad (19)$$

It is worth noting that the basic force – displacement relationship in the case of F mechanism is “base shear force V – roof displacement u ”. Because of Eq. (17) the displacement of the ESDOF system is equal to the roof displacement in MDOF system. The peak response of ESDOF system is easily expressed using response spectra.

G – mechanism

In the case of G mechanism the mathematical transform MDOF – ESDOF system is shown in Appendix B. This kind of transform is needed because the peak response of ESDOF system is easily evaluated through response spectra.

target capacity spectrum (TCS)

Target capacity spectrum (TCS) should comply with the performance requirements in largest extent. It should cover deformation criteria such as limited elastic displacement u_y^* for G mechanism and limited first storey elastic drift u_y , ductility demand should be less than ductility capacity (basic requirement of [9]). For F mechanism the elastic deformation criterion can be written in the form (see Figure 16):

$$u_y \leq \frac{H}{250} \quad (19a)$$

where H is the total height of the building. The ESDOF system should have prescribed values for the displacement ductility demand, behaviour factor. Prescribed values are entered by the design engineer as input.

Determination of target capacity spectrum is a geometric problem which is settled by iterations. All basic parameters are varying in previously specified limits in order to satisfy simultaneously all requirements in largest extent. In contrast with actual capacity spectrum the procedure of determination of the target capacity spectrum does not require any structural data, it just couples specified design regulations. Figures 16 and 17 are graphically illustrating the determination of the

target capacity spectrum (TCS) - Figure 16 for F mechanism and Figure 17 - for G - mechanism correspondingly.

Calculation procedure assuming F mechanism can be generalized in the following steps (Figure 16). The calculation process is iterative and the results are approximate. The iterative algorithm can be represented using the following steps:

1. Specify u_y using equality sign in Eq. 19a as upper limit for yielding displacement.
2. Calculate the ductility demand on the basis of the position of point PP.
3. Find the point EPP (elastic performance point) basing on the observation of Newmark for equal displacements.

4. Find the elastic (initial) stiffness for ESDOF system connecting EPP with the origin of the coordinate system.
5. Find the acceleration at yielding V_y / m (m - total mass of the structure).
6. Find the behaviour factor q_r as a ratio of (ordinate of EPP)/(ordinate of PP).

If the results from items 2), 3), 4), 5) and 6) do not comply with the prescribed values of same quantities then reduce u_y and go back to items 2), 3), 4), 5) and 6).

For G - mechanism (see Figure 17) the iterative algorithm is remaining the same but all quantities should be related to the equivalent single degree of freedom system described mathematically in Appendix B having the upper superscript (*).

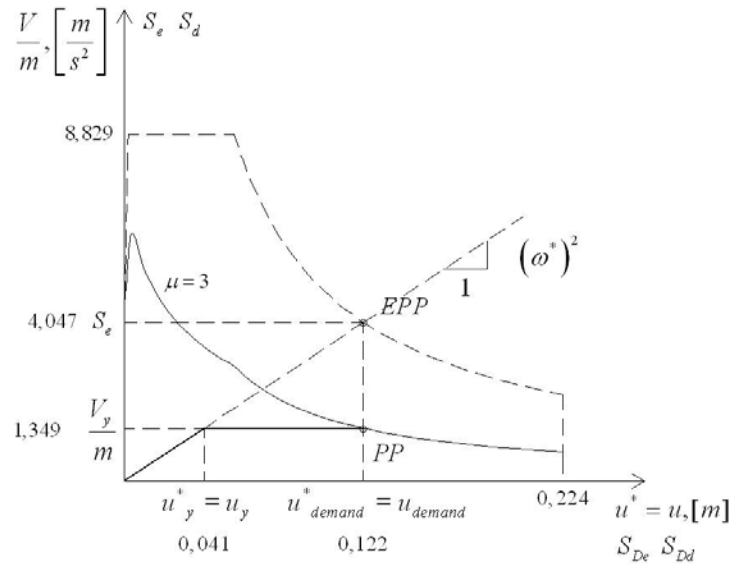


Figure 16. Determination of target capacity spectrum using base shear force – roof displacement relationship. Dashed line represents the elastic demand spectrum, solid line represents the design demand spectrum for accelerations using specified ductility, and dark solid line is the target capacity spectrum

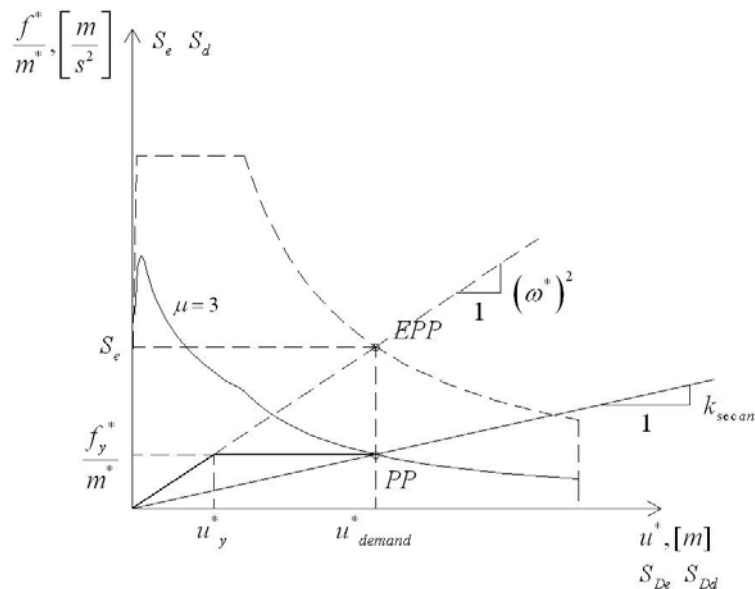


Figure 17. Determination of target capacity spectrum using effective force – effective displacement relationship. Dashed line represents the elastic demand spectrum, solid line represents the design demand spectrum for accelerations using specified ductility, and dark solid line is the target capacity spectrum

Following the current concept of design codes, it is relevant to represent the system of equations of the motion in drift oriented form. Interstorey drifts are the most important deformation indicators which are limited in elastic range. Figure 18 visualizes the connection between floor unknown displacements and drifts considering a simple vertical cantilever structure for the sake of simplicity.

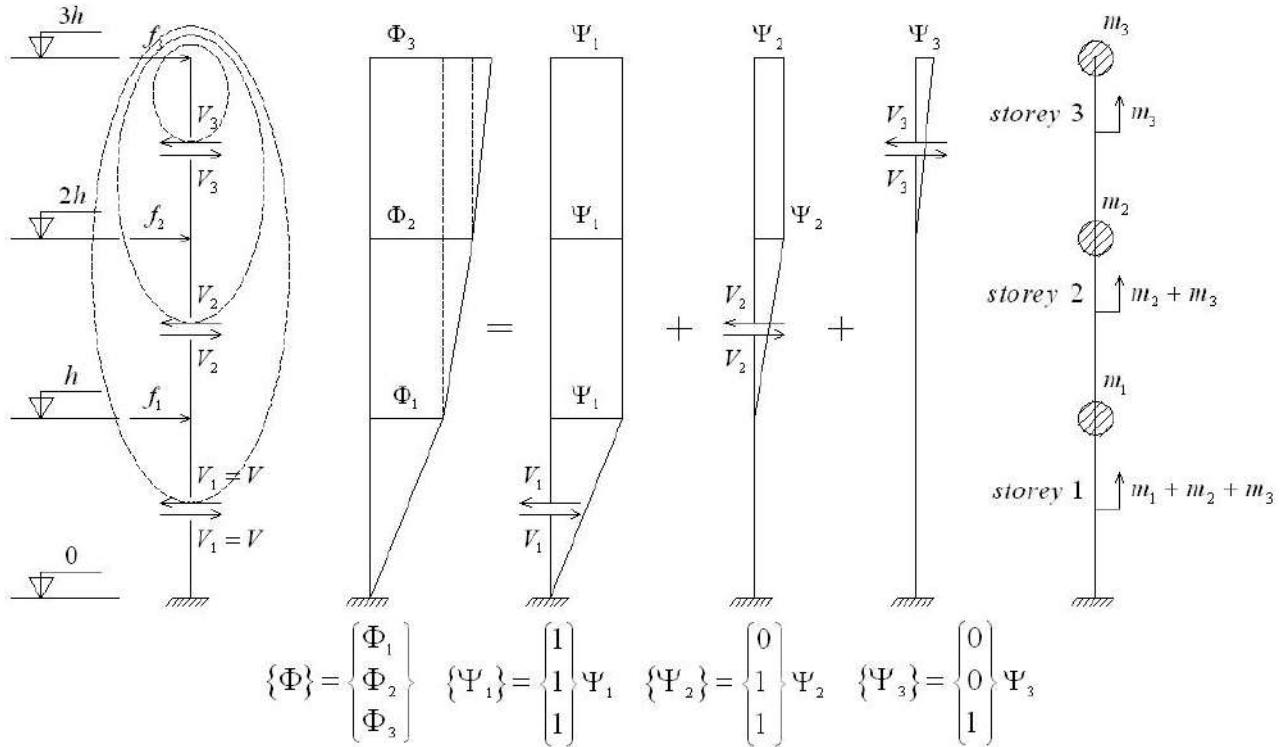


Figure 18. Drift-oriented decomposition in elevation of floor lateral displacements

The connection between relative floor displacements Φ and relative storey drifts Ψ is evident from Figure 18:

$$\begin{aligned} \Phi_1 &= \Psi_1 \\ \Phi_2 &= \Psi_1 + \Psi_2 \\ \Phi_3 &= \Psi_1 + \Psi_2 + \Psi_3 \end{aligned} \quad (20)$$

Further calculations require definition of the term “masses above storey level 1” for example m_1^* . This quantity requires summation of all storey masses which results in $m_1 + m_2 + m_3$. Similar definitions could be implemented for the remaining two masses.

$$\begin{aligned} m_1^* &= m_1 + m_2 + m_3 \\ m_2^* &= m_2 + m_3 \\ m_3^* &= m_3 \end{aligned} \quad (21)$$

The mass of ESDOF system is then obtained as:

$$m^* = \Psi_1 m_1^* + \Psi_2 m_2^* + \Psi_3 m_3^* \quad (22)$$

Considering now G – mechanism, it is worth implementation of floor accelerations following the ratios:

$$a_1 = \frac{V_1}{m_1^*} \quad a_2 = \frac{V_2}{m_2^*} \quad a_3 = \frac{V_3}{m_3^*} \quad (23)$$

Where V_1 , V_2 and V_3 are the storey shear forces below levels 1, 2 and 3.

Then mass acceleration of ESDOF system can be defined in drifts as:

$$\frac{f^*}{m^*} = \frac{\Psi_1 m_1^* a_1 + \Psi_2 m_2^* a_2 + \Psi_3 m_3^* a_3}{\Psi_1 m_1^* + \Psi_2 m_2^* + \Psi_3 m_3^*} \quad (24)$$

The ratio $\frac{f^*}{m^*}$ denotes the acceleration of the ESDOF system, which is averaged by Equation (24).

Let us assume that a simple building designed according to code of old generation is analyzed. The actual capacity spectrum of this structure without strengthening is ACS – 1. Let us imagine that the target capacity spectrum TCS looks like this shown in Figure 19. Comparison between ACS – 1 and TCS illustrates that the structure needs greater shear force capacity to withstand the design earthquake of [9]. The existing structure shows insufficient initial elastic stiffness and insufficient yield strength. This means that the necessity for strengthening is evident. After strengthening structure shows an improved capacity and it is capable of withstanding of the design seismic action. The actual capacity curve ACS – 2 has an excessive capacity with respect to TCS line and level of safety is increased due to the strengthening. Excessive elastic stiffness and excessive yield strength are also evident considering both ACS – 2 and TCS lines.

Looking at Figure 20 after comparison between idealized capacity spectra TCS and ACS one may conclude that the structure studied has insufficient

elastic stiffness and insufficient yield strength. Thus this structure needs strengthening. Figure 21 shows three different opportunities for strengthening. First one implies strengthening by using fibre reinforced polymers - FRP. Elastic stiffness and yield strength are increased by increasing the confinement. Second method implies the confinement to be implemented by R/C jackets. The third opportunity is based on inverted steel "V" – frame implementation into the R/C beams and columns sub assemblages.

Performance base seismic design method is applicable only for low rise building structures. Only single mode response is taken into account into this methodology and limitations are considered as consequence of this. For high-rise and tall building structures multi-modal methods are recommended because high frequency response may contribute essentially on overall response.

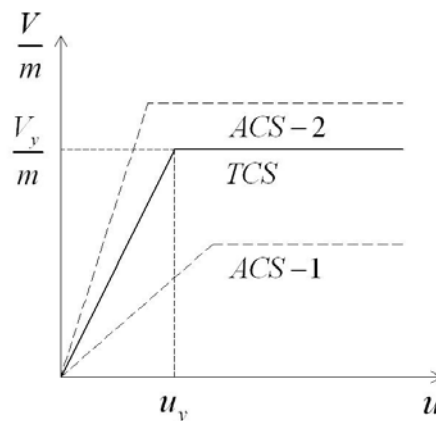


Figure 19. Comparison between TCS and ACS capacity spectra.
ACS-1 represents the actual capacity spectrum of existing structure before strengthening.
ACS-2 is the actual capacity spectrum after strengthening the existing structure.

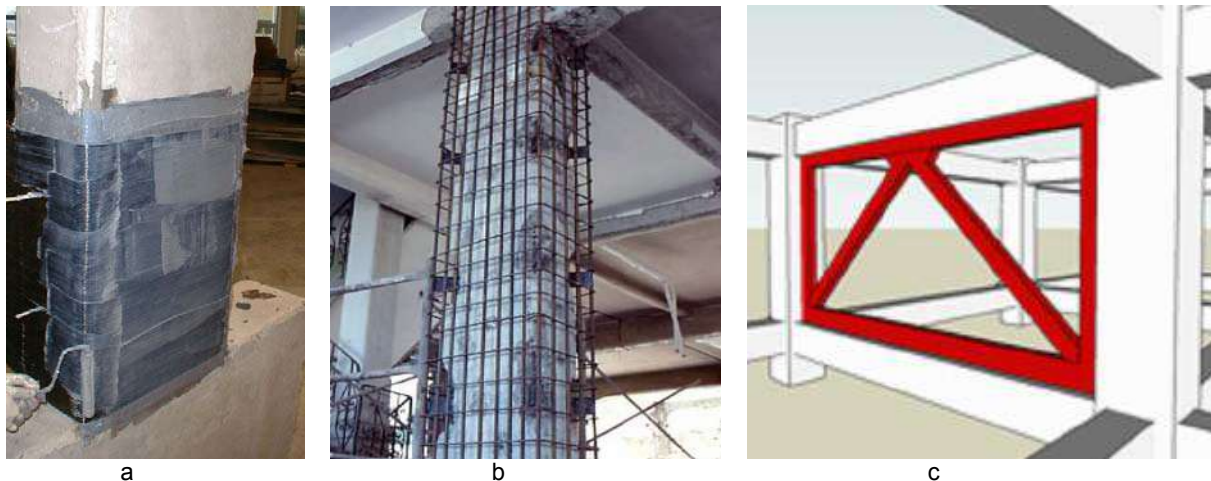


Figure 20. Different strengthening strategies and techniques:
a – improved confinement using FRP (fibre reinforced polymers), [14];
b – use of R/C jackets, [14];
c – use of internally implemented steel framework, [1].

3 CONCLUSIONS

The following conclusions are made as a result of proposed studies:

topic 1:

1. Inclusion of the rotational components results in larger action effects and unfavourable results.

2. Inclusion of rotational components leads to magnification of low period's response.

3. An efficient peak response reduction can be achieved by making use of supplemental stiffness proportional viscous damping.

topic 2:

1. Comparable analysis between target capacity spectrum (TCS) and actual capacity spectrum of existing

structure before strengthening (ACS 1) is capable of indicating whether strengthening is necessary or not.

2. Comparable analysis between target capacity spectrum (TCS) and actual capacity spectrum (ACS 2) of strengthened structure can be used to prove the benefit and efficiency of strengthening.

3. Target capacity spectrum (TCS) is the spectrum which satisfies the Eurocode 8 provisions. The scatter between TCS and ACS 1 shows how the parameters of existing structure should be changed. The scatter between TCS and ACS 2 can be used for prediction of level of safety after strengthening.

ACKNOWLEDGEMENTS

The encouragement and help of Professor emeritus Radomir Folic are greatly acknowledged by the authors.

4 REFERENCES

- [1] *Abdullah*. Seismic Strengthening of RC Building Structurer. FYPE Japan Co., Ltd. (PPT presentation).
- [2] *Bonev Z., E. Vaseva, D. Blagov and K. Mladenov*. Seismic Design of Slender Structures Including Rotational Components of the Ground Acceleration – Eurocode 8 Approach. Proceedings of the 14th European Conference on Earthquake Engineering, 30 August – 03 September, 2010, Ohrid, Macedonia, Paper 1793.
- [3] *Bonev Z., S. Dimova and P. Petrov*. Study of the Seismic Design of Irregular Structural Systems. European Association of Earthquake Engineering, Task Group 8: Asymmetric and Irregular Structures, Volume 1: Irregular Structures, Editors F. Karadogan and A. Rutenberg, October 1999, Istanbul, pp. 57-71.
- [4] *Bonev Z. and A. Taushanov*. Seismic Design of Structures According to Response Spectrum Method coupled with Linear Analysis. Integra Engineering, 2006 (book, in Bulgarian).
- [5] *Calvi Gian Michele, Stefano Pampann, P. Fajfar, M. Dolsek*. New Methods for Assessment and Design of Structures in Seismic Zones: Present State and Research Needs.
- [6] *Chopra A. K. and Rakesh K. Goel*. Capacity-Demand-Diagram Methods for Estimating Seismic Deformation of Inelastic Structures: SDF systems. Pacific Earthquake Engineering Research Center, PEER, 1999/02, April 1999.
- [7] *Dimova S., P. Petrov and Z. Bonev*. Precising of the Design Seismic Loading of Irregular Structures. Proceedings of the 3rd Japan-Turkey Workshop on Earthquake Engineering, Volume 1, Istanbul, 2000, pp. 63-77.
- [8] *Dimova S., Z. Bonev and P. Petrov*. Seismic Design of Irregular Structures Including Rotational Component of the Seismic Excitation. European Association of Earthquake Engineering, Task Group 8: Asymmetric and Irregular Structures, Volume 1: Irregular Structures, Editors F. Karadogan and A. Rutenberg, October 1999, Istanbul, pp. 73-87.
- [9] EN 1998-1 Eurocode 8 : Design of Structures for Earthquake Resistance – General Rules, Seismic Actions and Rules for Buildings.
- [10] EN 1998-6 Eurocode 8 : Masts, Chimneys and Towers
- [11] *Fajfar P.* A Nonlinear Analysis Method for Performance Based Seismic Design. Earthquake Spectra, Vol. 16, No 3, pp. 573-592, August 2000.
- [12] *Fajfar P.* Structural Analysis in Earthquake Engineering – a Breakthrough of Simplified Non-Linear Methods. Published by Elsevier Science Ltd., 12th European Conference on Earthquake Engineering, Paper reference 843.
- [13] *Fajfar P., D. Marusic, I. Perus*. The N2 Method for Asymmetric Buildings. First European Conference on Earthquake Engineering and Seismology, Geneva, Switzerland, 3-8 September, 2006, Paper Number 539
- [14] *Fardis M.* Seismic Design, Assessment and Retrofitting of Concrete Buildings, Based on EN Eurocode 8, Springer Science+Business Media B.V. 2009.
- [15] *Kuesel T. R.* Earthquake Design Criteria of Subways. Journal of the Structural Division, Proceedings of the American Society of Civil Engineers, Vol. ST 6, June 1969, pp. 1213-1231.

- [16] *Mestrovic G., D. Gizmar and M. Pende.* Nonlinear Analysis of Structures According to New European Design Code. Proceedings of the 14th World Conference on Earthquake Engineering, October 12-17, 2008, Beijing, China.
- [17] Static Pushover Analysis in Z_Soil PC & related EUROCODE 8 regulations R_070202, January 2007.
- [18] *St John C. M. and T. F. Zahrah.* Aseismic Design of Underground Structures, FEATURES SECTION: Seismic Effect on Underground Structures. Tunneling and Underground Space Technology, Vol. 2, Number 2, 1987, pp. 165-197.
- [19] *Tzenov L.* Basics of Earthquake Engineering. Professor Marin Drinov Academic Publishing House, Sofia, 2002.
- [20] *Tzenov L., S. Dimova, Z. Bonev and P. Petrov.* Seismic Resistant Design of Irregular Structures: Generalized Method for Determination of Design Seismic Loading, on issue of Turkish Earthquake Foundation, Technical Report TDV/TR 037-62, Istanbul Technical University, 2001.
- [21] *Todorovska M. and M.D. Trifunac.* Response Spectra for Differential Motion of Columns, Proceedings of the 12-th World Conference on Earthquake Engineering, 2000, paper 2638.
- [22] *Todorovska M.* Some Interferometry of Soil – Structure Interaction Model with Coupled Horizontal and Eocking Response, Bulletin of the Seismological Society of America, Vol. 99, No. 2A, pp. 611-625, April 2009.

SUMMARY

EUROCODE 8: USE OF ADVANTAGEOUS FORMULATIONS FOR IMPROVED AND SAFE DESIGN

*Zdravko BONEV
Stanislav DOSPEVSKI*

The purpose of the paper is to share the experience in application of Eurocode 8. Following the existing framework of the European standard two engineering development of two specific topics are proposed. First deals with modelling the seismic action aiming to take into account spatial variability of the seismic action. It is proven that the inclusion of rotational components may influence the action effects and the results provide unsafe design. Evaluation is carried out through response spectrum method. The second topic studies the use of performance based seismic design as a tool to prove the need for seismic strengthening and verification of the benefit. Both target and actual capacity spectra are compared to make assessment of the lateral resistance of existing and strengthened structure. Insufficient elastic stiffness and insufficient yield strength are considered as the most typical situations frequently met in the design practice and which can be settled by seismic strengthening. Discussions and conclusions concerning the philosophy of the assessment procedure are presented.

Key words: Seismic resistant design to Eurocode 8, taking into account spatial variability of seismic action, performance based seismic design

REZIME

EVROKOD 8: UPOTREBA POVOLJNE FORMULACIJE ZA POBOLJŠANO I SIGURNO PROJEKTOVANJE

*Zdravko BONEV
Stanislav DOSPEVSKI*

Svrha ovog rada jeste da se prenesu i podele iskustva iz primene Evrokoda 8 (EN 1998). Sledeći postojeći okvir Evropskih standarda, razvijena su dva inženjerska pravca delovanja, tj. dve zasebne oblasti rada. Prva se odnosi na modliranje seizmičkih dejstava sa ciljem uzimanja u obzir njihove prostorne promenljivosti. Provereno je i dokazano da uključanje rotacionih komponenti može da utiče na efekte od dejstava i da rezultati dovedu do nesigurnih projektnih rešenja. Procena je izvršena korišćenjem metode spektra odgovora. U drugoj oblasti izučava se upotreba metode projektovanja na bazi seizmičkih performansi kao sredstva provere i potvrde za seizmičkim pojačanjima kao i potvrde njihove efikasnosti. Da bi se ovo uradilo, upoređeni su spektar ciljanog kapaciteta i stvarni spektar kapaciteta. Slučaj nedovoljne elastične krutosti i nedovoljne čvrstoće pri tečenju smatra se najtipičnijim seizmičkim slučajem kada je potrebno izvesti pojačavanja. Diskutovane su obe ove teme i formulisani su zaključci koji se odnose na filozofiju Evropskih standarda.

Ključne reči: Projektovanje seizmički otpornih konstrukcija prema Evrokodu 8 (EN 1998), uzimanje u obzir prostornu promenljivost seizmičkih dejstava, seizmičko projektovanje zasnovano na performansama

APPENDIX A

RESPONSE SPECTRUM METHOD EXTENDED WITH APPLICATION OF ROTATIONAL COMPONENT

information concerning overall structure

X - superscript denoting translation transferred motion;

θ - superscript, denoting rotation transferred motion;

$\{v^x\}$ - dimensionless vector, describing mathematically the translation transferred motion;

$\{v^\theta\}$ - dimensionless vector, describing mathematically the rotation transferred motion;

M^x_{Tot} - total mass of the structure following the motion according to the vector $\{v^x\}$

M^θ_{Tot} - total mass of the structure following the motion according to the vector $\{v^\theta\}$

m_k - mass, associated with k -th degree of freedom

h_k - height of the mass m_k

h - total height of the structure

modal information:

modal subscript, mode i ;

modal vector $\{\Phi_i\}$;

modal mass m_i^* ;

modal participation factor – translation transferred motion Γ_i^x ;

modal participation factor - rotation transferred motion Γ_i^θ ;

design value of the modal seismic force E^x_{ik} , induced by translation transferred motion;

design value of the modal seismic force E^θ_{ik} , induced by rotation transferred motion;

Φ_{ik} - the modal ordinate, mode i , k -th degree of freedom;

$V^x_{i,base}$ - base shear force, mode i , translation transferred motion;

$V^\theta_{i,base}$ - base shear force, mode i , rotation transferred motion;

M^x_{base} - base flexural moment, mode i , translation transferred motion;

M^θ_{base} - base flexural moment, mode i , rotation transferred motion;

$S_e(T_i)$ - spectral ordinate (elastic response spectrum for horizontal accelerations, mode i);

T_i - i -th modal period of free undamped vibrations;

relationships when translation component is acting at the base of the structure (see fig. 8):

dimensionless vector of translational motion

$$\{v^x\}^T = \{1 \ 1 \ \dots \ 1\} \quad (A-1)$$

modal participation factor, mode i

$$\Gamma_i^x = \frac{\{\Phi_i\}^T [m] \{v^x\}}{m_i^*} \quad (A-2)$$

modal mass, mode i

$$m_i^* = \{\Phi_i\}^T [m] \{\Phi_i\} \quad (A-3)$$

total mass, translational motion

$$M^x_{Tot} = \{v^x\}^T [m] \{v^x\} = \sum_k m_k \quad (A-4)$$

design seismic force (see above)

$$E^x_{ik} = m_k \Phi_{ik} \Gamma_i^x S_e(T_i) \quad (A-5)$$

base shear force (see above)

$$V^x_{i,base} = \sum_k E^x_{ik} \quad (A-6)$$

base flexural moment (see above)

$$M^x_{i,base} = \sum_k h_k E^x_{ik} \quad (A-7)$$

relationships when rotation component is acting at the base of the structure (see fig. 8):

dimensionless vector of rotational motion

$$\{v^\theta\}^T = \{0 \ \dots \ \dots \ 1\} \quad (A-8)$$

correlation coefficients for modal combination

$$\rho_{ij} = \frac{8\xi^2 (1+r_{ij}) r_{ij}^{3/2}}{(1-r_{ij}^2)^2 + 4\xi^2 r_{ij} (1+r_{ij}^2)^2} \quad (A-9)$$

design seismic force (see above)

$$E_{ik}^{\theta} = m_k \Phi_{ik} \Gamma_i^{\theta} h S_e(T_i) \quad (\text{A-10})$$

modal participation factor, mode i

$$\Gamma_i^{\theta} = \frac{\{\Phi_i\}^T [m] \{v^{\theta}\}}{m_i^*} \quad (\text{A-11})$$

total mass, rotational motion

$$M_{Tot}^{\theta} = \{v^{\theta}\}^T [m] \{v^{\theta}\} = \sum_k m_k (v_k^{\theta})^2 \quad (\text{A-12})$$

APPENDIX B

APPLICATION OF RESPONSE SPECTRUM METHOD TO PEAK RESPONSE EVALUATION OF EQUIVALENT SINGLE DEGREE OF FREEDOM SYSTEM

The general design strategy used in the paper is based on mixed application of Capacity Spectrum Method (CSM) [6], [9], [17] and N2 method [11], [13], [16]. A mixed strategy to determine seismic demands assuming design seismic action is demonstrated in [5], [13] and [16]. The mixed application of both CSM and N2 methods has serious advantage because allows for determination of elastic and inelastic target parameters and their demands and the process of displacement is controlled through the ductility.

The governing system of equations is presented in the following usual presentation:

$$[m] \{\ddot{u}\} + \{f\} = -[m] \{v\} \ddot{u}_g \quad (\text{B-1})$$

where $[m]$ is diagonal matrix containing storey masses as diagonal elements, $\{v\}$ is the vector of the transferred horizontal seismic motion (all components have unit value), \ddot{u}_g represents the horizontal ground acceleration record, $\{\ddot{u}\}$ is the vector of horizontal storey accelerations relative with respect to the base. The vector $\{f\}$ is containing the storey resisting forces which are dependent on storey displacements.

Inelastic performance of the frame structure is studied by means of plastic mechanism formation using pushover analysis. Plastic mechanism is obtained on output of the pushover analysis and visualized by the vector $\{\Phi\}$ of dimensionless lateral floor displacements.

The basic assumption for lateral floor displacements distribution is written in the form:

$$\{u(t)\} \approx \{\Phi\} u(t) \quad (\text{B-2})$$

where $u(t)$ is the roof displacement as a function of the time. Equation (B-2) transforms the differential system of equations representing the behaviour of the dynamic model as multi degree of freedom system into a single equation. It is related to equivalent single degree of freedom (ESDOF) system. This transform can be carried out only after formation of the plastic mechanism. The following parameters are calculated for further steps:

mass parameter

$$\hat{m} = \{\Phi\}^T [m] \{\Phi\} \quad (\text{B-3})$$

mass of ESDOF system

$$m^* = \{\Phi\}^T [m] \{v\} = \sum_{i=1}^3 m_i \Phi_i \quad (\text{B-4})$$

internal force of ESDOF system

$$f^* = \{\Phi\}^T \{f\} = \sum_{i=1}^3 f_i \Phi_i \quad (\text{B-5})$$

modification factor

$$\hat{\Gamma} = \frac{m^*}{\hat{m}} = \frac{\{\Phi\}^T [m] \{v\}}{\{\Phi\}^T [m] \{\Phi\}} = \frac{\sum_{i=1}^3 m_i \Phi_i}{\sum_{i=1}^3 m_i \Phi_i^2} \quad (\text{B-6})$$

basic ESDOF equation of the motion

$$\frac{\ddot{u}(t)}{\hat{\Gamma}} + \frac{f^*}{m^*} = -\ddot{u}_g \quad (\text{B-7})$$

displacement of ESDOF system

$$u^*(t) = \frac{u(t)}{\hat{\Gamma}} \quad (\text{B-8})$$

peak total horizontal acceleration

$$\left| \frac{f^*}{m^*} \right|_{\max} = \left| \ddot{u}_g + \frac{\ddot{u}}{\hat{\Gamma}} \right|_{\max} \quad (\text{B-8})$$

displacement ductility demand

$$\mu_{demand} = \left| \frac{u_{demand}}{u_y} \right| \quad (\text{B-9})$$

displacement demand for ESDOF / actual system

$$u^*_{demand} = \frac{u_{demand}}{\hat{\Gamma}} \quad (\text{B-10})$$

TESTIRANJE FENOMENA PUZANJA MEKE STIJENE

TESTING OF CREEP PHENOMENA ON SOFT ROCK

Zvonko TOMANOVIĆ

ORIGINALNI NAUČNI RAD
ORIGINAL SCIENTIFIC PAPER
UDK: 624.131.54

1 UVOD

Test puzanja, po definiciji, karakteriše konstantno opterećenje pod kojim se materijal s vremenom deformiše. Uobičajeno je da se testovi puzanja sprovode povećanjem ili smanjenjem opterećenja na uzorak u inkrementima. Nakon svakog inkrementa, zadržava se konstantno opterećenje u toku odabranog intervala. Opterećivanje ili rasterećenje uzorka do određenog naponskog nivoa i održavanje konstantnog opterećenja u toku ovako dugog intervala, zahtijeva posebne uređaje prilagođene vrsti materijala koji se ispituje, veličini uzoraka i naponskom stanju (jednoaksijalno, biaksijalno ili triaksijalno) koje se održava na uzorku. Za sprovođenje testa jednoaksijalnog puzanja, odnosno za održavanje konstantnog opterećenja – napona na uzorcima, u toku relativno kratke istorije ovog testa, korišćeno je više različitih uređaja baziranih na polugama i okačenom teretu. U posljednje dvije decenije, konstruisani su i servo-uređaji za konvencionalne triaksijalne testove puzanja na standardnim cilindričnim uzorcima stijene.

Dug period testiranja i zahtjev da se naponsko stanje održi konstantnim, uz relativno mala odstupanja u toku dugog perioda koji se nekada mjeri i godinama, veoma komplikuje uređaje koji treba da odgovore tom zadatku. Pored navedenog, potrebno je obezbijediti pouzdano mjerenje relativno malih deformacija – sve od trenutka opterećivanja, pa do završetka testa. Pritom, treba imati u vidu da ukupna deformacija meke stijene može biti uzrokovana promjenom napona, vremenski zavisnim deformacijama (puzanje), promjenom temperature, promjenom vlage u stijeni, promjenom vlažnosti u vazduhu i slično.

1 INTRODUCTION

Creep test by definition represents a deformation of material with time under a constant stress. Commonly, creep tests are performed by incrementally increasing or decreasing the load on the specimen. After each increment, the constant load is maintained for a defined time interval. Application of stress or strain relief of specimen and maintaining constant load over this long time interval requires use of special devices that correspond to the type of tested material, specimen size and stress state (uniaxial, biaxial or three-axial) maintained in the specimen. In its quite short history, various dead weight and lever arm testing devices have been used for the purposes of uniaxial creep tests that are for maintaining constant stress state within the specimen. In the last two decades servo-hydraulic equipment has been designed for the conventional three-axial creep tests of standard cylindrical rock specimens.

The long time interval needed as well as the requirement for maintaining the constant stress state with relatively small variations over the long time interval which, sometimes can be measured by years, significantly complicate the devices that should response to this task. Additionally, it is necessary to enable reliable measuring of relatively small deformations from the moment the load is applied up to the test completion. Here it should be noted that total deformation of soft rock can be caused by stress changes, time-dependent deformations (creep), temperature changes, moisture changes, air humidity changes etc.

In addition to the above mentioned a change in the rock moisture content alone, without any changes in

Prof. dr Zvonko Tomanović, Građevinski fakultet,
Univerzitet Crne Gore, Cetinjski put bb, 81000 Podgorica,
Crna Gora, e-mail: zvonko@ac.me

Prof. dr Zvonko Tomanovic, Faculty of Civil Engineering,
University of Montenegro, Cetinjski put bb, 81000
Podgorica, Montenegro, e-mail: zvonko@ac.me

Pored navedenog, samo promjena vlažnosti stijene bez promjene napona ili temperature, može biti uzrok deformacija puzanja. Ovaj efekat, u literaturi poznat kao „hidraulično omekšanje“, među prvim uočili su *Griggs* i *Blacic* (1965) i *Griggs* (1967). Efekte vlažnosti vazduha oko uzoraka kamene soli pri testu puzanja izučavali su *Hunsche* i *Shulze* (1996). Ustanovljen je veliki uticaj na puzanje kamene soli, kada se vlažnost vazduha kreće u granicama od 0% do 65%. Dosad, u literaturi nije dokazano da vlažnost u vazduhu značajno utiče na puzanje drugih vrsta stijena (*sistematizovano kod: Cristescu, [4]*). Aparatura i procedure koje se sprovode u toku testiranja, treba da omoguće da se ukupna vremenska deformacija, koja je posljedica prethodne naponske promjene, razdvoji od ostalih komponenti vremenskih deformacija koje se razvijaju u stijeni u toku vremena (skupljanje zbog gubitka vlage, temperaturne dilatacije itd.).

Puzanje u stijeni počinje značajnije da se proučava početkom šezdesetih godina XX stoleća, nakon pionirskih radova *Michelson-a* (1917) koji je izvodio testove torzije na stijeni (po uzoru na ispitivanje metala). Početak istraživanja puzanja stijena karakterišu problemi u vezi s tehnikom izvođenja i interpretacijom rezultata testa. Testove puzanja pri jednoosijalnoj kompresiji izvodilo je više istraživača, na primer *Evans* i *Wood* (1937), na granitu, mermeru i soli. *Nichihara* (1958), *Hardy* (1959, 1966) i *Price* (1964) istraživali su puzanje sedimentnih stijena (*sistematizovano kod: Jaeger et al., [7]*).

Šezdesetih i sedamdesetih godina prošlog vijeka, značajan broj testova izveden je u BGR-u u Hanoveru, u Njemačkoj (BGR – Bundesanstalt für Geowissenschaften und Rohstoffe – Savezni zavod za geonauku i sirovine), na kamenoj soli pri jednoosijalnom i triaksijalnom stanju napona. *Gimm* (1968), *Dreyer* (1974) i *Baar* (1977) izveli su većinu testova puzanja stijenske mase „in situ“ u rudnicima kamene soli. Na osnovu rezultata mjerenja konvergencije u hodnicima rudnika kamene soli, reološki zakoni ponašanja kamene soli bili su predmet izučavanja *Hoeffler-a* (1958), *Schuppe-a* (1961), *Potts-a* i *Hendley-a* (1965) – *sistematizovano kod: Langer, [8]*. Laporci i laporovite stijene se u literaturi, kao predmet izučavanja vremenski zavisnih deformacija – puzanja, pojavljuju sporadično. *Cristescu* prikazuje rezultate jednoosijalnog testa puzanja na glinovitom laporcu u trajanju od 7–8 dana [4]. *Bergues* i *Tomanović* izučavali su puzanje tvrdih laporaca [1], [14] i [15].

Istraživanja vremenski zavisnih deformacija stijena (puzanje) praktičnu primjenu imaju pri analizi različitih naponsko-deformacijskih fenomena u stijenskoj masi, ali je najčešća pri analizi stabilnosti i deformacija oko tunelskih otvora. Mjerenjem konvergencije radijalnih deformacija konture tunelskog otvora, s jedne strane, ocjenjuje se stepen uspostavljenog balansa između sila u stijenskoj masi i podgradnoj konstrukciji, a s druge strane – prethodnim analizama procjenjuju se ukupne vremenske deformacije koje će se desiti oko tunelskog otvora ([2], [3], [13], [10], [11], [12]).

stress and temperature, can be a cause of the creep deformation. This effect, known as hydraulic weakening in literature, was among first ones identified by *Griggs* and *Blacic* (1965) and *Griggs* (1967). Effects of air humidity on the rock salt specimens at creep test were studied by *Hunsche* and *Shulze* (1996). A significant impact on the rock salt creep was identified in case when air humidity varied within range of 0-65%. The up to date literature records no proof of any significant impact of air humidity on the creep behaviour of other rocks (systematised at: *Cristescu* [4]). Apparatus and procedures used in the course of testing should enable separation of total time-dependent deformation, which results from the stress change from other components of time-dependent deformations which may occur within the rock over time (shrinkage due to moisture change, temperature change etc.).

In the early 60s, more consideration was given to the studying of a rock creep following the pioneering works of *Michelson* (1917), who carried out torsion tests of rock (by example of metal testing). The beginnings of the rock creep studies are marked by problems related to the testing technique interpretation of test results. Uniaxial compression creep tests were carried out on granite, marble and salt by many researchers such as *Evans* and *Wood* (1937). *Nichihara* (1958), *Hardy* (1959, 1966) and *Price* (1964) studied creep behaviour of sediment rocks (*systematised at: J. C. Jaeger et al., [7]*).

In the 60s and 70s of the last century, a great number of uniaxial and three-axial compression tests of rock salt was carried out at the BGR (BGR - Bundesanstalt für Geowissenschaften und Rohstoffe - Federal Institute for Geosciences and Natural Resources) *Gimm* (1968), *Dreyer* (1974) and *Baar* (1977) carried most of the creep tests of rock mass in situ in the rock salt mines. Based on the results of convergence measurements in the corridors of the rock salt mine, rheological behaviour of soft rock became a subject of research performed by *Hoeffler* (1958), *Schuppe* (1961), *Potts* and *Hendley* (1965), (systematised at: *Langer, [8]*). The literature records only sporadic occurrences of the marl and marlstone in terms of studying of the time-dependent deformations (creep). *Cristescu* (1993) has presented results of the uniaxial compression creep test of clayish marl carried out over the time interval of 7-8 days [4]. *Bergues* and *Tomanovich* studied creep behaviour of hard marls [1], [14] and [15].

Research of time-dependent rock deformations (creep) finds its practical application in analysis of different strain-dependent deformation phenomena in rock mass, yet it is mostly applied for the purposes of analysis of stability and deformations in the rock around the tunnel opening. Measurement of convergence of radial deformations of the tunnel opening contour enables to assess the achieved balance degree between the forces in rock mass and support system on one side, while on the other side, preliminary analyses are used to estimate total time-dependent deformations that may occur in the rock around the tunnel opening ([2], [3], [13], [10], [11], and [12]).

2 UREĐAJI ZA ODRŽAVANJE KONSTANTNOG NAPONSKOG STANJA PRI TESTOVIMA PUZANJA NA MEKOJ STIJENI

Za test puzanja, odnosno održavanje konstantnog opterećenja, do danas su korišćene dvije dominantne vrste uređaja: ramovi s primjenom poluga sa okačenim („mrtvim“) teretom i uređaji s hidrauličkim servo-kontrolisanim silama. Prednost uređaja s „mrtvim“ teretom jeste to što su jednostavne konstrukcije i pouzdani u toku dugog perioda, a prednost hidrauličkih sistema je što su malih gabarita. Za jedan broj testiranja korišćeni su i nešto manje pouzdani uređaji koji su zahtijevali manuelnu korekciju sile u toku vremena (dotezanjem matice i/ili opruge).

Poseban problem pri testu puzanja predstavlja konstruisanje ramova za održavanje konstantnog naponskog stanja na modelima, kao što su modeli kojima se simulira tunelski iskop pri dvoosnom stanju napona. Za realizaciju eksperimentalnog laboratorijskog istraživanja puzanja laporca koji se prezentuje u ovom radu, korišćeni su posebno konstruisane nestandardne aparature i uređaji za održavanje konstantnog naponskog stanja (prema nacrtima autora ovog rada). Za pojedine segmente istraživanja korišćena je i standardna laboratorijska oprema kao što su: laboratorijske prese, mjerači sile, deformetri i tako dalje. U nastavku teksta, opisuju se uređaji i instrumenti korišćeni za test puzanja laporca pri jednoosijalnom i biaksijalnom stanju napona.

2.1 Uređaj sa okačenim („mrtvim“) teretom za jednoosijalno opterećivanje

Za održavanje konstantnog opterećenja na jednoosijalnim prizmatičnim uzorcima laporca dimezija 15x15x40 cm korišćen je uređaj s dvostrukom polugom, kapaciteta 750 kN (slika 1 i slika 2). Okačeni teret na kraju poluge 2 prenosi se na polugu 1 i aplicira na uzorak kao sila pritiska. Zavisno od položaja uzorka duž poluge 1, težina tega multiplicira se od 10 do 150 puta. Za ispitivanje uzoraka laporca poprečnog presjeka 15x15 cm i jednoosijalne čvrstoće oko 8.8 MPa, optimalan položaj uzoraka je pri multipliciranju „mrtvog“ opterećenja za oko 100 puta.

Važna faza pri postavljanju testa puzanja jeste i centrisanje opterećenja. Neophodno je da se opterećenje na uzorak nanese što ravnomjernije, tako da početna deformacija uzorka indukuje minimalne inklinacije poprečnog presjeka. Postojla sa četiri zavrtnja omogućavala su da se uzorak podiže naviše, kako bi se zatvorili svi zazorci između pojedinih djelova poluga i rama i mjerača sile (vidi sliku 2.b) i obezbijedile približno iste deformacije na sve četiri strane prizmatičnih uzoraka.

Svaki uređaj od šest uređaja za jednoosijalne testove puzanja opremljen je prstenastim mjeračem sile kapaciteta 250 KN, posebno konstruisanim i proizvedenim za ovo eksperimentalno istraživanje puzanja laporca. Opterećenje na uzorak aplicirano je odozgo preko prstenastog mjerača sile, koji je istovremeno poslužio i kao zglob (slika 1 i 2.a). Na taj način, efekti dodatne ekscentričnosti opterećenja, uzrokovane rotacijom poluge 1 u toku spuštanja „mrtvog“ tereta, svedeni su na zanemarljive vrijednosti.

2 DEVICES FOR MAINTAINING CONSTANT STRESS STATE AT CREEP TESTING OF SOFT ROCK

For the creep test, that is for maintaining the constant load, two dominant device types have been used up to date - lever arm system in dead weight creep frame and hydraulic servo control compression testing device. The advantage of the dead weight creep test device is its simple structure and reliability over a long time period, while the advantage of hydraulic system lies in its small overall size. For a certain number of tests devices of somewhat lower level of reliability have been used, requiring adjustments of compression in the course of time (additional nut and/or lever tensioning).

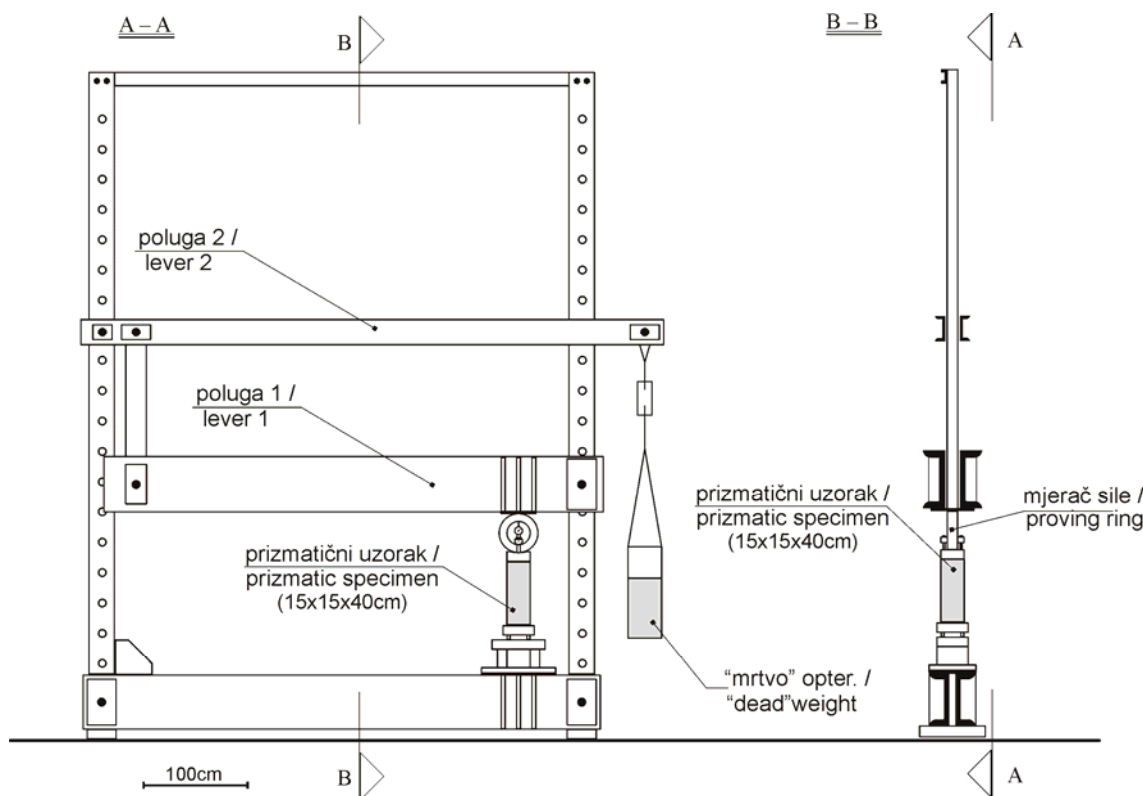
Particular issue at creep test arises with a view to the design of frames for maintaining of the constant stress state in models, such as the model for simulation of tunnel excavation at biaxial stress state. A specially designed non-standard apparatus and devices for maintaining stress state made by the author of this paper have been used for the purpose of experimental laboratory testing of the marl creep presented in this paper. Certain segments of the research involved the use of standard laboratory equipment as well - laboratory presses, dynamometers, deformeters etc. The text below describes devices and instruments that have been used for the creep test of marl at uniaxial and biaxial stress state.

2.1 Device with hanged (dead) weight for uniaxial compression

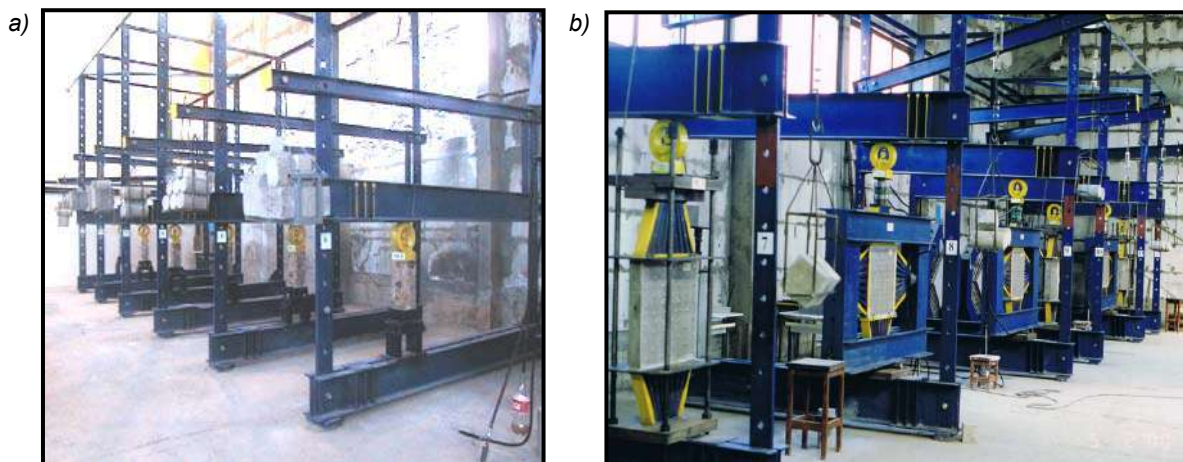
For maintaining the constant load on uniaxial prismatic marl specimens of 15x15x40cm in size, the two-lever arm device has been used, with capacity of 750kN, Figure 1 and Figure 2. Weight hanged at the end of the lever arm 2 is transmitted to lever arm 1 and then applied to the specimen acting as a compression. Depending on the position of the specimen along the lever arm 1, the weight is multiplied by 10 to 150 times. For testing of marl specimen of average section 15x15cm and uniaxial compression strength of approximately 8.8 MPa, an optimum position of the specimen is achieved when dead weight is multiplied by approximately 100 times.

An important phase in setting-up the creep test is centring the weight. It is required to apply the load onto the specimen as evenly as possible so to enable the initial deformation of the specimen to induce minimum inclinations of the cross section. Stands with four bolts provided for lifting the specimen upwards in order to close all the gaps between certain lever arms and frame and dynamometer (see Figure 2.b) and enable approximately even deformations at all four sides of prismatic specimen.

Each of the six used devices for uniaxial compression creep tests is equipped with ring dynamometer with capacity of 250kN which was specially designed and constructed for the purposes of this experimental research of the marl creep behaviour. The load was applied to the top of the specimen by means of ring dynamometer which at the same time served as a hinge (Figure 1 and Figure 2.a). In this way, the effects of the additional eccentricity of the loading, caused by rotation of lever arm 1 during lowering of the dead weight, have been reduced to negligible values.



Slika 1. Dispoziciona šema uređaja (rama) za jednoaksijalno opterećivanje
Figure 1. Layout of device (frame) for uniaxial compression



Slika 2. Uređaji za: a) jednoaksijalno opterećivanje; b) dvoosno opterećivanje
Figure 2. Devices for: a) uniaxial compression; b) biaxial compression

2.2 Uređaj sa okaćenim („mrtvim”) teretom za biaksijalno opterećivanje

Za održavanje konstantnog opterećenja na pločastim biaksijalno opterećenim uzorcima dimenzija 60x60x10 cm korišćen je uređaj s dvostrukom polugom, kapaciteta 1500 kN (slika 2b i slika 3), istog sistema prenošenja vertikalnih sila, kao i uređaj korišćen za jednoaksijalno opterećivanje. Trapezasti čelični elementi postavljeni su

2.2 Device with hanged (dead) weight for biaxial compression

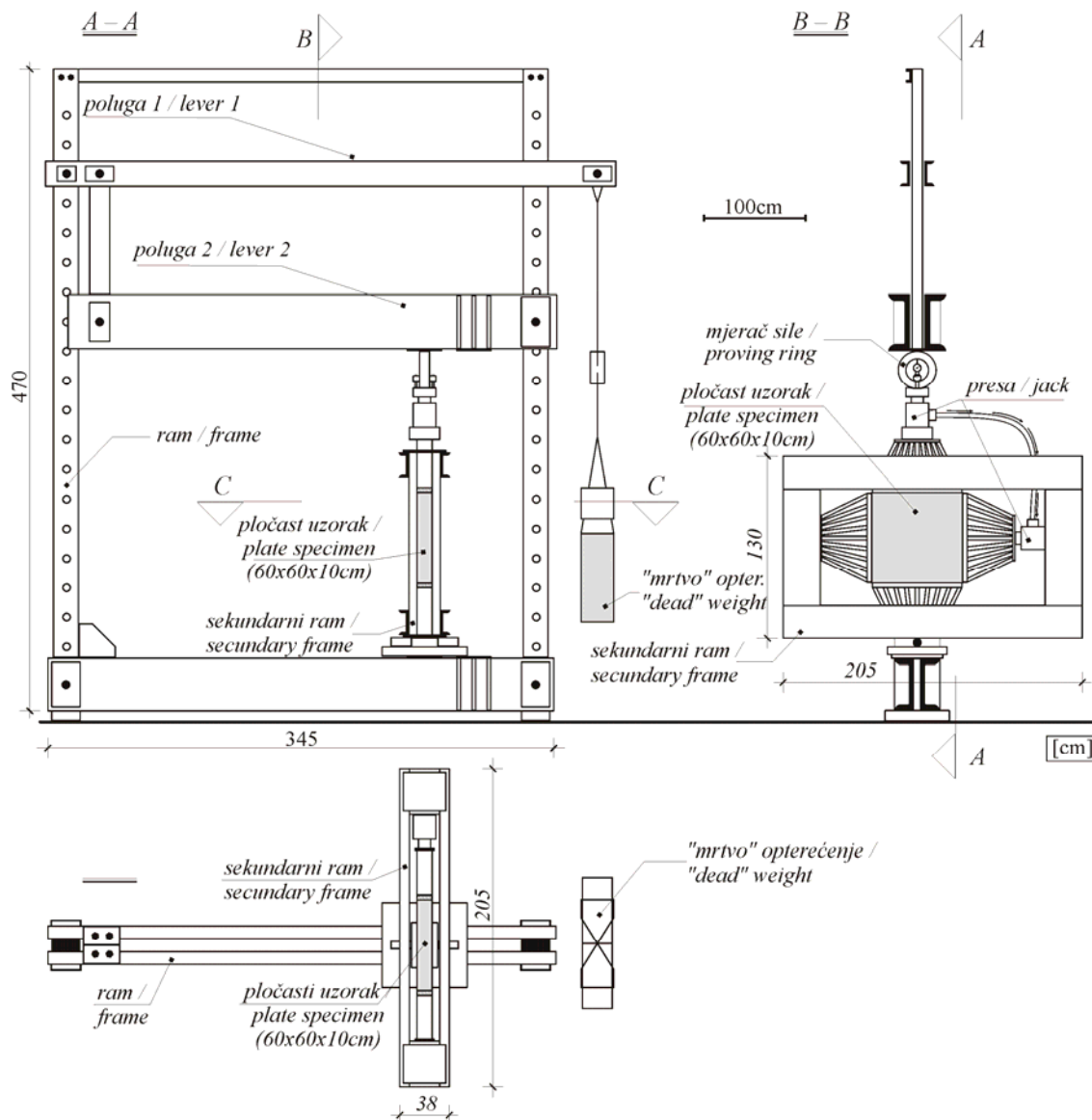
For maintaining the constant load on biaxial plate specimens of 60x60x10cm in size, the two-lever arm device has been used, with capacity of 1500kN, Figure 2b and Figure 3, with the same system for transmission of vertical load as used in case of the device for uniaxial compression. Trapeze-shaped steel elements were placed

između rama i uzorka da bi se obezbijedilo ravnomjerno prenošenje opterećenja s rama na uzorke širine 60 cm i debljine 10 cm.

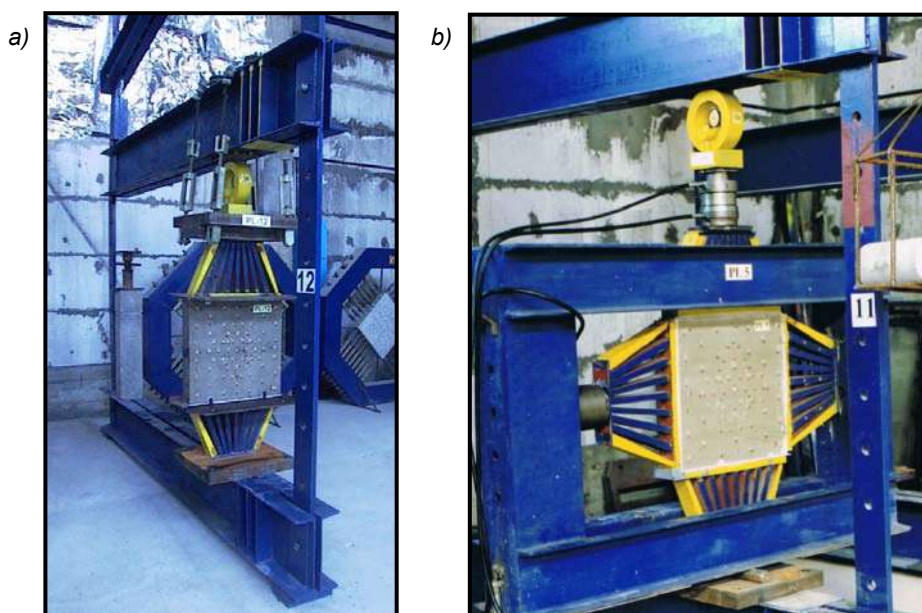
Za apliciranje horizontalnog opterećenja na pločast uzorak, korišćen je sekundarni zatvoreni ram zglobno oslonjen na postolje osnovnog uređaja za vertikalno opterećivanje i dvije hidrauličke prese povezane međusobno kao spojeni sudovi. Jedna presa postavljena je vertikalno između mjerača sile i prelaznog vertikalnog čeličnog trapezastog elementa (slika 3, presjek B-B), tako da prima vertikalno opterećenje i generiše pritisak u ulju (nanošena je aktivna sila na klip prese). Druga presa postavljena je horizontalno u zatvorenom sekundarnom ramu, tako da klip prese vrši pritisak na prelazni horizontalni trapezasti čelični element (kao što je prikazano na slikama 3 i 4. b). Ovaj jednostavan hidraulički sistem, bez servo-kontrole, primijenjen za nanošenje horizontalnog pritiska, nema gubitka sile u toku vremena.

between the frame and the specimen to enable even transmission of load from frame to the specimens of 60cm in width and 10 cm in thickness.

Application of horizontal load on the plate specimen involved the use of a secondary closed frame hinge supported against the stand of the main device for vertical loading and two hydraulic presses interconnected following the law of connecting tanks. One press was placed vertically between the dynamometer and transitional vertical trapeze-shaped steel element (Figure 3, section B-B), so to transmit the vertical load and generate oil pressure (active load was applied to the press cylinder). The second press was placed horizontally in the secondary frame, with the press cylinder generating pressure onto the horizontal trapeze-shaped steel element, as illustrated in Figure 3 and Figure 4b. This simple hydraulic system without servo control that was used for application of horizontal compression has no loss of force over the time.



Slika 3. Dispoziciona šema uređaja za biaksijalno opterećivanje
Figure 3. Layout of device for biaxial compression



Slika 4. a) Ram za jednoaksijalno opterećivanje pločastih uzoraka; b) Aparatura za biaksijalno opterećivanje; pločast uzorak PL-15, prva faza testa (odnos $Ph/Pv=1.0$)

Figure 4. a) Frame for uniaxial compression of plate specimens; b) Apparatus for biaxial compression; plate specimen PL-15, Phase 1 of test (ratio $Ph/Pv=1.0$)

Primjenom presa u paru, s različitim površinama klipova, moguće je aplicirati različite odnose horizontalne i vertikalne sile. Pritom, u toku vremena konstantnim se održavaju aplicirane sile i njihov međusobni odnos. U ovom eksperimentu korišćena su tri seta presa sa odnosom površina klipa horizontalne – bočne prese prema površini klipa vertikalne prese: 0.3, 0.5 i 1.0. Svaki uređaj od šest uređaja za testove na pločastim uzorcima opremljen je prstenastim mjeracem sile kapaciteta 350 kN. Na kontaktu između čelične konstrukcije, tj. prelaznih trapezastih elemenata i uzoraka postavljena je dvostruka folija od teflona radi eliminisanja kontaktnog trenja. Za jednoaksijalno opterećivanje pločastih uzoraka, korišćen je ram za nanošenje i održavanje vertikalnog opterećenja prikazan na slici 4. a (na fotografiji pločasti uzorak, PL-12).

2.3 Uređaj za triaksijalno opterećivanje

Konvencionalni test triaksijalne kompresije, pri kontrolisanim silama (pritiscima), sproveden je u aparaturi u kojoj su aksijalna sila i bočni pritisak aplicirani uz primjenu dva uređaja s dvostrukom polugom (konstruisano prema nacrtima autora ovog rada [slika 5]). Hook-ova triaksijalna ćelija postavljena je u jedan ram za opterećivanje kojim je nanošena aksijalna sila na uzorak (desni ram na slici 5). U drugi ram za opterećivanje postavljena je obična hidraulična presa koja je fleksibilnim crijevom povezana s triaksijalnom ćelijom (spojeni sudovi). Apliciranjem sile na klip prese, indukovan je željeni pritisak u ulju, odnosno bočni pritisak u triaksijalnoj ćeliji. Drugi izvod za ulje na triaksijalnoj ćeliji korišćen je za priključenje ćelije za mjerenje pritiska.

Using pair of presses with different cylinder surfaces, different ratios of horizontal and vertical load can be applied. Here, the applied loads and load ratio are maintained constant over the time. This experiment involved use of three sets of presses with the ratio of cylinder surface of the horizontal-lateral press to the cylinder surface of the vertical press: 0.3, 0.5 and 1.0. Each of the six used devices for creep tests of plate specimens is equipped with ring dynamometer with capacity of 350KN. At the contact point between the steel structure, i.e. transitional trapeze-shaped elements and specimens, a double teflon liner was placed to eliminate any contact friction. Frame for applying and maintaining the vertical load illustrated in Figure 4.a (photo of plate specimen PL-12) was used for uniaxial compression of plate specimens.

2.3 Three-axial loading device

A conventional strain-controlled three-axial compression test, is conducted in the apparatus applying axial load and lateral strain by means of two double-lever devices designed by the author of this paper, Figure.5. Hook's three-axial load cell is placed in one load frame that is used to apply axial load on the specimen (right frame in Figure 5). A standard hydraulic press is placed in the second load frame, connected to the three-axial cell by a flexible tube (interconnected tanks). Application of the load on the press cylinder induces the preferred oil compression, i.e. the lateral strain in the three-axial cell. The second oil outlet on the three-axial cell is used to connect the compression measuring cell.

Axial load and lateral strain are controlled manually

Aksijalna sila i bočni pritisak manuelno su kontrolisani dodavanjem tegova, a na osnovu mjerenja sile i pritiska primjenom ćelije za mjerenje sile i ćelije za mjerenje pritiska uz očitavanje na „mjernom mostu“. Primijenjena aparatura pokazala je lako održavanje konstantnog bočnog pritiska u toku testa i jednostavno rukovanje pri testu s kontrolisanim silama. Takođe, aparatura omogućava jednostavno izvođenje testova puzanja u konvencionalnoj triaksijalnoj ćeliji.

by adding weight and based on measurements of the load and strain by means of the compression measuring cell and reading of results on the "measuring bridge". The applied apparatus proved to provide the easy maintaining of the constant lateral strain during the test and that it is simple to operate in case of the strain-controlled test. Moreover, the apparatus enables simple performance of the creep tests in the conventional three-axial cell.



Slika 5. Aparatura za triaksijalni test
Figure 5. Three-axial compression test apparatus

3 MJERENJE SILE I DEFORMACIJE

Instrumenti i uređaji za test puzanja moraju da zadovolje dva osnovna uslova: a) održavanje konstantnog opterećenja u toku izvođenja testa; b) instrumenti za mjerenje deformacija treba da imaju mogućnost mjerenja deformacije od početka testa do nekog vremena t (nekoliko dana, mjeseci ili godina).

3.1 Mjerenje sile

Mjerenje sile pri nanošenju opterećenja na uzorke pri kratkotrajnim testiranjima (ili testovima puzanja u trajanju od nekoliko sedmica) i mjerenje sile za testove puzanja koji traju nekoliko mjeseci ili godina zahtijevaju potpuno različitu mjernu tehniku. Tako je pri kratkotrajnim testovima moguće koristiti standardne električne mjerače sile. Međutim, pri dugotrajnim testovima puzanja, mehanički mjerači sile imaju značajne prednosti u poređenju sa električnim, u pogledu kompleksnosti opreme, sistema za održavanje stalnog električnog napona, opreme za akviziciju podataka i cijene.

3 MEASUREMENT OF FORCE AND DEFORMATION

Instrumenti and devices for creep test should meet two basic requirements: a) maintaining constant load while the creep test is carried out; b) instruments for deformation measurement should provide deformation measurements from the commencement of the test to time t (several days, months or years).

3.1 Force measurement

Force measurement of load application on specimens at short-time tests (or creep tests with the duration of several weeks) and measurement of force for creep tests the duration of which is several months or years require completely different measurement technique. For the short-time tests standard electronic dynamometers can be used. However in the case of long-time creep tests, the mechanical dynamometers are far more suitable compared to the electronic dynamometers in terms of the complexity of equipment, system for maintaining constant electrical tension, data acquisition equipment and costs.

Za mjerenje sile koja se aplicira na uzorak i njenu kontrolu u toku testa puzanja, pri eksperimentalnom istraživanju puzanja laporca, konstruisani su prstenasti mjerači sile (prema nacrtima autora ovog rada). Mjerač sile sastoji se od čeličnog prstena, komparatera tačnosti 1/1000 mm i postolja (kako je prikazano na slici 6). Mjerači sile kapaciteta 250 kN korišćeni su za mjerenje sile jednoaksijalno opterećenih prizmatičnih uzoraka, a kapaciteta 350 kN korišćeni su za mjerenje sila kod pločastih biaksijalno opterećenih uzoraka. Različiti kapacitet mjerača sile postignut je povećanjem širine prstena, koja je iznosila 60 ili 80 mm.

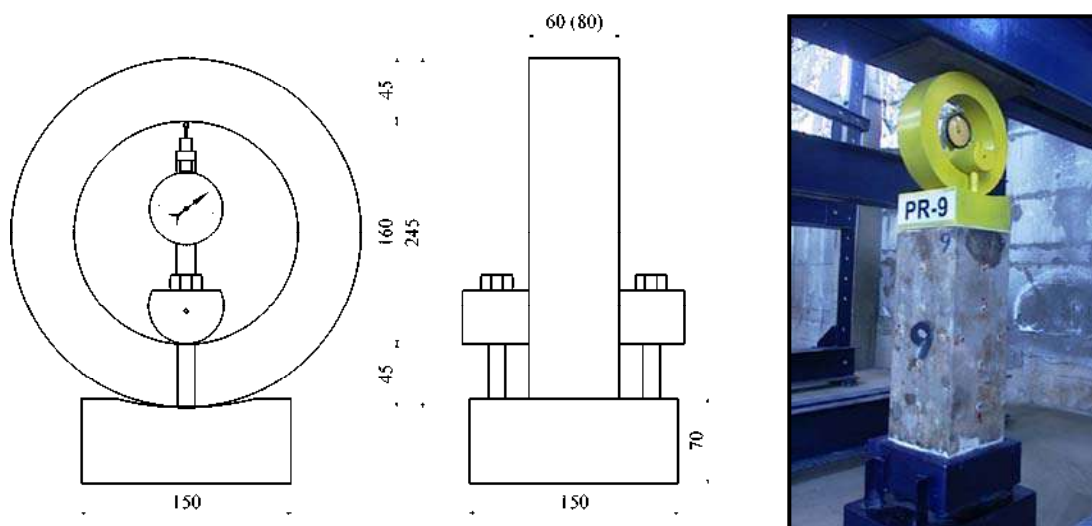
Svaki mjerač sile testiran je u laboratorijskoj presi i definisan je koeficijent proporcionalnosti između ugiba prstena i na prsten aplicirane sile. Veza ugib–sila jeste linearna: $F=k*u$, gdje je: F – vertikalna sila, u – vertikalni ugib prstena. Koeficijent proporcionalnosti k određen je metodom najmanjih kvadrata za svaki proizvedeni mjerač sile i kretao se u granicama od 462.00 do 491.04.

Test puzanja trajao je više od jedne godine, uz varijaciju temperature od 10°C do 32°C. Radi toga, izvršena je provjera uticaja promjene temperature na tačnost instrumenta. U opsegu temperature od 10°C do 40°C, ustanovljena je greška uzrokovana temperaturnim promjenama manja od 0.2%, a ukupna greška mjerenja u toku jedne godine je ispod prihvatljive granice od 1% za ovu vrstu testa [4]. Mehanički instrument obezbijedio je mjerenje sile u toku nanošenja opterećenja u inkrementima, ali i kontrolu sile u toku testa puzanja, u trajanju duže od jedne godine, na vrlo jednostavan i pouzdan način. Nakon završetka testa, kazaljka komparatera, ugrađenog u mjerač sile, vratila se na nulu – što je siguran pokazatelj da je mjerni prsten u toku čitavog testa bio elastično opterećen.

For measurement of the force that is applied to the specimen and control of such force during the creep test, in the course of experimental research of the marl creep behaviour, the ring dynamometers have been designed by the author of this paper. The dynamometer consists of a steel ring, comparator with the accuracy of 1/1000mm and stand pedestal as illustrated in Figure 6. Dynamometers with the capacity of 250kN were used for force measurement in case of uniaxially compressed prismatic specimens, while dynamometers with the capacity of 350kN were used for force measurement in case of biaxially compressed specimens. Different capacities of dynamometer have been achieved by increase in width of the ring which was 60 or 80 mm.

Each dynamometer was tested in the laboratory press with the defining of the coefficient of proportionality between the ring deflection and on the ring of the applied force. The deflection-force relation is linear: $F=k*u$, where: F - vertical force, u -vertical deflection of the ring. The coefficient of proportionality k was determined by the least squares method for each constructed dynamometer and its values ranged between 462.00 and 491.04.

The creep test lasted for a period of over one year with temperature variations from 10 oC to 32oC. Therefore, the accuracy of the instrument was tested against the effect of temperature variations. For the temperature range from 10oC to 40oC, a measurement error of 0.2% has been identified due to the changes in temperature, while total measurement error for one year period was beyond the acceptable limit of 1% for this type of test [4]. A mechanical instrument enabled very simple and reliable force measurement during the incremental application of load, and also the control of force during the creep test for a period of over one year. Upon test completion, the hand of the comparator integrated in the dynamometer returned to zero position, which indicated with certainty that the measuring ring remained within the range of elastic stress.



Slika 6. Prstenasti mjerač sile kapaciteta 250 kN
Figure 6. Ring dynamometer of capacity 250kN

3.2 Mjerenje deformacija

Mjerenja dilatacija izvedena su mehaničkim deformetrom tipa „Pfender“ (slika 7 – očitavanje pomjeranja 1/1000 mm na mjernoj bazi 100 mm) i pokazala su bolje rezultate pri testu puzanja, u poređenju s mjernim trakama, u pogledu tačnosti mjerenja u toku dugog intervala. Nakon dugotrajnih testiranja, ustanovljena je greška mjerenja ovog tipa uređaja 2-3/1000 mm. Mjerena promjena rastojanja između repera u toku testa puzanja na uzorcima od laporca kretala su se od 0.5 do 1 mm. Imajući u vidu ostvarene dilatacije, greška mjerenja od 3/1000 mm može se ocijeniti kao prihvatljiva.



Slika 7. Mjerenje deformetrom tipa „Pfender“ na pločastom uzorku
Figure 7. Measurement of deformations in plate specimen by deformer type "Pfender"

4 TEHNIKA FIKSIRANJA MJERNIH TAČAKA I MJERENJE DEFORMACIJA

Prizmatični i pločasti uzorci laporca, glavnih serija mjerenja, opremani su mrežom mjernih mjesta za mjerenje promjene dužine između mjernih baza mehaničkim deformetrom tipa „Pfender“. Mjerenje ovim deformetrom zahtijeva lijepljenje mjernih tačaka (mesingana pločica sa utisnutom čeličnom kuglicom) direktno na uzorak. Pritom, mek stijenski materijal i prirodna vlažnost uzorka pričinjavaju dosta poteškoća. Nakon proba učinjenih s nekoliko vrsta ljepkova i načina pripreme podloge na uzorku, ustanovljeno je da fiksiranje mesinganih pločica – mjernog mjesta ljepljenjem tipa „Hotinger-X60“ i lagano hrapavljenje podloge tj. površine uzorka, daju najbolje rezultate. Ovako fiksirana mesingana pločica ostaje adekvatno fiksirana za uzorak u toku perioda mjerenja od godinu dana i pri više desetina serija mjerenja.

4.1 Prizmatični uzorci

Svi prizmatični uzorci laporca dimenzija 15x15x40 cm opremljeni su mjernim tačkama koje su omogućile mjerenje deformacija u pravcu podužne ose uzorka i deformacija u porečnom pravcu (prikazano na slici 8). Mjerni opseg mehaničkog deformetra tipa „Pfender“ jeste 1 mm, a odabrana mjerna baza instrumenta iznosi oko 100.4 mm. Time je bilo moguće izmjeriti dilataciju od

3.2 Deformation measurement

Measurements of dilatations that were performed using mechanical deformer type Pfender, Figure 7 (reading displacements 1/1000mm on measuring base of 100mm) showed better results at creep test, compared to strain gauge with a view to the measurement accuracy over a long time interval. After long lasting tests, the measurement error of 2-3/1000mm was identified for this type of device. Measured changes in distance between the reference points during the creep testing of marl varied from 0.5 to 1mm. Taking into consideration the occurred dilatations, measurement error of 3/1000mm can be considered as acceptable

4 TECHNIQUE OF AFFIXING THE MEASURING POINTS AND DEFORMATION MEASUREMENT

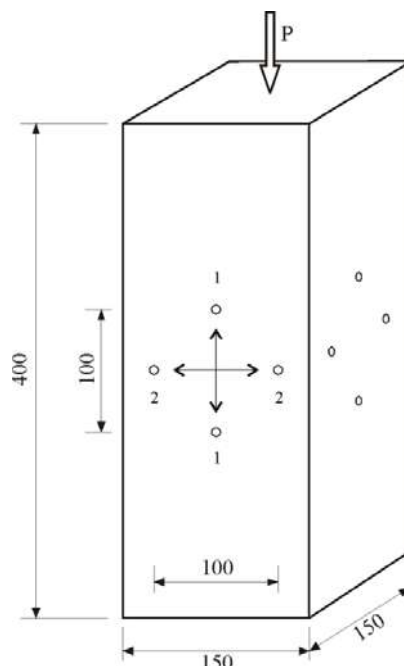
Prismatic and plate marl specimens of the main measurement series were provided with the network of measuring points for measuring the change in length between measuring bases by mechanical deformer type "Pfender". Measuring with this deformer requires the measuring points (brass plate with inlaid steel ball) to be affixed directly to the specimen. Soft rock material and natural moisture of the specimen caused lot of difficulties hereto. Upon trial attempts using several types of adhesives and methods of base preparation on the specimen, it was observed that fixing of brass plates - measuring points by means of adhesive type "Hotinger-X60" and slight coarsening of the base i.e. surface of the specimen provided the best results. The brass plate fixed in this way remained properly fixed to the specimen for a measurement period of one year even in the case of several tenths of measurement series.

4.1 Prismatic specimens

All prismatic specimens of 15x15x40cm in size were provided with measuring points, which enabled measurement of deformations in the direction of the longitudinal axis of the specimen and deformations in the horizontal direction as illustrated in Figure 8. Measuring range of the mechanical deformer type "Pfender" is 1mm, and selected measuring base of the instrument is

8 do 9 promila. Pripremljeno je osamnaest prizmatičnih uzoraka – šest uzoraka probne serije i dvanaest uzoraka glavne serije, od kojih je na šest sproveden test puzanja u trajanju oko godinu dana, a ostali su testirani na kratkotrajno opterećenje do loma [15].

about 100.4mm. This enabled measurement of a dilatation of 8-9 per mils. Eighteen specimens were prepared: 6 specimens of trial series and 12 specimens of main series, 6 of out of which were subject to creep testing for a period of about one year, while the remaining specimens were tested against short-time loading until failure occurred [15].



Slika 8. Prizmatični uzorak, šema mjernih mjesta
Figure 8. Prismatic sample, layout of measuring points

4.2 Pločasti uzorci

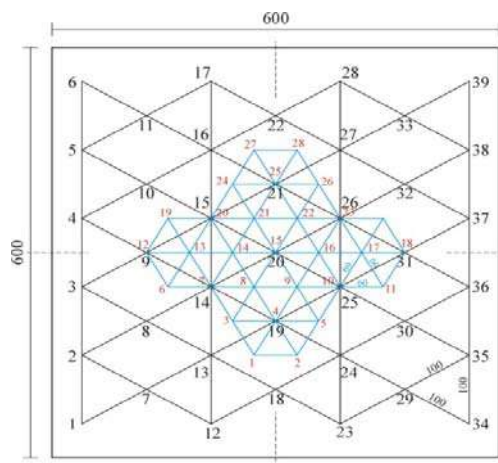
Svi pločasti uzorci opremljeni su sa po dvije mreže mjernih tačaka, sa obje strane uzorka, koje su omogućile mjerenje polja deformacija u ravni ploče. Mreža baze mjerenja 100 mm postavljena je na čitavoj površini uzorka, a mreža baze mjerenja 60 mm formirana je u centralnom dijelu uzorka (prikazano na slici 9). Gušćom mrežom mjernih mjesta obuhvaćen je uži dio oko otvora koji će se izbušiti u drugoj fazi testa. Mjerenje deformacije po stranama trouglova mreže omogućuje definisanje deformacije u bilo kom željenom pravcu.

Postavljanje mjernih baza za mrežu trouglova predstavlja izuzetno komplikovan zadatak zbog malog mjernog opsega instrumenta (1mm). Da bi se mogla obavljati mjerenja, sve tačke su međusobno morale biti postavljene na rastojanju 100 mm \pm 0.2 mm. Nakon promjene naponskog stanja, mjerene su deformacije puzanja na mreži mjernih tačaka (u sve tri faze testa) i to nakon 1, 6 i 24 sata od nanošenja opterećenja, zatim nakon tri dana i sedam dana, a u daljem periodu – svakih petnaest dana. Intervali mjerenja odabrani su tako da razlike prethodne i tekuće mjerene deformacije budu približno jednake.

4.2 Plate specimens

Every plate specimen was provided with two networks of measuring points on both sides of the specimen, which enabled measuring of deformation field in the plane of the plate. Network of the measuring base of 100mm was placed over the total surface of the specimen, while the network of the measuring base of 60mm was formed in the central part of the specimen, as illustrated in Figure 9. A network with higher density of measuring points covered the immediate area around the opening which would be bored in the phase 2 of the test. Measurement of deformation on the sides of triangles of the network enables the deformation to be determined in any preferable direction required.

Setting the measuring bases for the network of triangles is a quite complicated task due to the small measuring range of the instrument, this being 1mm. It was required for all points to be set at the mutual distance of 100mm \pm 0.2mm for measurement purposes. Upon the change of stress state, creep deformations were measured on the network of measuring points a (in all three phases of the test), within 1, 6 and 24 hours after application of the load, then after 3 and 7 days and on every 15 days in the further period. Measuring intervals were selected to ensure approximately even differences in previously and currently measured deformation.



Slika 9. Pločasti uzorak: a) šema mjernih mjesta; b) uzorak za kompenzaciona mjerenja
Figure 9. Plate specimen: a) layout of measuring points; b) specimen for compensation measurements

4.3 Triaksijalni uzorci

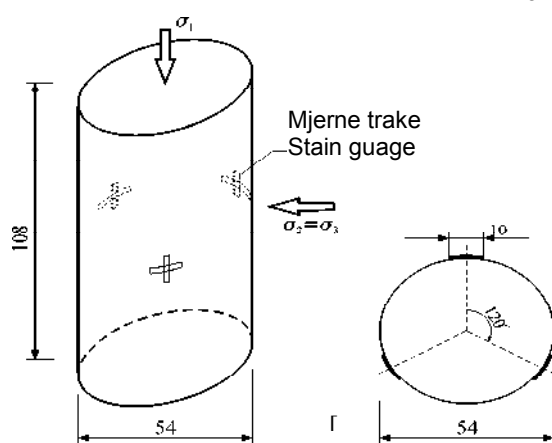
Za mjerenje deformacija uzoraka u konvencionalnom triaksijalnom testu, u standardnoj Hook-ovoj ćeliji, upotrijebljene su mjerne trake i rozete koje mjere deformacije u dva upravna pravca (proizvođač: TML-Japan). Za lijepljenje rozeta korišćeno je ljepilo P2 (TML-Japan), koje ima veliku rastegljivost, što omogućava mjerenje velikih dilatacija kakve su očekivane na predmetnom materijalu.

Svaki uzorak opremljen je sa po tri rozete ili trake, postavljene u sredini visine uzorka, pod centralnim uglom 120° , posmatrano u poprečnom presjeku uzorka (kako je prikazano na slici 10). Za povezivanje traka s „data logger-om“ korišćen je trakasti kabl debljine oko 0.3 mm. Nakon postavljanja kabla i povezivanja s rozetama, preko uzorka je navlačena zaštitna membrana. Pripremljena su i ispitana ukupno dvadeset četiri uzorka u triaksijalnom aparatu, uz mjerenje deformacija, a još desetak uzoraka dovedeno je do loma bez mjerenja deformacija (uz mjerenje aksijalne sile loma i bočnog pritiska) [16].

4.3 Tree-axial specimens

Measurement of the specimens' deformations by conventional tree-axial test in the standard Hook's cell included the use of a strain gauge and rosettes for deformation measurement in the two normal directions (accuracy 10-3mm, producer TML - Japan). Glue (TML - Japan), with a high deformation power, was used for the gluing of the rosettes, which enabled the measurement of the high strain expected in the examined material.

Each specimen was equipped with tree rosettes or a strain gauge set in the middle of specimen height under the central angle of 120° , seen through the cross-section of the specimen, as shown in Figure 10. A stripe cable, about 0.3mm thick, was used to connect the strain gauge with the "data logger". After the cable was set and the rosettes were connected, a protective membrane was put over the specimens. A total of 24 specimens were prepared and examined in the tree-axial device along with deformation measurement and about ten more specimens were led to failure without any deformation measurement (with a measurement of the axial stress of the failure and lateral pressure) [16].



Slika 10. Cilindrični uzorak za konvencionalni triaksijalni test;
a) dispozicija mjernih rozeta; b) rozeta postavljena na uzorak
Figure 10. Cylindrical specimen for a conventional tree-axial test;
a) disposition of measurement rosetta; b) rosettes attached to the specimen

5 NEOPTEREĆENI UZORCI ZA MJERENJE DEFORMACIJE SKUPLJANJA I DEFORMACIJE OD PROMJENE TEMPERATURE

5.1 Osnovne fizičko-mehaničke osobine ispitivanog laporca, mineralni i hemijski sastav

Testovi puzanja sprovedeni su na sivom cementnom laporcu. Prosječna vrijednost suve zapreminske težine ovog laporca, iz kojega su uzorci uzeti, iznosi oko 18.8 kN/m³ (od 17.2 do 20.38 kN/m³), a prosječna pritisna jednoosijalna čvrstoća monolita oko 8.8 MPa. Ispitivani laporac – u pogledu mineralnog sastava – dominantno predstavljaju kalcit (46–48%) i kvarc (12–13%), dok su u okviru glinovite faze – ilit+smektit, montmorijonit, kaolinit, glaukonit, transformisani feldspat i liskun. Prema hemijskom sastavu, sadržaj CaCO₃ je u granicama 48.10–48.30%, dok je sadržaj nerastvornog ostatka (glinovito+kvarc) u granicama 51.03–51.87%.

5.2 Promjene vlažnosti u toku dugotrajnog testiranja

Nakon vađenja iz prirodno vlažne sredine, na sobnoj temperaturi, laporac brzo gubi vlagu. Zbog znatnog sadržaja glinovitih minerala i velike poroznosti, posledica gubitka vlage u uzorcima jeste skupljanje materijala. Pri intenzivnom sušenju i većem stepenu gubitka vlage, skupljanje uzrokuje pojavu pukotina i raspadanje materijala. Deformacije koje se javljaju kao posljedica gubitka vlage tj. skupljanja, imajući u vidu cilj istraživanja, bilo je neophodno svesti na prihvatljiv nivo, kako ne bi imale uticaj na mehaničke karakteristike materijala. Radi redukovanja promjene vlažnosti u toku testa puzanja, nakon postavljanja mjernih baza (pločica), na uzorak je nanošen tanak sloj parafina. Promjena vlage ovom mjerom je znatno redukovana, pa je skupljanje stijenskog materijala, u toku ispitivanja od godinu dana, svedeno na prihvatljiv nivo – od nekoliko procenata.

U toku testova puzanja, pri svakoj seriji mjerenja deformacija, mjereni su temperatura i vlažnost vazduha u laboratoriji u kojoj su rađeni testovi. Vlažnost uzorka određivana je metodom sušenja na temperaturi od 105°C. Prirodna vlažnost uzoraka kretala se od 11 do 12%. Nakon završetka testa puzanja probne serije prizmatičnih uzoraka, koji je trajao tri mjeseca, ustanovljena je prosječna vlažnost od 10.65%, a nakon završetka testa puzanja glavne serije mjerenja, koji je trajao dvanaest mjeseci, izmjerena je prosječna vlažnost 7.40%.

5.3 Uzorci za mjerenje deformacije skupljanja i deformacije od promjene temperature

Pored preduzetih mjera da se spriječi promjena vlage u uzorcima za vrijeme dugotrajnih testova puzanja, dolazi do izvjesne promjene vlage u uzorcima, a time i do deformacije skupljanja uzrokovane gubitkom vlage. Takođe, nije bilo moguće obezbijediti konstantnu temperaturu u laboratoriji u toku godinu dana, te je

5 NON-LOADED SAMPLES FOR MEASUREMENT OF SHRINKAGE DEFORMATION AND DEFORMATION DUE TO TEMPERATURE CHANGE

5.1 Basic physical and mechanical properties of the tested marl, mineral and chemical composition

Creep tests were carried out on gray cement marl. Average value of dry volumetric weight of this marl, which was sampled, is approximately 18.8kN/m³ (from 17.2-20.38 kN/m³), and average uniaxial compression strength of monoliths is about 8.8MPa. In terms to the mineral composition, the marl is represented by calcite (46-48%) and quartz (12-13%), and within the scope of the clayish phase - illite-smectite, montmorillonite, kaolinite, glauconite, transformed feldspar and mica. With a view to its chemical composition, CaCO₃ is within the limits of 48.10 - 48.30%, while the remaining insoluble content (clayish + quartz) is within the limits of 51.03 - 51.87%.

5.2 Change in moisture during long-time testing

Having been extracted from the natural moist environment, marl loses moisture quickly at room temperature. Due to a significant content of clayish minerals and high porosity, the loss of moisture in the specimens results in shrinkage of material. At intensive drying and high moisture loss conditions, the shrinkage causes cracking and decomposition of material. With a view of the objective of the research, it was necessary to reduce deformations resulting from the moisture loss, i.e. shrinkage to the acceptable level to prevent their impact on mechanical properties of the material. For reduction of moisture changes during the creep test, after placing the measuring bases (plates) a thin layer of paraffin was applied to the specimen. This measure enabled significant reduction in moisture change, hence the shrinkage of rock material during the one year period of testing, was reduced to the acceptable level of several percents.

In the course of creep tests, at every deformation measuring series, temperature and air humidity were measured in the laboratory in which the tests were carried out. Humidity of specimen was defined by a method of drying at temperature of 105°C. Natural humidity of specimen varied in the range from 11% to 12%. Upon completion of the creep test of trial series of prismatic specimens, which lasted three months, the measured average humidity was 10.65%. After the completion of creep test main series of measurements, which lasted for 12 months, the measured average humidity was 7.40%.

5.3 Specimens for measurement of shrinkage deformation and deformation due to temperature changes

Despite the measures taken to prevent changes in moisture within samples during the long-time creep tests, certain moisture changes in the samples still appear, and consequently the shrinkage deformations caused by the moisture loss occur. Moreover, it was

temperatura varirala u rasponu od 10 do 32°C, pa su i te temperature promjene uzrokovale izvjesne dilatacije uzoraka.

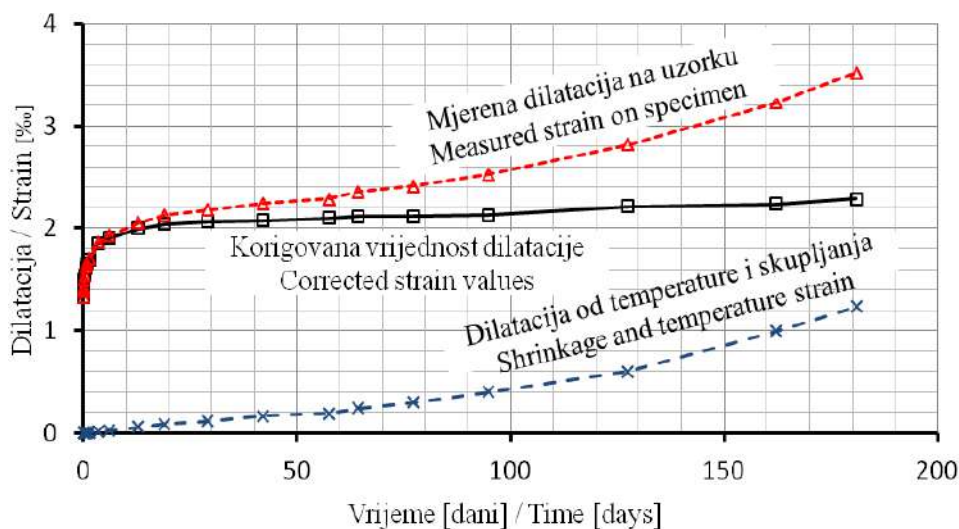
Da bi se razdvojila dilatacija koja je posljedica naponske promjene od dilatacija koje su posljedica promjene vlage i promjene temperature, pripremljeni su dodatni uzorci koji nijesu opterećivani (kompenzacioni uzorci ili uzorci blizanci [slika 9. b]). Ovi uzorci opremljeni su mjernim bazama kao i opterećivani uzorci (prizmatični i pločasti) i čuvani su u vertikalnom položaju u blizini opterećenih uzoraka. Mjerenja na neopterećenim uzorcima (blizancima) vršena su uvijek kada i mjerenja na opterećenim uzorcima. Time je na neopterećenim uzorcima mjerena deformacija koja je posljedica promjene vlažnosti i promjene temperature, a na opterećenim uzorcima ukupna deformacija. Pri kasnijoj analizi rezultata, mjerene vrijednosti deformacija, dobijene pri testu puzanja, korigovane su (umanjene) za vrijednosti deformacije skupljanja i temperature mjerene na kompenzacionim uzorcima.

Na slici 11 prikazani su rezultati mjerenja dilatacije izmjerene na uzorcima pri testu puzanja, dilatacija izmjerena na kompenzacionim uzorcima (skupljanje uzrokovano gubitkom vlage i temperaturnim promjenama) i korigovani dijagram – dobijen kao razlika ove dvije dilatacije. Iz dijagrama se jasno vidi da se korekcijom mjerenih vrijednosti skupljanja dobija glatka kriva puzanja za dug period nakon opterećivanja.

impossible to enable constant temperature at the laboratory for a period of one year, but the temperature varied in the range from 10 to 32°C, which in turn caused certain sample dilatations.

Due to make differentiation between the dilatation caused by a change in stress and dilatation resulting from moisture change and temperature change, additional specimens were prepared to which load was not applied (compensation specimens or twin specimens), Figure 9.b. These specimens were provided with measuring bases as in the case of the loaded specimens (prismatic and plate-shaped) and were kept in vertical position in the vicinity of the loaded specimens. Measurements of non-loaded specimens (twin specimens) were made always when the measurements of loaded specimens were performed. Here, deformations caused by moisture change and temperature change were measured for non-loaded specimens and total deformation was measured for loaded specimens. Thereafter, during the analysis of the results, measured deformation values obtained from the creep test were adjusted (reduced) for the value of the shrinkage deformation and temperature change as measured on the compensation specimens.

Figure 11 illustrates the results of dilatation measured at creep test, dilatation measured on compensation specimens (shrinkage due to moisture loss and temperature changes) and adjusted diagram resulting from the difference between these two dilatations. The diagram clearly indicates that the adjustment of the shrinkage measuring values results in the smooth creep curve for a long period of time after the load application.



Slika 11. Rezultati mjerenja dilatacije na uzorku pri jednoosijalnom testu puzanja na 2.0MPa i dilatacije skupljanja na kompenzacionom uzorku

Figure 11. Results of dilatation measurement on specimen at uniaxial compression creep test at 2.0MPa and shrinkage dilatation on compensation specimen

6 REZULTATI TESTIRANJA

6.1 Test jednoaksijalne kompresije laporca pri kratkotrajnom opterećenju

Jednoaksijalni test na prizmatičnim uzorcima, pri nespriječenom bočnom širenju, kao najjednostavniji za izvođenje i interpretaciju, obično predstavlja početni korak pri istraživanju naponsko-deformacijskog ponašanja čvrstih materijala. Iako s vrlo jednostavnim poljem napona i deformacija, ovaj test daje vrlo jasne materijalne konstante i/ili parametre koji se mogu korisno upotrijebiti i pri analizi veoma složenih naponski zavisnih fenomena.

Ispitivani uzorci laporca, pri jednoaksijalnom testu, pokazuju nelinearnu vezu između napona i deformacija ovog materijala, čak i pri malom nivou napona. Na slici 12 prikazan je reprezentativan $\sigma - \varepsilon$ dijagram laporca, dobijen pri jednoaksijalnom testu. Uzorci su opterećivani jednoaksijalno, u pravcu duže ose prizme, u inkrementima od 1.0 MPa. Deformacije su mjerene u podužnom i poprečnom pravcu. Pri svakom inkreментu sile, deformacije su mjerene jedan minut nakon nanošenja opterećenja. Brzina opterećivanja je oko 3–4 minuta po inkreментu, tako da je uzorak dovođen do loma za oko 30 minuta.

Brojne stijene pokazuju osobinu da imaju različita deformabilna svojstva u različitim pravcima ispitivanja. Ova osobina je prvenstveno posljedica teksture tj. slojevitosti ili orijentacije zrna u mikrokompoziciji stijenskog materijala. Generalno je poznato da stijenski materijal pokazuje veću deformabilnost u pravcu upravnom na slojeve, a manju u pravcima paralelnim ravnima slojevitosti. Ispitivanje naponsko deformacijske veze laporca u različitim pravcima izvedeno je na prizmatičnim uzorcima pri jednoaksijalnom testu s nespriječenim bočnim širenjem. Uzorci su rezani u tri ortogonalna pravca: jedan vertikalni pravac koji odgovara vertikalnoj osi neporemećene stijene „in situ” i u dva upravna horizontalna pravca.

Na dijagramu slike 12, prikazani su rezultati jednoaksijalnih testova (oznaka EZ ukazuje na opterećivanje upravno na slojeve, EX u ravni slojeva; oznaka v i h ukazuje na pravac mjerenja dilatacija; v - u pravcu dejstva opterećenja, a h - u upravnom pravcu). Jasno se uočava veća deformabilnost laporca u pravcu upravnom na slojeve u odnosu na druga dva ortogonalna pravca. Modul elastičnosti (sračunat pri nivou napona 2.0 MPa) u pravcu X dva puta je veći od modula elastičnosti u pravcu Z, $E_z / E_x = 2.0$. Početni moduli elastičnosti u x-y ravni, pokazuju jednake vrijednosti (horizontalna ravan „in situ”). Navedeno deformacijsko ponašanje laporca ukazuje na to da se adekvatni proračuni naponski zavisnih fenomena u laporcima moraju sprovoditi reološkim modelima koji obuhvataju efekte transverzalne izotropije.

6 TEST RESULTS

6.1 Uniaxial compression test of marl at short-term loading

Uniaxial compression test of prismatic samples, with unconstrained lateral expansion, being the simplest to carry out and interpret usually represents the initial step in research of strain-dependent deformation behaviour of rigid materials. Notwithstanding its quite simple field of stress and deformations, this test provides very clear material constants and/or parameters which can have a purposeful application even for an analysis of highly complex strain-dependent phenomena.

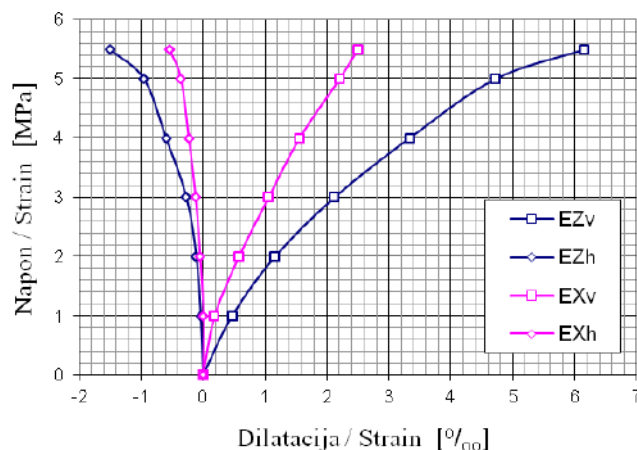
Tested marl specimens, at uniaxial compression test, show non-linear relation between the stress and deformation of this material even at low stress level.

Figure 12 illustrates a typical $\sigma - \varepsilon$ diagram of marl obtained from the uniaxial compression test. Uniaxial load was applied to the specimens in the direction of the longer axis of the prism, in increments of 1.0 MPa. Deformations were measured in the longitudinal and transverse direction. At each increment, the deformation forces were measured one minute after the load application. With the loading speed of 3-4 minutes per increment, every specimen was brought to failure within approximately 30 minutes.

The feature common in large number of rocks shows different deformability properties in different directions of testing. This feature comes as a result of the texture and/or layering or orientation of grain in micro-composition of rock material. It is generally known that the rock material shows higher deformability in the direction which is perpendicular to the layers, and lower deformability in the directions that are parallel to the layering planes. Testing of strain-dependent deformation relation of marls in different directions was carried out on prismatic specimens at uniaxial compression test with constrained lateral expansion. The specimens were cut in three orthogonal directions: one vertical direction which corresponds to the vertical axis of the undisturbed rock in situ and two perpendicular horizontal directions.

The Diagram illustrated in Figure 12 shows the results of uniaxial compression tests (where EZ means loading perpendicular to the layers; EX means loading in the layering plane; v and h denote direction of the dilatation measurement; v - in the load effect direction; h - in the perpendicular direction). It is easily observed that the marl exhibits higher deformability in the direction perpendicular to the layers compared to the other two orthogonal directions. Elastic modulus (calculated at the stress level of 2MPa) in the X direction is twice larger than the elastic modulus in the Z direction, $E_z / E_x = 2.0$.

The initial elastic modulus in the x-y plane show even values (horizontal plane in situ). The said deformation behaviour of marl indicates that proper calculations of strain-dependent phenomena in marls need to be carried out on rheological models which include the effects of transverse isotropy.



Slika 12. Rezultati jednoaksijalnih testova upravno na slojeve i u ravni slojevitosti
 Figure 12. Results of uniaxial compression tests carried out perpendicularly to the layers and in the layering plane

6.2 Rezultati jednoaksijalnih testova pri testu puzanja

Jednoaksijalni test puzanja na laporcu, predstavljen u ovom istraživanju, izveden je na dvije grupe po tri prizmatična uzorka dimezija 15x15x40 cm. Ukupno trajanje testa puzanja bilo je oko 180 dana. Opterećivanje uzoraka izvedeno je u inkrementima od 25% od krajnjeg napona testa puzanja, za svaku grupu uzoraka.

Srednje vrijednosti mjerenja deformacija na po tri prizmatična uzorka svake različito opterećene grupe uzoraka, pri aksijalnom naponu od 2.0MPa i 4.0MPa, prikazane su na slici 13. Na dijagramu se jasno izdvaja zona intenzivnog puzanja materijala u aksijalnom pravcu u prvih dvadeset dana nakon opterećivanja. Priraštaj deformacija u ovom periodu jeste nelinearan u odnosu na vrijeme. Nakon ovog perioda, deformacije puzanja su manje i priraštaj deformacija je približno linearan.

Na uporednom dijagramu prikazanom na slici 13, vidi se da je – pri aksijalnom naponu od 2.0 i 4.0 MPa – gradijent prirasta deformacije u toku vremena veći kod uzoraka opterećenih većim naponom pritiska. Značajno je naglasiti i to da aksijalna deformacija puzanja koja se razvije u toku šest mjeseci dostiže red veličine trenutne deformacije koju indukuje inicijalna promjena napona. Tako, pri naponu od 2.0 MPa, prosječna trenutna deformacija (prosječna deformacija na tri uzorka jedne serije) iznosi 1.41‰, a prosječna vremenska deformacija 0.98‰, dok pri naponu 4.0 MPa prosječna trenutna deformacija iznosi 3.27‰, a prosječna vremenska deformacija 2.74‰.

Poprečne dilatacije su oko deset puta manje od aksijalnih (ako se upoređuju njihove apsolutne vrijednosti), odnosno Poisson-ov koeficijent ima vrijednost $\nu = 0.1$. Ovaj odnos je približno isti za trenutnu dilataciju uzrokovanu naponskom promjenom i vremenski zavisne komponente ukupnih dilatacija. S povećanjem naponskog nivoa, ovaj odnos raste za ukupnu deformaciju (trenutna + vremenska) u sličnom odnosu kao i kod kratkotrajno opterećenih uzoraka (slika 13). Pri lomu, kod ispitivanog laporca, Poisson-ov koeficijent ima vrijednost $\nu = 0.25$.

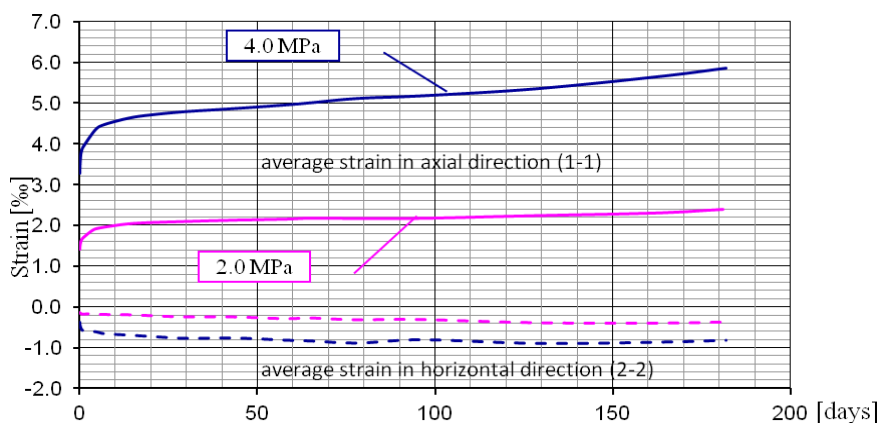
6.2 Results of uniaxial compression tests at creep test

Uniaxial marl creep test in experimental research presented here was conducted on two groups with three prismatic specimens, 15x15x40cm each. Total duration of the creep test was about 180 days. Loading of the specimen was conducted in increments of 25% of defined level of stress in the creep test, for every group of specimens.

Average values of deformation measurements on three prismatic specimens out of each group of specimens that were subjected to different loading, at axial compression load of 2.0MPa and 4.0MPa are illustrated in Figure 13. A zone of an intensive creep of material in the axial direction in the first twenty days after the load application is clearly seen in the diagram. Increase in deformations over this time interval is not-linear to time. After this period, the creep deformations are smaller and the increase in deformations is almost linear.

Comparative diagram illustrated in Figure 13 shows that at axial compression of 2.0MPa and 4.0MPa, the gradient of deformation increase in time is larger in case of specimens that are subject to a larger compression load. It is important to note that axial creep deformation which occurs within 6 months reaches the order of magnitude of the instantaneous deformation induced by initial change in compression load. Therefore, at the compression load of 2.0MPa, an average instantaneous deformation (average deformation on three samples of one series) is 1.41‰, and an average time-dependent deformation is 0.98‰; while at compression load of 4.0MPa an average instantaneous deformation is 3.27‰, and an average time-dependent deformation is 2.74‰.

Transverse dilatation are about 10 times smaller compared to axial (when absolute values are compared), meaning the value of Poisson ratio is $\nu = 0.1$. This ratio is almost the same in the case of an instantaneous dilatation caused by change in compression and time-dependent component of total dilatations. With the increase of the compression level, this ratio grows for total deformation (instantaneous + time-dependent) in the same proportion as in the case of short-term loaded



Slika 13. Dijagram puzanja aksijalno opterećenih prizmatičnih uzoraka
Figure 13. Creep diagram of axially compressed prismatic specimens

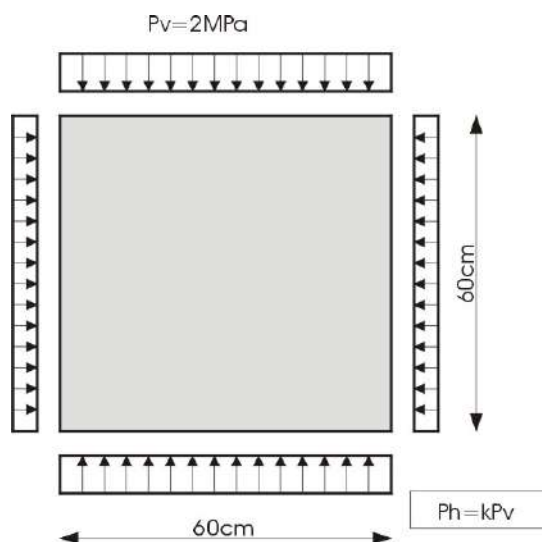
specimens (Figure 13). At the failure of the tested marl, the Poisson ratio is $\nu = 0.25$.

6.3 Test na pločastim uzorcima

Prilikom testa na pločastim uzorcima (slika 14), nanijeto je opterećenje, jednoaksijalno i biaksijalno u svojoj ravni ploče, u inkrementima od 0.5 MPa, u toku jednog sata, do vertikalnog napona od 2.0 MPa, što je oko 25% od vršne čvrstoće ispitivanog laporca. Tri uzorka opterećena su jednoaksijalno, a u sljedeće tri grupe uzoraka variran je odnos horizontalnog i vertikalnog pritiska, $P_h/P_v = 0.3, 0.5$ i 1.0 . Inicirano naponsko stanje (uz održavanje konstantnog odnosa $P_h/P_v = \text{const.}$) održavano je narednih 45 dana, uz mjerenja polja deformacija na oba lica ploče.

6.3 Test on plate specimens

Test on plate specimens (Figure 14) consisted of applying uniaxial and biaxial load on the plate in its own plane, in increments of 0.5 MPa during a period of one hour up to vertical stress of 2.0 MPa, which makes for about 25% of the peak strength of the examined marl. Three specimens were loaded uniaxially, while in the following three groups of specimens the ratio P_h/P_v between horizontal and vertical load components was varied, 0.3, 0.5 and 1.0. The initiated stress state (with maintained constant ratio between horizontal and vertical stress) was retained in the following 45 days, with measurement of the deformation fields on both sides of the plate specimen.



Slika 14. Biaksijalno opterećenje na pločastim uzorcima
Figure 14. Biaxial load on plate specimens

Procedura ove faze testa definisana je tako da se ustanovi uticaj bočnog napona na puzanje u vertikalnom pravcu, te da se ustanovi varijacija mjerenih deformacija (trenutnih i vremenskih), zavisno od oblika uzorka (prizmatičan/pločast).

Bočno opterećenje biaksijalno opterećenih pločastih uzoraka značajno mijenja deformacijsku sliku, kako početne deformacije indukovane naponskom promjenom, tako i deformacije puzanja. Na slici 15 prikazani su rezultati mjerenja deformacije na tri grupe uzoraka opterećenih pri različitom odnosu horizontalnog i vertikalnog napona. Kao uporedna vrednost na svim dijagramima, prikazana je prosječna ukupna vertikalna (PR-v) i horizontalna (PR-h) deformacija prizmatičnih uzoraka pri istom vertikalnom naponu 2.0 MPa.

Pri odnosu $k = \sigma_h / \sigma_v = 1.0$ kod pločastih uzoraka, početna i vremenska vertikalna deformacija vrlo malo se razlikuje od deformacije jednoaksijalno opterećenih prizmatičnih uzoraka, kako je prikazano na dijagramu slike 15. Prirast vremenskih deformacija nešto je veći kod pločastih uzoraka nego kod prizmatičnih, i to nakon 10–15 dana od opterećivanja. Veći prirast vremenskih deformacija, prema tome, jeste posljedica većeg sekundarnog puzanja kod pločastih uzoraka (sekundarno puzanje dobija na značaju s protokom vremena, dok primarno puzanje, nakon desetak dana, praktično nema dalji uticaj na prirast deformacija). Ove razlike su očigledno posljedica oblika uzorka, jer je ispitivanje izvršeno pod istim uslovima na istom materijalu.

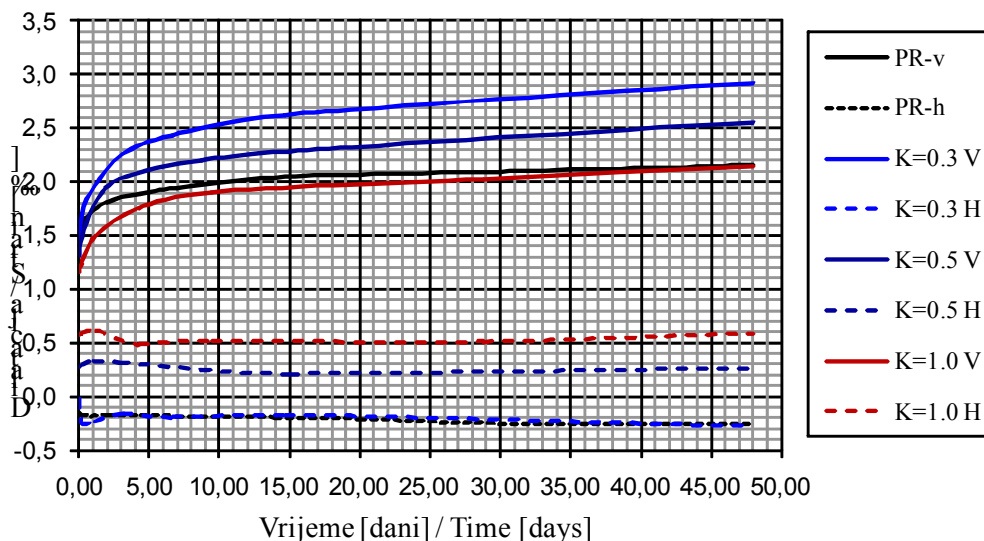
Sa smanjenjem odnosa $k = \sigma_h / \sigma_v$ od vrijednosti 1.0 prema jednoaksijalnom stanju, prirast inicijalnih i vremenski zavisnih vertikalnih deformacija raste, kao što je prikazano na dijagramima slike 15, što je posljedica oslobađanja bočnog širenja uzorka.

The procedure of this phase of the test was designed to determine effects of the lateral stress on the creep in the vertical direction as well as to determine variations of the measured deformations (instantaneous and time-dependent) depending on the shape of specimen i.e. prismatic – plate shaped.

Lateral loading in the case of biaxially compressed plate specimens significantly changes the deformation behaviour of both the initial deformations induced by a stress change and creep deformations. Figure 15 shows results of deformation measurements on three group of specimens loaded at different horizontal-vertical stress ratio. A comparative value presented in each diagram is an average total vertical (PR-v) and horizontal (PR-h) deformation of prismatic specimens at the same vertical stress of 2.0MPa.

At ratio $k = \sigma_h / \sigma_v = 1.0$ in the case of plate specimens, the initial and time-dependent vertical deformation slightly defers from the deformation of uniaxially compressed prismatic specimens, as illustrated in diagram, Figure 15. Increment of time-dependent deformations is somewhat larger in the case of plate specimens compared to prismatic specimens, after 10–15 days following the load application. Therefore, larger increment of time-dependent deformations is a consequence of larger secondary creep of the plate specimens (secondary creep grows in line with time, while primary creep after about 10 days practically has no further impact on the increase of deformations). These differences obviously come as a result of the shape of specimen, given that the tests were carried out under the same conditions on the same material.

With decrease of the ratio $k = \sigma_h / \sigma_v$ from the value of 1.0 towards the uniaxial state, the increment of initial and time-dependent deformations grows, as illustrated in Figure 15, which is a consequence of the unconstrained lateral expansion of the specimen.



Slika 15. Dijagram puzanja biaksijalno opterećenih uzoraka (PR– označava prizmatičan jednoaksijalno opterećen uzorak, a K označava odnos horizontalnog i vertikalnog napona na pločastim uzorcima)
Figure 15. Creep diagram of biaxially loaded specimens (PR means uniaxially loaded prismatic specimen, K means ratio of horizontal and vertical stress on plate specimens)

Horizontalna deformacija, kod biaksijalno opterećenih pločastih uzoraka, pokazuje kolebanje u prvih 5–7 dana od opterećivanja. U kasnijem periodu, puzanje u horizontalnom pravcu može se evidentirati samo kod jednako vertikalno i horizontalno opterećenih uzoraka. Kod ostalih uzoraka odnosa $k = \sigma_h / \sigma_v = 0.5$ horizontalne deformacije u toku vremena zadržavaju vrijednost inicijalne deformacije, a kod odnosa $k = \sigma_h / \sigma_v = 0.3$ horizontalne deformacije su skoro iste kao i horizontalne deformacije prizmatičnih uzoraka. Pri odnosu $k = \sigma_h / \sigma_v = 1.0$ i 0.5, horizontalna deformacija jeste deformacija skupljanja, a pri odnosu $k = \sigma_h / \sigma_v = 0.3$ horizontalna deformacija jeste deformacija širenja.

6.4 Konvencionalni test triaksijalne kompresije pri dugotrajnom opterećenju

Konvencionalni test triaksijalne kompresije daje mogućnost analize uticaja bočnog napona na deformisanje. Pritom, bočni pritisak $\sigma_2 = \sigma_3$ (koji se varira u setu testova) obično ne prelazi vrijednost od 50% vršne čvrstoće dobijene u jednoaksijalnom testu bez spriječenog bočnog širenja. Generalno, ovaj tip testa moguće je sprovesti uz kontrolisane sile kojim se uzorak opterećuje ili uz kontrolisanje brzine aksijalne deformacije. Test puzanja, koji je sproveden na laporcu u nešto kraćem vremenu (sedam dana), predstavlja specifičan triaksijalno test pri kontrolisanoj sili, koja je u ovom slučaju nakon nanošenja konstantna u toku testa.

Test puzanja na laporcu u konvencionalnom triaksijalnom aparatu sproveden je na deset uzoraka, pri konstantnom opterećenju od 2.0 MPa, u toku tri dana, te pri 4.0 MPa, u toku naredna tri dana. Tri uzorka testirana su bez bočnog pritiska, kod četiri bočni napon je 1.0 MPa, a kod tri 2.0 MPa. Ovaj relativno kratak test puzanja dao je neke kvalitativne pokazatelje ponašanja ispitivane stijene u toku vremena pri dejstvu jednakog bočnog pritiska.

Na dijagramu na slici 16. prikazani su rezultati testa puzanja triaksijalno opterećenih cilindričnih uzoraka pri različitim bočnim naponima pritiska. Pune linije ukazuju na aksijalnu (vertikalnu) dilataciju, a isprekidana linija na horizontalnu (radijalnu) dilataciju. Radijalna deformacija kod svih uzoraka, nakon jednog dana od opterećivanja, zadržava dostignuti nivo, bez obzira na intenzitet radijalnog napona u razmatranom domenu, dok aksijalna deformacija ukazuje na postojanje uticaja bočnog napona na tok vremenskih deformacija [16].

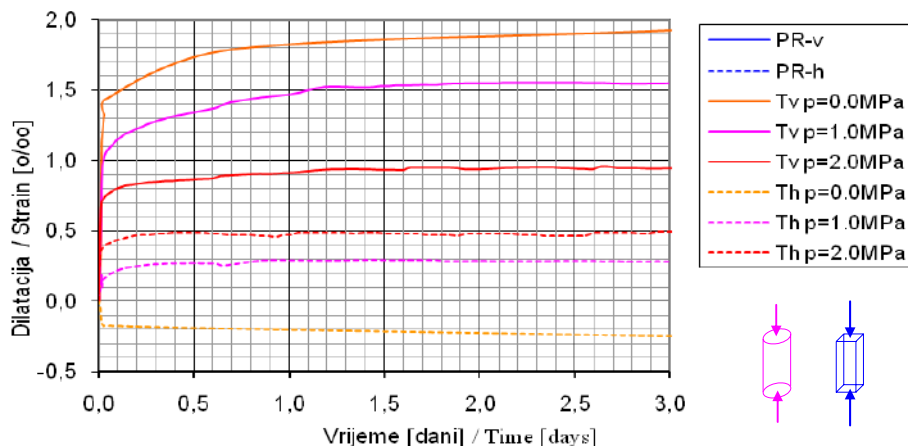
Horizontal deformation in the case of biaxially compressed plate specimens exhibits fluctuations in the first 5-7 days after the load application. In the later period, the creep in the horizontal direction can be observed only in specimens with even vertical and horizontal loading. In the case of other specimens with ratio $k = \sigma_h / \sigma_v = 0.5$, horizontal deformations retain the value of the initial deformation over the time, while at ratio $k = \sigma_h / \sigma_v = 0.3$, horizontal deformations are almost the same as horizontal deformations of the prismatic specimens. At ratio $k = \sigma_h / \sigma_v = 1.0$ and 0.5, horizontal deformation is a shrinkage deformation, and at ratio $k = \sigma_h / \sigma_v = 0.3$, horizontal deformation is an expansion deformation.

6.4 Conventional test of three-axial compression under long term loading

Conventional tests of three-axial compression give the possibility of analysis of influence of lateral stress on deformations. Lateral pressure $\sigma_2 = \sigma_3$ (which varies in the set of tests) usually does not exceed value of 50% of peak strength obtained in uniaxial test with free lateral deformations. Generally speaking, this type of test can be conducted with controlled forces with load against the specimen or with control of velocity of axial deformation. Creep test carried out on marl in a shorter period of time (seven days), represents a specific type of three-axial test with controlled force that is stress state which after the application remains constant during the test.

Creep test on marl in conventional three-axial device was carried out on 10 specimens with constant vertical load of 2.0 MPa over the period of 3 days and with 4.0MPa load within the following 3 days. Three specimens were tested without lateral pressure, the fourth one had lateral pressure of 1.0MPa, and three specimens had a 2.0MPa lateral pressure. This short creep test offered some relative indicators of behaviour of the examined rock in time with influence of rotation symmetrical lateral pressure.

Diagram in Figure 16. shows the creep test results of three-axially loaded cylindrical specimens with different lateral pressure. Full lines indicate axial (vertical) strain and dash lines indicate tangential (horizontal) strain. Radial deformation with all the specimens after one day of loading preserves the obtained level regardless the intensity of radial stress in the considered domain, while axial deformation indicates influence on lateral stress on the flow of time deformations [16].



Slika 16. Rezultati triaksijalnog testa puzanja na prizmatičnim i cilindričnim uzorcima pri aksijalnom naponu 2.0 MPa
 Figure 16. Results of three-axial creep tests on cylindrical specimens and of uniaxial test on prismatic specimens with pre-axial stress of 2.0MPa

7 ZAKLJUČAK

Ispitivanje puzanja laporca pri jednoaksijalnom i biaksijalnom naponskom stanju zahtijevalo je konstruisanje nestandardne opreme i uređaja za opterećivanje i mjerenje sile u toku dugog perioda. Uređaji sa okačenim teretom za nanošenje i održavanje sile u toku dugog perioda omogućili su potpuno i uspješno sprovođenje kompleksnih testova puzanja, u trajanju i od više od jedne godine, uz prihvatljive varijacije napona. Mehanički prstenasti mjeraci sile korišćeni su za mjerenje sile u toku nanošenja opterećenja u inkrementima i mjerenje zadatog opterećenja na uzorcima u toku testa puzanja. Ovaj mehanički instrument obezbijedio je mjerenje sile u toku nanošenja opterećenja u inkrementima, ali i kontrolu sile u toku testa puzanja u trajanju od više od jedne godine, na vrlo jednostavan i pouzdan način, uz obezbjeđenje varijacije opterećenja manje od 1%.

Mjerenje deformacija puzanja mehaničkim deformetrom, na uzorcima od laporca, pokazalo se kao vrlo pouzdano u toku dugog perioda trajanja testa puzanja. Obezbijeđena tačnost mjerenja ovog tipa uređaja od 2–3/1000 mm u potpunosti je zadovoljavajuća, jer su mjerene promjene rastojanja između repera (oko 100 mm) od 0.5 do 1 mm. Mana upotrebe mehaničkog deformetra jeste dugotrajno mjerenje na brojnim mjernim mjestima, kao što je to bio slučaj s pločastim uzorcima-modelima.

Rezultati jednoaksijalnih testova ukazuju na to da materijal pokazuje nelinearnost u pogledu napona i deformacija, čak i pri niskom nivou napona, ali se značajna nelinearnost javlja tek kada napon dostigne vrijednost od oko 80% od vršne čvrstoće σ_c pri jednoaksijalnom testu. Laporac je nastao sedimentacijom u dubokoj jezerskoj vodi, a posljedica toga jeste poseban oblik mikrostrukture zbog slaganja čestica s različitom orijentacijom u vertikalnom, odnosno horizontalnom pravcu. Ispitivanje mehaničkih karakteristika u vertikalnom i horizontalnom pravcu pokazalo je da se materijal ponaša izuzetno transversalno izotropno.

7 CONCLUSION

Testing of marl creep behaviour at uniaxial and biaxial stress state required designing non-standard equipment and devices for loading and force measurement over a long time interval. Devices with hanged dead weight for application and control of force over a long time interval enabled the creep tests to be completely and successfully carried out for a period of over one year, with the acceptable stress variations. Mechanical ring-type dynamometers were used for force measurement during incremental application of load and measurement of the predefined load on the specimens at the creep test procedure. In addition to the force measurement in the course of incremental application of load, this mechanical instrument also enabled simple and reliable control of the force at the creep test carried out over a period of more than one year, with the load variations below 1%.

Measurement of creep deformations in marl specimens by mechanical deformer showed to be reliable for a long time interval of the creep test. This type of device provides measurement accuracy of 2–3/1000mm which is fully satisfying, considering that the measured changes in distance from the reference point (at the distance of about 100mm) range from 0.5 to 1mm. Downside of the use of mechanical deformer is a time-consuming measurement on the large number of measuring points, as it was the case with the plate specimens-models.

Results of the uniaxial compression tests indicate that material shows non-linearity in relation to the stress and strain even at the low level of stress; however a significant non-linearity is observed only when the stress reaches the value of 80% of the peak strength σ_c at uniaxial compression test. Marl is formed by sedimentation in deep lake water, which resulted in a specific shape of the microstructure due to the layering of particles with different orientation in the vertical and/or horizontal direction. Testing mechanical properties in the vertical and horizontal direction showed a distinctive

Značajno različito deformacijsko ponašanje laporca u različitim pravcima ukazuje na to da se proračuni naponski zavisnih fenomena u laporcima i sličnim stijenama moraju sprovesti na reološkim modelima koji obuhvataju efekte transverzalne izotropije.

Testovi puzanja, sprovedeni na jednoaksijalno opterećenim prizmatičnim uzorcima, ukazuju na to da laporac, pri konstantnom jednoaksijalnom naponu pritiska, pokazuje značajne vremenske deformacije - puzanje. U prvih dvadeset dana nakon opterećivanja, priraštaj deformacija je nelinearan u odnosu na vrijeme. To je zona intenzivnog puzanja materijala u aksijalnom pravcu - primarno puzanje. Nakon tog perioda, deformacije puzanja su manje i priraštaj deformacija je približno linearan - sekundarno puzanje. Pritom, gradijent prirasta deformacije u toku vremena je veći kod uzoraka opterećenih većim naponom pritiska.

Bočni pritisak kod biaksijalno opterećenih pločastih uzoraka značajno mijenja deformacijsku sliku, kako početnih deformacija indukovanih naponskom promjenom, tako i deformacija puzanja. Sa smanjenjem odnosa $k = \sigma_h / \sigma_v$ od vrijednosti 1.0 prema (ka) jednoaksijalnom stanju napona, prirast inicijalnih i vremenski zavisnih vertikalnih deformacija raste, što je posljedica oslobađanja bočnog širenja uzorka. Uporedna analiza vremenski zavisnih deformacija jednoaksijalno opterećenih prizmatičnih uzoraka i radijalnih deformacija oko kružnog otvora (kod dvoosno opterećenih pločastih uzoraka - modela), ukazuje na to da nema bitne razlike u obliku i u ukupnoj veličini vremenskih deformacija. Ovo opet ukazuje na to da se rezultati puzanja dobijeni na vrlo jednostavnim jednoaksijalnim testovima mogu koristiti u inženjerskoj praksi za ocjenu vremenski zavisnih deformacija meke stijene, pri znatno složenijem naponskom stanju - kakvo je stanje napona oko tunelskih otvora.

Efekat uticaja bočnog napona pritiska na aksijalnu deformaciju, pri konvencionalnom testu triaksijalne kompresije, znatno je veći nego na uticaj bočnog napona kod biaksijalnog opterećenja. Aksijalna deformacija, u uslovi- ma rotaciono simetričnog pritiska, može biti manja i do 100% (pri hidrostatičkom stanju napona, $k=1.0$) od aksijalne deformacije, razvijene bez djelovanja bočnog pritiska.

transversal isotropic behaviour of material. The significant differences in the behaviour of marl in different directions indicate that calculations of stress-dependent phenomena in marls and similar rocks should be performed on rheological models which include the effects of the transversal isotropy.

The creep tests of the uniaxially and biaxially loaded specimens suggest that when marl is under constant uniaxial stress state, significant time-dependent deformations - creep are observed. In the first twenty days following the load application, the increment of deformations is non-linear in relation to time. This is a zone of intensive creep of material in the axial direction - primary creep. After this period, the extent of creep deformations is smaller and the increment of deformations is approximately linear - secondary creep. In addition, the gradient of deformation increment is higher in the case of the specimens under higher compression pressure.

Lateral compression in the case of biaxially compressed plate specimens significantly changes the deformation both the initial deformations induced by a change in stress and creep deformations. With the decrease in value of the ratio $k = \sigma_h / \sigma_v$ from value of 1.0 towards uniaxial stress state, the increment of initial and time-dependent vertical deformations grows as a result of the relief from lateral expansion of the specimen. Comparative analysis of time-dependent deformations in uniaxially compressed prismatic specimens and radial deformations around the circular opening (in the case of biaxially compressed plate specimens-models) suggests that there is no relevant difference in the shape and total extent of the time-dependent deformations. This indicates that the results obtained from the quite simple uniaxial compression tests can be applied in the engineering practice for the purposes of assessment of time-dependent deformations in soft rock at far more complex stress state, such as the stress state within the rocks around the tunnel opening.

In the conventional three-axial compression test, the effect of lateral strain on the axial deformation is significantly larger compared to the effect of the lateral strain in the case of the biaxial compression. At rotationally symmetric pressure, the axial deformation can be even up to 100% (at hydrostatic stress state $k=1.0$) smaller than the axial deformation that is generated without an impact of the lateral strain.

8 LITERATURA REFERENCES

- [23] Bergues J. & Nguyen D., Hoetit N. 1998. Time dependent behaviour of hard marls, *The Geotechnics of hard Soils-Soft Rock*, Evangelista & Picarelli, Balkema, Rotterdam.
- [24] Baryshnikov V. D., 2012, Estimating Remaining Life of Underground Tunnel Concrete Lining by Convergence Measurements, *Journal of Mining Science*, 2012, Vol. 48, No. 3, pp. 440–444
- [25] Bosman, J., Malan, D., and Drescher, K. 2000. „Time-dependent tunnel deformation at Hartebeestfontein mine.” *J. S. Afr. Inst. Min. Metall.*, 100(6), pp. 333–340.
- [26] Cristescu, N.D. and Hunsche, U. 1998. Time effects in Rock Mechanics. John Willey & Sons.
- [27] Cristescu, N.D. 2009. Time Effects in Rock Mechanics. Proceedings of the SEM Annual Conference, June 1–4, Albuquerque New Mexico USA ©2009 Society for Experimental Mechanics Inc.

- [28] Goodman, R. E. 1989. Introduction to rock mechanics, Wiley, New York. John Wiley & Sons.
- [29] Jaeger J.C. & Cook N.G.W., and Zimmerman R.W. 2007. Fundamentals of Rock Mechanics, Chapman and hall Ltd. And Science Paperbanks.
- [30] Langer M., 1979, Rheological behaviour of rock masses, Proc. 4th Int. Con. On Rock Mech., Montreux, Vol.3., pp 29–62.
- [31] Pan Y.W. and Dong J.J. 1991a. Time-Dependent Tunnel Convergence - I. Formulation of the Model, J.Rock Mech. and Mining Sci., pp. 469–475
- [32] Pan Y.W. and Dong J.J., 1991b. Time-Dependent Tunnel Convergence - II. Advance Rate and Tunnel-Support Interaction, J.Rock Mech. and Mining Sci., pp. 475–488
- [33] Pande G.N., Beer G. & Williams J.R. 1995. Numerical Methods in Rock Meshanics, John Wiley & Sons Ltd.
- [34] Phienweij, N., Thakur, P. K., and Cording, E. J. 2007. „Time-dependent response of tunnels considering creep effect.” Int. J. Geomech., 7(4), p.p 296–306.
- [35] Sakurai, S., 1978, „Approximate time-dependent analysis of tunnel support structure considering progress of tunnel face.” Int. J. Numer.Analyt. Meth. Geomech., 2, 59–175.
- [36] Tomanovic, Z. 2006. Rheological model of soft rock based on test on marl. Int. J. Mechanics of Time-Dependent Materials, Springer, pp. 135–154.
- [37] Tomanovic, Z. 2007. Reološki model puzanja matriksa meke stijene / Rheological model of matrix of soft rock creep, Građevinski materijali i konstrukcije / Building matrilas end structure, vol. 50, br. 1-2, str. 3-19
- [38] Tomanovic, Z. 2009. Influence of Ko on creep properties of marl. Int. J. Acta Geotechnica Slovenica, pp. 14-29.

REZIME

TESTIRANJE FENOMENA PUZANJA MEKE STIJENE

Zvonko TOMANOVIĆ

Test puzanja karakteriše konstantno opterećenje pod kojim se materijal s vremenom deformiše. Zbog toga je za korektno izvođenje testa puzanja veoma važno održavanje - kontrolisanje konstantnog naponskog stanja koje je aplicirano na uzorak. Naime, uticaj napona pritiska na veličinu deformacije puzanja izrazito je nelinearan, pa zbog toga nivo napona, odnosno eventualne varijacije napona u toku vremena imaju veliki uticaj na prirast vremenski zavisnih komponenti deformacija. Radi toga, u toku testa puzanja – koji nekada traje i godinama – treba obezbijediti da varijacije napona budu u granici od $\pm 1\%$. U ovom radu predstavlja se konstrukcija aparature s „mrtvim” opterećenjem za održavanje konstantnog naponskog stanja u toku dugog perioda (dana, nedjelja ili godina), kapaciteta od 750 kN i 1500 kN, kao i mjerenje sile i deformacija u toku testa puzanja. Testovi puzanja sprovedeni su na uzorcima laporca, u trajanju do jedne godine. Predstavljeni su rezultati jednoaksijalno opterećenih prizmatičnih uzoraka dimenzija 15x15x40 cm i rezultati testa puzanja biaksijalno opterećenih pločastih modela dimezija 60x60x10 cm, s kružnim otvorom u sredini. Takođe, prikazani su i rezultati testa puzanja u triaksijalnom aparatu na uzorcima dimenzija $d/h = 5.4/108$ cm.

ključne riječi: puzanje, aparatura za opterećivanje, laporac, mjerenje sile i deformacija, meka stijena

SUMMARY

TESTING OF CREEP PHENOMENA ON SOFT ROCK

Zvonko TOMANOVIĆ

Creep test involves deformation of material with time under a constant stress. Hence, for proper conducting of the creep test it is highly important to maintain, i.e. constant control the stress applied to a specimen. Namely, impact of the compression on the extent of deformation is distinctively non-linear; therefore the stress level or eventual variations of stress over time largely affect the increment of time-dependent components of deformation. Therefore, it is necessary to ensure that variations of stress are kept within limits of $\pm 1\%$ during the creep test the duration of which sometimes may last for several years. This paper presents structure of the dead-weight creep apparatus for maintaining constant stress over long time interval (day, week or year) with a capacity of 750kN and 1500kN, as well as for measuring of force and deformations at creep test. The creep tests have been conducted on marl specimens in duration of up to one year. The creep test results are presented for the uniaxially compressed prismatic specimens of dimensions 15x15x40cm and biaxially compressed plate models of dimensions 60x60x10cm, with circular opening at centre.

Key words: creep, load-application apparatus, marl, force and deformation measurements, soft rock

PRIMENA MODIFIKOVANOG RASPLINUTOG TOPSIS METODA ZA VIŠEKRITERIJUMSKE ODLUKE U GRAĐEVINARSTVU

APPLICATION OF MODIFIED FUZZY TOPSIS METHOD FOR MULTICRITERIA DECISIONS IN CIVIL ENGINEERING

Živojin PRAŠČEVIĆ
Nataša PRAŠČEVIĆ

ORIGINALNI NAUČNI RAD
ORIGINAL SCIENTIFIC PAPER
UDK: 624:519.816

1 UVOD

TOPSIS metod (*Technique for Order Preference by Similarity to Ideal Solution* – Tehnika za redosled prioriteta prema sličnosti sa idealnim rešenjem) za rešavanje višekriterijumskih problema (MCDMP) sa više alternativa predložili su i razvili Hwang i Yoon [7] 1981. godine.

Metod je baziran na činjenici da izabrana ili najbolja alternativa treba da ima najkraće rastojanje od pozitivnog idealnog rešenja (PIS) i najduže rastojanje od negativnog idealnog rešenja (NIS). Pozitivno idealno rešenje maksimizuje kriterijume koji se odnose na korisnosti, a minimizuje kriterijume koji se odnose na troškove ili gubitke. Negativno idealno rešenje minimizuje kriterijume koji se odnose na korisnosti, a maksimizuje kriterijume koji se odnose na troškove. Izabrana alternativa ima maksimalnu sličnost (bliskost) sa PIS i minimalnu sličnost (bliskost) sa NIS.

Chen i Hwang [3] su ovaj metod sa fiksnim (nerasplnutim) podacima transformisali u metod s rasplnutim podacima. U poslednjih više od trideset godina, mnogi autori učestvovali su u razvoju ovog metoda i predložili brojne modifikacije. Metod se često uspešno koristio kao pomoć donosiocima odluka za rešavanje mnogih praktičnih problema u različitim oblastima primene. Opricović [12] je predložio i razvio metod nazvan VIKOR, za višekriterijumsku optimizaciju složenih sistema. Ovaj metod koristi se za rangiranje i izbor alternativa u slučaju postojanja konfliktnih kriterijuma. On

Prof. dr Živojin Prašćević, dipl. građ. inž.,
Univerzitet u Beogradu, Građevinski fakultet, Beograd
e-mail: zika@grf.bg.ac.rs
Doc. dr Nataša Prašćević, dipl. građ. inž.,
Univerzitet u Beogradu, Građevinski fakultet, Beograd
e-mail: natasa@grf.bg.ac.rs

1 INTRODUCTION

TOPSIS method (*Technique for Order Preference by Similarity to Ideal Solution*) for solving multiple criteria decision problem (MCDMP) with several alternatives was proposed and developed by Hwang and Yoon [7] 1981.

The method is based on the fact that the chosen or most appropriate alternative should have the shortest distance from positive ideal solution (PIS) and the longest distance from negative ideal (anti ideal) solution (NIS). Positive ideal solution maximizes the criteria that are related to the benefits and minimizes the criteria that are related to the costs or losses. The negative ideal solution minimizes the criteria that are related to the benefits and maximizes the criteria that are related to the costs and losses. The chosen alternative has the maximum similarity (closeness) with PIS and minimum similarity (closeness) with NIS.

Chen and Hwang [3] have transformed this method with the crisp (nonfuzzy) data to the method with the fuzzy data. In more than last thirty years a lot of authors participated in development of this method and proposed numerous modifications. The method was applied successfully in the practice as a help to decision makers for solving many problems in different fields of application. Opricović [12] has proposed and developed a method, named VIKOR, or multiple criteria optimization of complex systems. This method focuses on ranking and selecting alternatives in the presence of conflicting

Professor Živojin Prašćević, DSc Tech, Dipl. Civ. Eng.
University of Belgrade, Faculty of Civil Engineering
Belgrade, e-mail: zika@grf.bg.ac.rs
Nataša Prašćević, DSc Tech., Dipl. Civ. Eng., Assistant.
Professor, University of Belgrade, Faculty of Civil
Engineering, Belgrade, e-mail: natasa@grf.bg.ac.rs

je uveo indeks višekriterijumskog rangiranja, koji se određuje na osnovu bliskosti idealnom rešenju.

Opricović i Tzeng [13] upoređivali su osnovne karakteristike VIKOR i TOPSIS metoda u svim koracima rešavanja problema: proceduralna baza, normalizacija, agregacija i konačno rešenje. Kasnije je Opricović proširio VIKOR metod za rešavanje rasplnutih višekriterijumskih problema s konfliktnim i nekonfliktnim kriterijumima i razvio metod VIKOR-F [14]. Metod VIKOR više puta je korišćen za višekriterijumsko rangiranje alternativa prilikom rešavanja mnogih problema u građevinarstvu, hidrotehnici i saobraćaju, kao i u drugim inženjerskim oblastima. Pored ove dve metode, u literaturi postoji još metoda za višekriterijumsko donošenje odluka (AHP, PROMETHEE, ELECTRE i dr.).

Wang i Elhang [17] predložili su fuzzy TOPSIS metod, zasnovan na alfa preseccima rasplnutih skupova za rešavanje problema upravljanja rizikom kod mostova. Za svaku alternativu i izabrani alfa nivo, definisali su nelinearni program (NLP) s gornjom i donjom vrednošću relativne bliskosti od NIS kao funkcijama cilja i u već definisanim gornjim i donjim vrednostima kao ograničenjima. Na taj način, relativne bliskosti posmatrane su kao rasplnuti brojevi, a kasnije, posle defazifikacije, rangirane su alternative. U stranoj i domaćoj literaturi postoje brojni primeri primene TOPSIS metode s fiksnim i rasplnutim brojevima u svim područjima građevinarstva i realizacije investicionih projekata za rangiranje alternativa ili subjekata imajući u vidu propisane kriterijume. Kraći prikaz jednog broja tih radova dali su autori u njihovom ranijem radu [16].

Procena rizika objekata (mostova, zgrada i ostalih objekata) najčešće se koristi za određivanje optimalnog plana ili rangiranja održavanja objekata u odnosu na rizik. Ovaj problem proučavali su mnogi autori, a u literaturi postoje različiti metodi procene rizika. Na primer, Adey, Hajdin i Brühwiler [1] predstavili su pristup određivanju optimalnog plana održavanja mostova, baziranog na rizicima koje je izazvalo više hazarda. Wang i Elhang [18] predložili su pristup grupnom donošenju odluka za procenu rizika, koristeći rasplnuti TOPSIS metod.

Mnogi radovi u kojima je reč o oceni stanja, održavanju i sanaciji građevinskih objekata i naselja publikovani su u zbornicima radova s međunarodnih konferencija, čiji je editor Folić [9], [10].

U ovom radu razmatra se problem višekriterijumskog rangiranja objekata za rekonstrukciju na osnovu definisanih kriterijuma, korišćenjem modifikovane rasplnute TOPSIS procedure koju su predložili autori, a koja je detaljno prikazana u radu [16]. U ovom metodu, svi ulazni podaci predstavljeni su kao trougaoni rasplnuti brojevi. Za ove brojeve i njihove proizvode određene su generalisane očekivane vrednosti, varijanse, standardne devijacije i koeficijenti varijacija. Ove vrednosti, dalje, korišćene su u matematičkim formulama za određivanje relativnih rastojanja svake alternative do PIS i NIS za njihovo rangiranje. Predložena procedura je opštija od procedure u kojoj se koriste fiksni brojevi i donosiocu odluka pruža realnije podatke za donošenje najprijatljivije odluke.

criteria. He introduced the multiple criteria ranking index based on the particular measure of closeness to the ideal solution.

Opricović and Tzeng [13] compared main features of VIKOR and TOPSIS methods in all steps of problem solution: procedural basis, normalization, aggregation and final solution. Opricović later extended VIKOR method for solving fuzzy multiple criteria problems with conflicting and non conflicting criteria and developed VIKOR-F [14]. VIKOR method has been used many times for multiple criteria ranking of alternatives for solving many problems in civil, hydro technical and transportation engineering and other branches of practice as well. Besides these two methods, there are more methods for multiple criteria decision making (AHP, PROMETHEE, ELECTRE, etc.) in the literature considering this field of research.

Wang and Elhang [17] proposed fuzzy TOPSIS method based on alpha level sets with application to the bridge risk management. For every alternative and chosen alpha level, they formulated nonlinear programs (NLP) with lower and upper value of relative closeness to NIS as the objective functions and with prescribed lower and upper values as the constraints. In such a way these relative closeness are considered as fuzzy numbers, and then after defuzzification, the alternatives are ranked according to these closeness. In the foreign and domestic literature there is large number of examples of application of the TOPSIS method in all area of civil engineering and construction project realization for ranking alternatives or subjects related to the prescribed criteria. Short review of these works is presented in the author's work [16].

The risk assessment of an object (bridge, building, etc) is usually performed to determine the optimal scheme or rank order of the object maintenance. This problem has been investigated by numerous authors and there are different methods for the risk assessment. For instance, Adey, Hajdin and Brühwiler [1] presented risk-based approach to the determination of optimal interventions for bridges affected by multiple hazards. Wang and Elhang [18] proposed a fuzzy group decision making approach for the risk assessment using fuzzy TOPSIS method.

Numerous papers related to the assessment, maintenance and rebuilding of structures and settlements are given in the proceedings of international conferences, edited by Folić [9],[10].

This paper deals with a problem of multiple criteria ranking of objects for reconstruction against prescribed criteria using modified fuzzy TOPSIS procedure proposed by authors in the paper [16]. In this method all input data are presented as probabilistic triangular fuzzy numbers. Generalized expected values, variances, standard deviations and coefficients of variations are found for these fuzzy numbers and their products. These values are, further, used in mathematical formulas to determine relative closeness of every alternative to the PIS and NIS for their ranking. This proposed procedure is more general than the procedure based on crisp data and gives to the decision maker more realistic data to make the most acceptable decision.

2 DEFINICIJA PROBLEMA

U ovom radu razmatra se neka firma ili institucija (vlasnik) koja je odgovorna za održavanje n objekata (zgrada, mostova i drugih) koji su označeni sa A_1, A_2, \dots, A_m . Da bi se smanjile posledice rizika koje utiču na sigurnost, funkcionalnost, održivost, raspoloživost, uticaje okoline i druge bitne faktore, neophodno je uložiti određenu količinu novca za održavanje tih objekata. Raspoloživa količina novca obično nije dovoljna za održavanje svih objekata, pa je zbog toga neophodno objekte rangirati prema nivou rizika, te novac uložiti u objekte shodno listi rangiranja. Pomenuti faktori, koji se zovu *kriterijumi*, označeni su sa C_1, C_2, \dots, C_n , dok objekti predstavljaju *alternative* višekriterijumskog odlučivanja (MCDM). Svaku alternativu A_i u odnosu na kriterijum C_j numerički su ocenili eksperti vrednošću f_{ij} ($i = 1, 2, \dots, m; j = 1, 2, \dots, n$). Ove vrednosti jesu elementi *matrice odlučivanja*, koja je označena sa $F = [f_{ij}]_{m \times n}$.

Skup kriterijuma Ω sadrži dva disjunktna skupa Ω_b i Ω_c , tj.

$$\Omega = (C_1, C_2, \dots, C_n) = (\Omega_b \cup \Omega_c), (\Omega_b \cap \Omega_c) = \emptyset. \quad (1)$$

Podskup Ω_b predstavlja *dobiti* ili *kriterijume s povoljnim efektima* koje treba maksimizovati, dok podskup kriterijuma Ω_c predstavlja *troškove* ili *kriterijume s nepovoljnim efektima* koje treba minimizovati.

Svaki kriterijum C_j eksperti ocenjuju *relativnom težinom* ili *faktorom značajnosti* w_j ($j = 1, 2, \dots, n$). Ove vrednosti formiraju *vektor težina* $w = [w_j]_{1 \times n}$. Cilj rešavanja problema jeste da se odredi najprihvatljivija ili najbolja alternativa – A_c koja zadovoljava sve kriterijume i koja je najbliža *pozitivnom idealnom rešenju*, a najudaljenija od *negativnog idealnog rešenja*, kao i da se alternative rangiraju prema navedenom pravilu.

Idealno pozitivno rešenje F^* sadrži vrednosti f_{ij} koje predstavljaju maksimume kriterijuma dobiti i minimume kriterijuma troškova to jest

$$F^* = \{f_1^*, \dots, f_i^* \dots f_n^*\} = \{(\max_j f_{ij}, i \in \Omega_b), (\min_j f_{ij}, i \in \Omega_c)\}. \quad (2)$$

Idealno negativno rešenje F^- sadrži vrednosti f_{ij} koje odgovaraju minimumima kriterijuma dobiti i maksimumima kriterijuma troškova to jest

$$F^- = \{f_1^-, \dots, f_i^- \dots f_n^-\} = \{(\min_j f_{ij}, i \in \Omega_b), (\max_j f_{ij}, i \in \Omega_c)\}. \quad (3)$$

3 TOPSIS PROCEDURA SA FIKSNIM BROJEVIMA

Ako su elementi matrice odlučivanja f_{ij} ($i = 1, 2, \dots, m; j = 1, 2, \dots, n$) i koeficijenti značajnosti ili težine kriterijuma w_j ($j = 1, 2, \dots, n$), fiksni ili nerasplinuti brojevi, onda se primenjuje TOPSIS procedura s fiksnim brojevima, koja se izvršava u sledećim koracima.

1. *Normalizacija*. Pošto kriterijumi mogu imati različita značenja i različitu prirodu, elementi matrice odlučivanja izražavaju se različitim dimenzionalnim merama i skalama

2 DEFINITION OF THE PROBLEM

A firm or institution (owner) which is responsible for the maintenance of n objects (buildings, bridges or other objects) A_1, A_2, A_m is considered in this paper. To reduce consequences of a risk that influence safety, functionality, sustainability, availability, environmental and other important factors, a corresponding amount of money should be invested in the maintenance of these objects. The available amount of money usually is insufficient for all objects or projects, so that they should be ranked according to the risk rating, and the money should be invested in the objects according to this rank list. The mentioned factors are named as *criteria* denoted by C_1, C_2, \dots, C_n , while the objects represent *alternatives* for multi-criteria decision making (MCDM). Each alternative A_i is numerically evaluated by experts with respect to the criterion C_j by values f_{ij} ($i = 1, 2, \dots, m; j = 1, 2, \dots, n$). These values are elements of the decision matrix denoted by $F = [f_{ij}]_{m \times n}$.

The set of criteria Ω contains two disjunctive subsets Ω_b and Ω_c , i.e.

The subset of criteria Ω_b represents *benefits* or *criteria with favourable effects* that should be maximised, while subset of criteria Ω_c represents *costs* or *criteria with unfavourable effects* that should be minimized in the procedure.

Every criterion C_j is assessed by experts with relative *weight values* or *factors of importance* w_j ($j = 1, 2, \dots, n$). These values form the *vector of weights* $w = [w_j]_{1 \times n}$. The goal of the problem solution is to find the most preferable or the best (compromise) alternative A_c that satisfies all criteria together and which is closest to the *positive ideal solution* and farthest to the *negative ideal solution*, and rank alternatives according to this rule as well.

The positive ideal solution F^* contains the values f_{ij} that are maximal for the benefit criteria and minimal for the cost criteria, i.e.

The ideal negative solution F^- contains values f_{ij} that are minimal for the benefit criteria and maximal for the cost criteria, i.e.

3 TOPSIS PROCEDURE WITH CRISP NUMBERS

If elements of the decision matrix f_{ij} ($i = 1, 2, \dots, m; j = 1, 2, \dots, n$) and coefficients of importance or weights of criteria w_j ($j = 1, 2, \dots, n$), are crisp or non fuzzy numbers, then the TOPSIS procedure with crisp numbers is applied, which performs in the next steps.

1. *Normalization*. Since the criteria may have different meanings and nature, then elements of the decision matrix are expressed by different dimensional

vrednosti. Stoga, treba izvršiti normalizaciju elemenata matrice odlučivanja F . U literaturi postoji više predloga za normalizaciju, a ovdje će biti prikazana dva koja se najčešće primenjuju.

Prema prvom postupku, za svaki kriterijum C_j ($j = 1, 2, \dots, m$) odredi se maksimalna vrednost

$$f_j^* = \max_i f_{ij} \quad (i = 1, 2, \dots, m; j = 1, 2, \dots, n) \quad (4)$$

i s tom vrednošću podele sve vrednosti f_{ij} u koloni C_j matrice F . Na taj način, dobijaju se normalizovane i bezdimenzionalne vrednosti a_{ij} koje sačinjavaju normalizovanu matricu odlučivanja $A = [a_{ij}]$

$$a_{ij} = f_{ij} / f_j^*, \quad (i = 1, 2, \dots, m; j = 1, 2, \dots, n). \quad (5)$$

Drugi postupak naziva se *vektorski postupak* i u njemu se za svaki kriterijum nađu dužine odgovarajućih vektora po formuli

$$f_j^* = \sqrt{f_{1j}^2 + f_{2j}^2 + \dots + f_{mj}^2}, \quad (j = 1, 2, \dots, n). \quad (6)$$

Kao i u prethodnom slučaju, sa ovim vrednostima dele se elementi matrice odlučivanja F i tako dobijaju elementi normalizovane matrice A .

2. *Određivanje težinske matrice C*. Svaki element normalizovane matrice A množi se sa odgovarajućim težinskim koeficijentom ili koeficijentom značajnosti kriterijuma w_j i tako se dobiju elementi c_{ij} težinske matrice $C = [c_{ij}]$

$$c_{ij} = a_{ij} w_j, \quad (i = 1, 2, \dots, m; j = 1, 2, \dots, n). \quad (7)$$

3. *Određivanje pozitivnog idealnog rešenja (PIS) i negativnog idealnog rešenja (NIS)*

Za svaku alternativu A_i određuju se komponente c_i^* pozitivnog idealnog rešenja i c_i^- negativnog idealnog rešenja prema sledećim formulama

$$c_i^* = \max_j c_{ij}; C_j \in \Omega_b \text{ or } c_i^- = \min_j c_{ij}; C_j \in \Omega_c; \quad i = 1, 2, \dots, m; j = 1, 2, \dots, n. \quad (8)$$

$$c_i^* = \min_j c_{ij}; C_j \in \Omega_b \text{ or } c_i^- = \max_j c_{ij}; C_j \in \Omega_c; \quad i = 1, 2, \dots, m; j = 1, 2, \dots, n. \quad (9)$$

4. *Određivanje udaljenosti i relativnih bliskostii alternativa A_i pozitivnom idealnom (PIS) i negativnom idealnom rešenju (NIS)*

Za svaku alternativu A_i određuje se distanca od pozitivnog idealnog rešenja D_i^* i negativnog idealnog rešenja D_i^{*-} prema sledećim formulama

$$D_i^* = \left[\sum_{j=1}^m (c_{ij} - c_i^*)^2 \right]^{1/2}; \quad D_i^- = \left[\sum_{j=1}^m (c_{ij} - c_i^-)^2 \right]^{1/2}; \quad i = 1, 2, \dots, m; j = 1, 2, \dots, n; \quad (10)$$

measures and scales of values. Because of that, the normalization of elements of the decision matrix F should be performed to obtain dimensionless values. There are several proposals for this normalization in literature and here will be presented two of them that are most frequently applied.

According to the first proposal for every criterion C_j ($j = 1, 2, \dots, m$) maximal value is determined

and with this value all values f_{ij} in the column C_j of the matrix F are divided. Thus, normalized and non dimensional values a_{ij} that compose normalized decision matrix $A = [a_{ij}]$ are obtained

The second proposal is named a vector procedure in which lengths of corresponding vectors are determined for every criterion

As in the previous case, elements of the decision matrix F are divided by these values and obtained elements a_{ij} of the normalized decision matrix A .

2. *Determination of the weighted matrix C*. Every element of the normalized matrix A is multiplied by the corresponding *weighted coefficient* or *coefficient of significance* w_j to obtain elements c_{ij} of the weighted matrix $C = [c_{ij}]$

3. *Determination of the positive ideal solution (PIS) and negative ideal solution (NIS)*

For every alternative A_i are determined components c_i^* of positive ideal solution and components c_i^- of negative ideal solution according to the next formulas

4. *Determination of distances and relative closeness of the alternatives A_i to positive ideal solution (PIS) and negative ideal solution. (NIS)*

For every alternative A_i the distances D_i^* from the positive ideal solution and D_i^{*-} from the negative ideal solution are determined by the following formulas

i relativne bliskosti RC_i^* pozitivnom idealnom rešenju i RD_i^- i negativnom idealnom rešenju

and relative closeness RC_i^* to positive ideal solution and RC_i^- and to negative ideal solution

$$RC_i^* = D_i^* / (D_i^* + D_i^-), \quad RC_i^- = D_i^- / (D_i^* + D_i^-); \quad i = 1, 2, \dots, m; \quad j = 1, 2, \dots, n. \quad (11)$$

$$RC_i^* + RC_i^- = 1. \quad (12)$$

Ove relativne bliskosti nazivaju se još i *koeficijenti bliskosti* alternative A_i pozitivnom idealnom rešenju i negativnom idealnom rešenju.

Alternative se rangiraju prema ovim koeficijentima. Alternative s manjom relativnom bliskosću RC_i^* pozitivnom idealnom rešenju, i većim relativnom bliskosću RC_i^- negativnom idealnom rešenju, bolje su rangirane. Najbolje rangirana alternativa jeste ona koja ima najmanji koeficijent bliskosti idealnom pozitivnom rešenju RC_i^* .

The relative closeness are named *coefficients of closeness* of the alternative A_i to the positive ideal solution and negative ideal solution respectively. The alternatives are ranked according to these coefficients.

Alternatives with the smaller relative closeness RC_i^* to the positive ideal solution and greater relative closeness RC_i^- to the negative ideal solution are better ranked. The best ranked alternative has the smallest coefficient RC_i^* .

3.1 Primer

Radi lakšeg razumevanja ove procedure, razmotriće se jedan jednostavan primer. Neka postoje tri alternative A_1, A_2 i A_3 i dva kriterijuma C_1 i C_2 , i neka se kriterijum C_1 odnosi na trošak, a kriterijum C_2 na korisnost (dobit), tako da su skupovi kriterijuma

3.1 Example

For the easiest understanding of this procedure, one simple example will be considered. Let exists three alternatives A_1, A_2, A_3 and two criteria C_1, C_2 , and let the criterion C_1 is related to the cost, and criterion C_2 to the benefit (profit), so that the sets of criteria are

$$\Omega_b = C_2, \quad \Omega_c = C_1, \quad (\Omega_c \cap \Omega_b) = \emptyset.$$

Neka su procenjene vrednosti matrice odlučivanja

Let assess values of the decision matrix

$$\mathbf{F} = \begin{matrix} & \begin{matrix} C_1 & C_2 \end{matrix} \\ \begin{bmatrix} 1.00 & 2.00 \\ 3.00 & 1.00 \\ 4.00 & 3.00 \end{bmatrix} & \begin{matrix} A_1 \\ A_2 \\ A_3 \end{matrix} \end{matrix}.$$

Kriterijum C_1 se minimizuje, a kriterijum C_2 se maksimizuje, tako da su prema (3) elementi pozitivnog idealnog rešenja (PIS)

The criterion C_1 is minimised, while criterion C_2 is maximised, so the elements of positive ideal solution (PIS), according to (3), are

$$f_1^\# = \min(1.00, 3.00, 4.00) = 1.00, \quad f_2^\# = \max(2.00, 1.00, 3.00) = 3.00,$$

i negativnog idealnog rešenja (NIS)

and negative ideal solution (NIS)

$$f_1^- = \max(1.00, 3.00, 4.00) = 4.00, \quad f_2^- = \min(2.00, 1.00, 3.00) = 1.00.$$

Ova rešenja predstavljaju dve zamišljene idealne alternative, PIS - $A^* = [1.00 \ 3.00]$ i NIS - $A^- = [4.00 \ 1.00]$.

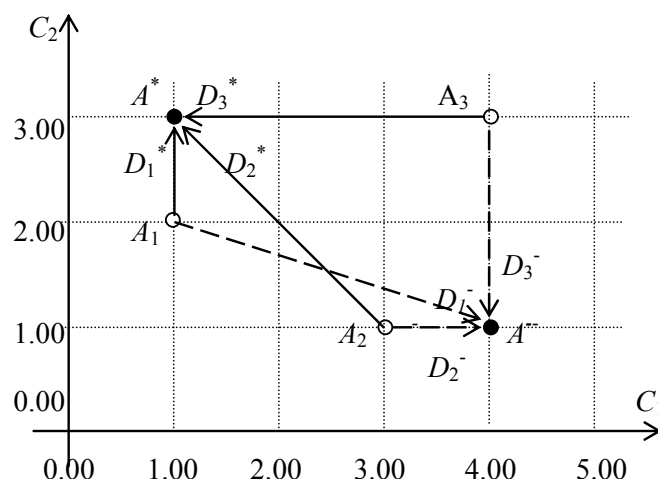
These solutions represent imaginary ideal alternatives, PIS - $A^* = [1.00 \ 3.00]$ and NIS $A^- = [4.00 \ 1.00]$.

U koordinatnom sistemu kriterijuma C_1 i C_2 , na slici 1, sve ove alternative prikazane su kao tačke.

In the coordinate system of criteria C_1 and C_2 , shown in Fig. 1, all the alternatives are presented as points.

Pod uslovom da su koeficijenti težina (značajnosti) oba kriterijuma isti i da su vrednosti elementata matrice \mathbf{F} za oba kriterijuma izraženi u istim jedinicama mere nije neophodno vršiti normalizaciju ovih vrednosti. Određuju se udaljenosti od tačaka A_1, A_2 i A_3 , koje predstavljaju alternative od tačaka A^* i A^- , koje predstavljaju pozitivno (PIS) i negativno (NIS) idealno rešenje respektivno se određuju u sledećem koraku..

Provided that the coefficients of weights (coefficients of importance) for the both of criteria are the same and that the values of elements of the matrix \mathbf{F} for both of criteria are expressed in the same units of measure, it is unnecessary to perform normalisation of these values. Distances of the points A_1, A_2 and A_3 , that represent alternatives, from the points A^* i A^- , that represent positive ideal solution (PIS) and negative ideal solution (NIS) respectively are determined in the next step.



Slika 1. Grafički prikaz alternativa i kriterijuma
Figure 1. Graphical presentation of the alternatives and criteria

Udaljenosti D_i^* ($i = 1,2,3$) alternativa od pozitivnog idealnog rešenja (PIS) jesu:

$$D_1^* = [(1.00 - 1.00)^2 + (2.00 - 3.00)^2]^{1/2} = 1.00,$$

$$D_2^* = [(3.00 - 1.00)^2 + (1.00 - 3.00)^2]^{1/2} = 2.82,$$

$$D_3^* = [(4.00 - 1.00)^2 + (3.00 - 3.00)^2]^{1/2} = 3.00.$$

The distances D_i^* ($i = 1,2,3$) of the alternatives from the positive ideal solution (PIS) are according to (10):

Udaljenosti d_i^{*-} ($i = 1,2,3$) alternativa od negativnog idealnog rešenja (NIS) jesu:

$$D_1^- = [(1.00 - 4.00)^2 + (2.00 - 1.00)^2]^{1/2} = 3.16,$$

$$D_2^- = [(3.00 - 4.00)^2 + (1.00 - 1.00)^2]^{1/2} = 1.00,$$

$$D_3^- = [(4.00 - 4.00)^2 + (3.00 - 1.00)^2]^{1/2} = 2.00.$$

The distances D_i^- ($i = 1,2,3$) of the alternatives from the negative ideal solution (NIS) are according to (10):

Na kraju, sračunavaju se relativne bliskosti alternativa od PIS RC_i^* ($i = 1,2,3$) i relativne udaljenosti alternativa od NIS RC_i^- ($i = 1,2,3$):

$$RC_1^* = 1.00 / (1.00 + 3.16) = 0.24, \quad RC_1^- = 3.16 / (1.00 + 3.16) = 0.76,$$

$$RC_2^* = 2.82 / (2.82 + 1.00) = 0.74, \quad RC_2^- = 1.00 / (2.82 + 1.00) = 0.26,$$

$$RC_3^* = 3.00 / (3.00 + 2.00) = 0.60, \quad RC_3^- = 2.00 / (3.00 + 2.00) = 0.40.$$

At the end, are calculated *relative closeness* to the alternatives RC_i^* ($i=1,2,3$) from PIS and RC_i^- ($i=1,2,3$) from NIS, according to (11), :

Na osnovu ovih rezultata, može se zaključiti da alternativa A_1 ima najmanju udaljenost $D_1^* = 1.00$ i najmanju relativnu bliskost PIS pozitivnom idealnom rešenju $RC_1^* = 0.24$ koje je predstavljeno tačkom A^* . Ova alternativa ima najveću udaljenost $D_1^- = 3.16$ i najmanju relativnu bliskost NIS $RC_1^- = 0.76$ od NIS, koje je predstavljeno tačkom A^- na slici 1. Prema tome, alternativa A_1 je najbliža ili „najsličnija“ pozitivnom idealnom rešenju A^* , pa je zbog toga – najprihvatljivija. Ako se izvrši rangiranje prema relativnoj udaljenosti od pozitivnog idealnog rešenja, onda je redosled alternativa A_1, A_3, A_2 .

From these results may be concluded that alternative A_1 has the smallest distance $D_1^* = 1.00$ and smallest relative closeness from PIS $RC_1^* = 0.24$, which is represented by the point A^* . This alternative has the largest PIS distance $RC_1^- = 3.16$ and the largest relative closeness to NIS $RC_1^- = 0.76$, that is represented by the point A^- in Fig. 1. Therefore, the alternative A_1 is the nearest or "most similar" to the positive ideal solution A^* , and because of that it is most acceptable. If alternatives are ranked according to the relative distance of alternatives from the positive ideal solution, then order of alternatives is A_1, A_3, A_2 .

4 POJAM RASPLINUTOG SKUPA I RASPLINUTOG BROJA

U mnogim realnim situacijama, elementi f_{ij} matrice odlučivanja \mathbf{F} i elementi w_j vektora težina \mathbf{w} ne mogu se tačno izmeriti ili proceniti i prikazati fiksnim realnim brojevima, nego se izražavaju približnim vrednostima. Neki od tih elemenata prikazuju se lingvističkim vrednostima, kao što su „dobar”, „loš”, „visok”, „nizak” i slično. Zbog toga, za ulazne podatke treba koristiti rasplinite brojeve, kao posebnu klasu rasplinitih skupova, pa se tako problem transformiše u problem rasplinitog višekriterijumskog odlučivanja (FMCDMP).

Pojam i definiciju rasplinitog skupa uveo je Lotfi Zadeh 1965. godine, u svom čuvenom radu „Raspliniti skupovi” [19]. On je postavio osnove teorije rasplinitih skupova, i rasplinite logike, teorije mogućnosti, teorije rasplinitih sistema i upravljanja ovim sistemima. Ove teorije su posle toga imale veoma intenzivan razvoj i našle široku primenu u razmatranju i rešavanju brojnih problema teorije i prakse u različitim disciplinama. U stranoj i domaćoj literaturi, postoji veoma mnogo radova, knjiga i publikacija koje se odnose na rasplinite skupove i njihove primene. Ovde se daju kratke definicije pojma rasplinitog skupa i rasplintog broja i neke aritmetičke operacije s tim brojevima.

4.1 Definicija rasplinitog skupa i rasplinitog broja

Neka $X=\{x\}$ označava neku kolekciju objekata ili tačaka prikazanih sa x , onda fuzzy skup \tilde{A} u X jeste skup uređenih parova x i $\mu_{\tilde{A}}(x)$

$$\tilde{A} = \{x, \mu_{\tilde{A}}(x) \mid x \in X\}, \quad (13)$$

gde se $\mu_{\tilde{A}}(x)$ naziva funkcija pripadnosti ili stepen pripadnosti objekta x skupu \tilde{A} . (Zadeh,[19], Zimmermann, [21]).

Skup X Zadeh naziva univerzalni skup, čije elemente x funkcija pripadnosti $\mu_{\tilde{A}}(x)$ preslikava u elemente podskupa realnih brojeva $[0, 1]$, što se simbolički piše

$$\mu_{\tilde{A}}(x) : X \rightarrow [0, 1].$$

Mogu se navesti mnogi primeri fuzzy skupova. Na primer „skup mladih ljudi” jeste fuzzy skup, čija funkcija ili stepen pripadnosti $\mu_{\tilde{A}}(x)$ zavisi od starosti svakog člana toga skupa. Isto tako, „skup odličnih studenata” jeste fuzzy skup, jer funkcija ili stepen pripadnosti svakog studenta ovom skupu zavisi od ostvarene prosečne ocene i nekih drugih bitnih pokazatelja uspeha.

Ako je \tilde{A} fuzzy podskup skupa X , onda je njegov α -nivo ili α -presek neraspliniti skup A_α koji sadrži sve elemente čija je funkcija pripadnosti veća ili jednaka broju α , tj.

$$A_\alpha = \{x \in X \mid \mu_{\tilde{A}}(x) \geq \alpha, 0 < \alpha \leq 1\}. \quad (14)$$

4 NOTION OF FUZZY SET AND FUZZY NUMBER

In many real situations elements f_{ij} of the decision matrix \mathbf{F} and elements w_j of the vector of weights \mathbf{w} cannot be measured or assessed precisely and expressed by the crisp numbers, since they are expressed by approximate values. Some of these elements sometimes may be quantified by linguistic values “good”, “bad”, “high”, “low” and in some other similar way. For these reasons, the fuzzy numbers for input data should be used, and the problem transformed to the fuzzy multiple criteria decision making problem (FMCDMP).

The notion and definition of the fuzzy set has introduced Lotfi Zadeh in his famous paper "Fuzzy sets" [19]. He founded theory of the fuzzy sets and fuzzy logics, theory of possibility, theory of fuzzy systems and control of these systems. These theories have had very intensive development and found wide application in consideration and solution of numerous problems of the theory and practice in different disciplines. In the foreign and domestic literature there are numerous papers, books and other publications that are related on the fuzzy sets and their applications. Here are given some short mathematical definitions of the fuzzy set and fuzzy number and some arithmetic operations with these numbers.

4.1 Definition of the fuzzy set and the fuzzy number

Let $X=\{x\}$ represents some collection of objects or points denoted by x , then a fuzzy set \tilde{A} in X is the set ordered pairs x i $\mu_{\tilde{A}}(x)$

Where $\mu_{\tilde{A}}(x)$ is named a membership function or grade of membership of the object x to the set \tilde{A} . (Zadeh, [19], Zimmermann, [21]).

Zadeh has called the set X universe of discourse, whose elements x membership function $\mu_{\tilde{A}}(x)$ copies into elements of a subset of the real numbers $[0, 1]$, which is written symbolically

Many examples of the fuzzy sets could be cited. For example, a "set of young people" is the fuzzy set, whose membership function or grade of membership $\mu_{\tilde{A}}(x)$ depends on the age of every member of that set. In the same way, a set of excellent students is the fuzzy set, since its membership function of every student depends on an achieved average grade and other basic indicators of his success.

If \tilde{A} is a fuzzy subset of the fuzzy set X , then its α -level or α -cut is a crisp (non fuzzy) set A_α that contains all elements with the membership function which is more or equal to the number α , i.e.

Rasplinuti skup je *konveksan* ako su mu svi α -preseci A_α konveksni skupovi.

Ako univerzalni skup predstavlja skup realnih brojeva R , čiji su elementi x predstavljeni brojnou pravom, onda se rasplinuti skup $\tilde{A} \in R$ naziva *rasplinuti (fuzzy) broj*, s funkcijom pripadnosti $\mu_{\tilde{A}}(x) : R \rightarrow [0,1]$, ako ispunjava sledeće uslove (Dubois and Prade, [5]):

- \tilde{A} je normalan broj, što znači da postoji broj $x_0 \in R$ za koji je $\mu_{\tilde{A}}(x_0) = 1$;
- \tilde{A} je rasplinuto konveksan broj, tj. $\mu_{\tilde{A}}(\lambda x + (1 - \lambda)y) \geq \min\{\mu_{\tilde{A}}(x), \mu_{\tilde{A}}(y)\}$, za sve $x, y \in R, \lambda \in [0,1]$;
- \tilde{A} je odozgo semikontinualan broj (tj. $\mu_{\tilde{A}}^{-1}([\alpha,1])$ zatvoren je za sve $\alpha \in [0,1]$),
- Osnova rasplnutog broja \tilde{A} ($Supp(\tilde{A})$) zatvoren je skup za koji je $\mu_{\tilde{A}}(x) > 0, x \in R$.
- A_α – je α presek rasplnutog (fuzzy) broja je nerasplinuti broj
- $A_\alpha = \{x \in R \mid \mu_{\tilde{A}}(x) \geq \alpha, 0 < \alpha \leq 1\}$, koji predstavlja zatvoreni *interval poverenja*

$$A_\alpha = [A_l(\alpha), A_u(\alpha)], 0 < \alpha \leq 1, \quad (15)$$

$A_l(\alpha)$ i $A_u(\alpha)$ jesu donja i gornja granica ovog intervala. Par funkcija $A_l(\alpha)$ i $A_u(\alpha)$ predstavlja parametarsku prezentaciju rasplnutog broja \tilde{A} .

$$A_l(\alpha) = \inf\{x \in R : \mu_{\tilde{A}}(x) \geq \alpha\}, A_u(\alpha) = \sup\{x \in R : \mu_{\tilde{A}}(x) \geq \alpha\}. \quad (16)$$

Zavisno od funkcije pripadnosti, postoji više tipova rasplnutih brojeva: trougaoni, trapezoidni, broj oblika S i π i drugi. U teoriji i praksi, najčešće se zbog linearnosti funkcija pripadnosti koriste trougaoni i trapezoidni rasplinuti brojevi. U ovom radu se koristi trougaoni rasplinuti broj, prikazan na slici 1. Ovaj broj se obično prikazuje s tri karakteristične vrednosti: donjom a_l , modalnom a_m (za koju je $\mu(a_m)=1$) i gornjom a_u , tj.

$$\tilde{A} = (a_l, a_m, a_u). \quad (17)$$

Funkcije pripadnosti ovog broja jesu:

$$\begin{aligned} \mu_{\tilde{A}}(x) &= 0 \text{ za } x \leq a_l, \\ \mu_{\tilde{A}}(x) &= (x - a_l)/(a_m - a_l) \text{ za } a_l \leq x \leq a_m, \\ \mu_{\tilde{A}}(x) &= (a_u - x)/(a_u - a_m) \text{ za } a_m \leq x \leq a_u, \\ \mu_{\tilde{A}}(x) &= 0 \text{ za } x \geq a_u. \end{aligned} \quad (18)$$

The fuzzy set is *convex* one if all its α -cuts A_α are convex sets.

If universe of discourse is the set of real numbers R , whose elements x are represented by the numeric straight line, then the fuzzy set $\tilde{A} \in R$ is named a *fuzzy number*, with the membership function $\mu_{\tilde{A}}(x) : R \rightarrow [0,1]$, if satisfies the following conditions (Dubois and Prade, [5]):

- \tilde{A} is a normal number, which means that exists a number $x_0 \in R$ for which is $\mu_{\tilde{A}}(x_0) = 1$;
- \tilde{A} is fuzzy convex number, i.e. $\mu_{\tilde{A}}(\lambda x + (1 - \lambda)y) \geq \min\{\mu_{\tilde{A}}(x), \mu_{\tilde{A}}(y)\}$, for all $x, y \in R, \lambda \in [0,1]$;
- \tilde{A} is upper semi continuous (i.e. $\mu_{\tilde{A}}^{-1}([\alpha,1])$ is closed for all $\alpha \in [0,1]$),
- The support of \tilde{A} ($Supp(\tilde{A})$) is bounded for which is $\mu_{\tilde{A}}(x) > 0, x \in R$.
- A_α is α cut of the fuzzy number \tilde{A} , that is a crisp number
- $A_\alpha = \{x \in R \mid \mu_{\tilde{A}}(x) \geq \alpha, 0 < \alpha \leq 1\}$, which represents a closed *interval of confidence*

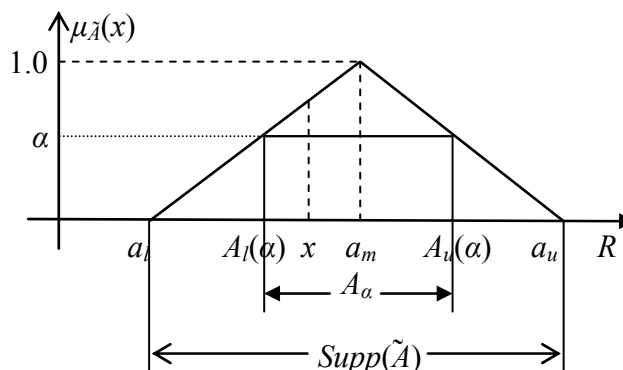
$A_l(\alpha)$ i $A_u(\alpha)$ are lower and upper limits of this interval. The pair of functions of this interval $A_l(\alpha)$ and $A_u(\alpha)$ expresses a parametric presentation of the fuzzy number \tilde{A} .

There are several types of fuzzy numbers depending of membership function: triangular, trapezoidal, S and π shape and others. In the theory and practical applications triangular and trapezoidal fuzzy numbers are used most frequently. Triangular fuzzy number, shown in Fig. 1, is used in this paper. This number is usually represented by three characteristic values: lower a_l , modal a_m (for which is $\mu(a_m)=1$) and upper a_u , i. e.

Za izabrani presek α , parametarska prezentacija rasplinutog broja \tilde{A} jeste

For the chosen α – cut , parametric presentation of the fuzzy number \tilde{A} is

$$A_l(\alpha) = a_l + (a_m - a_l)\alpha, \quad A_u(\alpha) = a_u - (a_u - a_m)\alpha, \quad 0 < \alpha \leq 1. \quad (19)$$



Slika 2. Trougaoni rasplinuti broj
Figure 2. Triangular fuzzy number

4.2 Aritmetičke operacije s rasplnutim brojevima

4.2 Arithmetic operations with fuzzy numbers

Neka su data dva rasplinuta broja \tilde{A} i \tilde{B} pisana u parametarskoj formi

If are given two fuzzy numbers \tilde{A} and \tilde{B} , written in the parametric form

$$A_\alpha = [A_l(\alpha), A_u(\alpha)] \text{ i } B_\alpha = [B_l(\alpha), B_u(\alpha)], \quad (20)$$

onda, primenjujući aritmetičke operacije s tim brojevima, dobija se rasplinuti broj \tilde{C} pisan u parametarskoj formi $C_\alpha = [C_l(\alpha), C_u(\alpha)]$

then, a fuzzy number \tilde{C} written in the parametric form $C_\alpha = [C_l(\alpha), C_u(\alpha)]$ is obtained by applying arithmetic operations with these numbers.

Aritmetičke operacije za $C_l(\alpha)$ i $C_u(\alpha)$, kada su $A_l(\alpha) > 0, B_l(\alpha) > 0$, jesu:

Arithmetic operations for $C_l(\alpha)$ and $C_u(\alpha)$, when, $A_l(\alpha) > 0, B_l(\alpha) > 0$ are:

- za sabiranje:

- for addition:

$$C_l(\alpha) = A_l(\alpha) + B_l(\alpha), \quad C_u(\alpha) = A_u(\alpha) + B_u(\alpha); \quad (21)$$

- za oduzimanje:

- for subtraction:

$$C_l(\alpha) = A_l(\alpha) - B_u(\alpha), \quad C_u(\alpha) = A_u(\alpha) - B_l(\alpha), \quad (22)$$

- za množenje:

- for multiplication:

$$C_l(\alpha) = A_l(\alpha)B_l(\alpha), \quad C_u(\alpha) = A_u(\alpha)B_u(\alpha); \quad (23)$$

- za deljenje:

- for division:

$$C_l(\alpha) = A_l(\alpha) / B_u(\alpha), \quad C_u(\alpha) = A_u(\alpha) / B_l(\alpha), \quad A_l(\alpha) > 0, \quad A_u(\alpha) > 0. \quad (24)$$

4.3 Generalisana očekivana vrednost, varijansa i standardna devijacija slučajnog rasplinutog broja

4.3 Generalized expected value, variance and standard deviation of a random fuzzy number

Ovde predloženi metod za rangiranje alternative zasnovan je na generalisanoj očekivanoj (srednjoj) vrednosti, varijansi i standardnoj devijaciji slučajnog rasplinutog broja, koji predstavlja neki rasplinuti događaj, kako je to definisao Zadeh [20].

The proposed method for ranking alternatives is based on the generalized expected (mean) value, variance and standard deviation of a random fuzzy number that represents some probabilistic fuzzy event, as it is defined by Zadeh [20].

Neka je $P(\tilde{A}) \geq 0$ mera verovatnoće na skupu realnih brojeva R , gde je \tilde{A} slučajni rasplinuti događaj predstavljen slučajnim rasplnutim brojem u skupu realnih brojeva R ($\tilde{A} \in R$); onda je, prema Zadehu [20], verovatnoća slučajnog rasplnutog događaja (rasplnutog broja)

$$P(A) = \int_R \mu_{\tilde{A}(x)} dP = E(\mu_{\tilde{A}}(x)), \quad (25)$$

gde E označava operator očekivane vrednosti funkcije pripadnosti.

Očekivana vrednost $E(\tilde{A})$ rasplnutog broja \tilde{A} u odnosu na meru verovatnoće P jeste

$$E(\tilde{A}) = x_e = \frac{1}{P(\tilde{A})} \int_R x \mu_{\tilde{A}}(x) \frac{dP}{dx} dx. \quad (26)$$

Varijansa $V(\tilde{A})$ slučajnog rasplnutog broja \tilde{A} u odnosu na meru verovatnoće P jeste

$$V(\tilde{A}) = \frac{1}{P(\tilde{A})} \int_R (x - x_e)^2 \mu_{\tilde{A}}(x) dP = \frac{1}{P(\tilde{A})} \int_R x^2 \mu_{\tilde{A}}(x) \frac{dP}{dx} dx - x_e^2. \quad (27)$$

\tilde{A} je, dakle, rasplinuti broj koji ima funkciju pripadnosti $\mu_{\tilde{A}}(x)$, funkciju raspodele verovatnoće $P(\tilde{A})$ i funkciju gustine raspodele verovatnoće $g(x)$. Karakteristične statističke vrednosti $E(\tilde{A})$ i $V(\tilde{A})$, koje se sračunavaju pomoću ovih formula nazivaju se *generalisana očekivana (srednja) vrednost* i *generalisana varijansa slučajnog broja \tilde{A}* .

Ako je funkcija raspodele verovatnoća uniformna za fuzzy broj $\tilde{A} = (a_l, a_m, a_u)$

$$P(\tilde{A}) = 0 \text{ za } x < a_l, P(\tilde{A}) = (x - a_l)/(a_u - a_l) \text{ za } a_l \leq x \leq a_u, P(\tilde{A}) = 0 \text{ za } x > a_u, \quad (28)$$

onda je

$$g(x) = \frac{dP}{dx} = \frac{1}{a_u - a_l}.$$

Kada se ovaj izraz uvrsti u izraze (26) i (27), dobija se za uniformnu raspodelu verovatnoća:

- generalisana očekivana vrednost

$$x_e^U(\tilde{A}) = \frac{\int_R x \mu_{\tilde{A}}(x) dx}{\int_R \mu_{\tilde{A}}(x) dx} \quad (29)$$

- generalisana varijansa

Let $P(\tilde{A}) \geq 0$ be a probability measure over the measurable space of real numbers R , where \tilde{A} is random fuzzy event represented by the fuzzy number in R ($\tilde{A} \in R$), then according to Zadeh [20], the probability of this random fuzzy event (fuzzy number) is

where E denotes an operator of expected value of the membership function.

The expected value (mean) $E(\tilde{A})$ of the fuzzy number \tilde{A} , related to the probability measure P , is

Variance $V(\tilde{A})$ for the random fuzzy number \tilde{A} , related to the probability measure P , is

\tilde{A} is, therefore, the random fuzzy number which has membership function $\mu_{\tilde{A}}(x)$, probability distribution function $P(\tilde{A})$ and probability density function $g(x)$. Characteristic statistical values $E(\tilde{A})$ and $V(\tilde{A})$ calculated from these formulas are called *generalized expected (mean) value* and *generalized variance* of the random fuzzy number \tilde{A} .

If the probability distribution function is uniform for the fuzzy number $\tilde{A} = (a_l, a_m, a_u)$

then

Introducing this expression in the expressions (26) and (27), one obtains for the uniform probability distribution:

- generalized expected (mean) value

- generalized variance

$$V_e^U(\tilde{A}) = \frac{\int_R x^2 \mu_{\tilde{A}}(x) dx}{\int_R \mu_{\tilde{A}}(x) dx} - (x_e^U)^2. \quad (30)$$

Za trouglasti rasplinuti broj $\tilde{A} = (a_l, a_m, a_u)$ ove vrednosti su

For the triangular fuzzy number $\tilde{A} = (a_l, a_m, a_u)$ these values are

$$x_e^U(\tilde{A}) = (a_l + a_m + a_u)/3, \quad (31)$$

$$V_e^U(\tilde{A}) = (a_l^2 + a_m^2 + a_u^2 - a_l a_m - a_l a_u - a_m a_u)/18. \quad (32)$$

Ako je raspodela verovatnoće $P(x)$ trougaona, tako da je proporcionalna funkciji pripadnosti $\mu_{\tilde{A}}(x)$

If the probability distributions function $P(x)$ is triangular, so that it is proportional to the membership function $\mu_{\tilde{A}}(x)$

$$P(x) = k\mu_{\tilde{A}}(x), \quad (33)$$

gde je k factor proporcionalnosti, onda su:

– generalisana očekivana vrednost rasplinutog broja

where k is factor of proportionality then is:

– generalized expected value

$$x_e^T(\tilde{A}) = \frac{\int_R x(\mu_{\tilde{A}}(x))^2 dx}{\int_R (\mu_{\tilde{A}}(x))^2 dx}, \quad (34)$$

– generalisana varijansa

– generalized variance

$$V_e^T(\tilde{A}) = \frac{\int_R x^2(\mu_{\tilde{A}}(x))^2 dx}{\int_R (\mu_{\tilde{A}}(x))^2 dx} - (x_e^T(\tilde{A}))^2. \quad (35)$$

Za trouglasti rasplinuti broj $\tilde{A} = (a_l, a_m, a_u)$ ove vrednosti su

For the triangular fuzzy number $\tilde{A} = (a_l, a_m, a_u)$ these values are

$$x_e^T(\tilde{A}) = (a_l + 2a_m + a_u)/4, \quad (36)$$

$$V_e^T(\tilde{A}) = (3a_l^2 + 4a_m^2 + 3a_u^2 - 4a_l a_m - 2a_l a_u - 4a_m a_u)/80. \quad (37)$$

5 MODIFIKOVANA RASPLINUTA (FUZZY) TOPSIS PROCEDURA

Elementi rasplinite matrice odlučivanja $\tilde{\mathbf{F}}$ su trougaoni rasplinuti brojevi $\tilde{f}_{ij} = (f_{ij}^{(l)}, f_{ij}^{(m)}, f_{ij}^{(u)})$, tako da se ova matrica može prikazati pomoću tri matrice s fiksnim (nerasplnutim) elementima $\tilde{\mathbf{F}} = (\mathbf{F}_l, \mathbf{F}_m, \mathbf{F}_u)$. Rasplinuta TOPSIS procedura izvršava se u nekoliko koraka koji su objašnjeni u ovom radu, uz predloženu modifikaciju. Ovi koraci su: normalizacija, računanje generalisane očekivane vrednosti i standardne devijacije, rangiranje alternativa i izbor najbolje alternative.

MODIFIED FUZZY TOPSIS PROCEDURE

Elements of the fuzzy decision matrix $\tilde{\mathbf{F}}$ are triangular fuzzy numbers $\tilde{f}_{ij} = (f_{ij}^{(l)}, f_{ij}^{(m)}, f_{ij}^{(u)})$, so that this matrix can be expressed by three crisp matrices $\tilde{\mathbf{F}} = (\mathbf{F}_l, \mathbf{F}_m, \mathbf{F}_u)$. Fuzzy TOPSIS procedure performs in several steps that will be explained in this paper with some proposed modification. These steps are: normalization, calculation of generalized expected values and standard deviations, ranking alternatives and choice of the best alternative.

5.1 Normalizacija

Normalizacija se i ovde vrši iz istih razloga iz kojih se to čini i u TOPSIS metodi s fiksnim (nerasplnutim) brojevima – da bi se dobile bezdimenzionalne vrednosti u matrici odlučivanja $\tilde{\mathbf{F}}$. Međutim, zbog rasplnutosti njezinih elemenata, u literaturi postoji nekoliko predloga za normalizaciju (Wang i Elhang, [17]). Ovde će se koristiti metod koji su predložili Ertugrud i Karakasagly [6]. Normalizovane vrednosti elementa \tilde{f}_{ij} rasplnute (fuzzy) matrice odlučivanja $\tilde{\mathbf{F}}$ označeni su sa \tilde{a}_{ij} , i one sačinjavaju normalizovanu rasplnutu matricu odlučivanja $\tilde{\mathbf{A}}$ i sračunavaju se po sledećoj formuli

$$\tilde{a}_{ij} = (f_{ij}^{(l)} / f_i^{*(u)}, f_{ij}^m / f_i^{*(u)}, f_{ij}^u / f_i^{*(u)}); i = 1, 2, \dots, m; j = 1, 2, \dots, n; \quad (38)$$

gde za svaki kriterijum C_i

$$f_i^{*(u)} = \max_j f_{ij}^{(u)}, i = 1, 2, \dots, m. \quad (39)$$

5.2 Određivanje karakterističnih vrednosti elemenata težinski normalizovane matrice odlučivanja $\tilde{\mathbf{C}}$

Elementi \tilde{c}_{ij} težinske normalizovane matrice odlučivanja $\tilde{\mathbf{C}}$ računaju se kao proizvodi dva rasplnuta trouglasta broja \tilde{a}_{ij} i težine w_j koja u većini slučajeva predstavlja *koeficijent značajnosti* kriterijuma C_j

$$\tilde{c}_{ij} = \tilde{a}_{ij} v_i, i = 1, 2, \dots, m; j = 1, 2, \dots, n; \quad (40)$$

Rasplnuti brojevi \tilde{a}_{ij} i \tilde{w}_j se mogu prikazati prema (17)

$$\tilde{a}_{ij} = (a_{ij}^{(l)}, a_{ij}^{(m)}, a_{ij}^{(u)}), \tilde{w}_j = (w_j^{(l)}, w_j^{(m)}, w_j^{(u)}), i = 1, 2, \dots, m; j = 1, 2, \dots, n.$$

Lako se može zaključiti, iz pravila o množenju rasplnutih brojeva (23), da proizvod dva trougaona rasplnuta broja nije trougaoni rasplnuti broj, tako da elementi \tilde{c}_{ij} matrice $\tilde{\mathbf{C}}$ nisu trouglasti rasplnuti brojevi. Međutim, mnogi autori pretpostavljaju, radi uprošćenja procedure, da ovi elementi jesu trouglasti brojevi i sračunavaju elemente težinske fuzzy matrice $\tilde{\mathbf{C}}$ prema sledećoj formuli

$$\tilde{c}_{ij} = (\tilde{a}_{ij}^{(l)} \tilde{w}_j^{(l)}, \tilde{a}_{ij}^{(m)} \tilde{w}_j^{(m)}, \tilde{a}_{ij}^{(u)} \tilde{w}_j^{(u)}), i = 1, 2, \dots, m; j = 1, 2, \dots, n. \quad (41)$$

U svom prethodnom radu [16], autori su izveli obrasce za tačno određivanje ovih rasplnutih brojeva koji nisu trougaoni, i predložili proceduru s generalisanim očekivanim vrednostima e_{ij} i varijansama v_{ij} proizvoda rasplnutih brojeva $\tilde{c}_{ij} = \tilde{a}_{ij} \tilde{w}_j$

5.1 Normalization

Normalization is performed here due to the same reasons as in TOPSIS method with the crisp numbers to obtain dimensionless values in the decision matrix $\tilde{\mathbf{F}}$. However, due to fuzziness of its elements, there are several proposals for the normalization (Wang and Elhang, [17]). Here, a method which is proposed by Ertugrud and Karakasagly [6] is used. Normalized values of elements \tilde{f}_{ij} are denoted as \tilde{a}_{ij} , and they constitute the normalized fuzzy matrix $\tilde{\mathbf{A}}$ and they are calculated by the following formula

$$\tilde{a}_{ij} = (f_{ij}^{(l)} / f_i^{*(u)}, f_{ij}^m / f_i^{*(u)}, f_{ij}^u / f_i^{*(u)}); i = 1, 2, \dots, m; j = 1, 2, \dots, n; \quad (38)$$

where for every criterion C_i

$$f_i^{*(u)} = \max_j f_{ij}^{(u)}, i = 1, 2, \dots, m. \quad (39)$$

5.2 Determination of characteristic values of the weighted normalized decision matrix $\tilde{\mathbf{C}}$

Elements \tilde{c}_{ij} of the weighted decision matrix $\tilde{\mathbf{C}}$ are calculated as a product of two fuzzy numbers \tilde{a}_{ij} and the weight \tilde{w}_j , which in many cases represents *coefficient of significance* of the alternative C_j

$$\tilde{c}_{ij} = \tilde{a}_{ij} v_i, i = 1, 2, \dots, m; j = 1, 2, \dots, n; \quad (40)$$

Fuzzy numbers \tilde{a}_{ij} i \tilde{w}_j may be shown according to (17)

$$\tilde{a}_{ij} = (a_{ij}^{(l)}, a_{ij}^{(m)}, a_{ij}^{(u)}), \tilde{w}_j = (w_j^{(l)}, w_j^{(m)}, w_j^{(u)}), i = 1, 2, \dots, m; j = 1, 2, \dots, n.$$

It is easy to conclude from the rule of multiplication of fuzzy numbers (23), that product of two fuzzy triangular numbers is not a triangular fuzzy number, hence elements \tilde{c}_{ij} of the fuzzy matrix $\tilde{\mathbf{C}}$ are not triangular fuzzy numbers. However many authors suppose, due to simplicity of the procedure, that these numbers are triangular ones and calculate elements of this matrix by the simplified formula

In the earlier paper written by these authors [16], a procedure with the generalized expected values e_{ij} and variances v_{ij} of the fuzzy numbers products $\tilde{c}_{ij} = \tilde{a}_{ij} \tilde{w}_j$ has been proposed.

$$e_{ij} = x_e(\tilde{c}_{ij}), \quad v_{ij} = V(\tilde{c}_{ij}); \quad i = 1, 2, \dots, m; \quad j = 1, 2, \dots, n. \quad (42)$$

U toj proceduri, brojevi \tilde{c}_{ij} tretiraju se kao slučajni fuzzy događaji koji s jedne strane imaju odgovarajuću raspodelu verovatnoće događanja, a s druge funkciju pripadnosti rasplinutom (fuzzy) skupu \tilde{A} .

Ove vrednosti su elementi matrica \mathbf{E} i \mathbf{V} respektivno, a računaju se prema formulama izvedenim u pomenutom radu [16], zavisno od izabrane raspodele verovatnoća fuzzy događaja, koje mogu biti uniformne ili trougaone (proporcionalne).

In this procedure, the fuzzy numbers \tilde{c}_{ij} are assumed as fuzzy events that have a corresponding probability distribution as well as membership function to the fuzzy set \tilde{A} .

These values are elements of matrices \mathbf{E} and \mathbf{V} respectively and they are calculated by the formulas that are given in the mentioned paper [16], depending on the chosen probability distribution of fuzzy events, which may be uniform or triangular (proportional) one.

$$e_{ij} = x_e(\tilde{c}_{ij}) = \frac{M_1(\tilde{c}_{ij})}{F(\tilde{c}_{ij})}, \quad v_{ij}(\tilde{c}_{ij}) = \frac{M_2(\tilde{c}_{ij})}{F(\tilde{c}_{ij})} - (x_e(\tilde{c}_{ij}))^2, \quad \sigma_{ij} = (v_{ij}(\tilde{c}_{ij}))^{1/2}. \quad (43)$$

Za uniformnu raspodelu slučajne rasplinite promenljive:

For the uniform distribution of a random fuzzy variable are:

$$F(\tilde{c}_{ij}) = \frac{\bar{B}_l - \bar{B}_u}{2} + \frac{2(\bar{C}_l - \bar{C}_u)}{3}, \quad (44)$$

$$M_1(\tilde{c}_{ij}) = \frac{\bar{A}_l \bar{B}_l - \bar{A}_u \bar{B}_u}{2} + \frac{\bar{B}_l^2 - \bar{B}_u^2}{3} + \frac{3(\bar{B}_l \bar{C}_l - \bar{B}_u \bar{C}_u)}{4} + \frac{2(\bar{A}_l \bar{C}_l - \bar{A}_u \bar{C}_u)}{3} + \frac{2(\bar{C}_l^2 - \bar{C}_u^2)}{5}, \quad (45)$$

$$M_2(\tilde{c}_{ij}) = \frac{\bar{A}_l^2 \bar{B}_l - \bar{A}_u^2 \bar{B}_u}{2} + \frac{\bar{B}_l^3 - \bar{A}_u^3}{4} + \frac{5(\bar{B}_l \bar{C}_l^2 - \bar{B}_u \bar{C}_u^2)}{6} + \frac{2(\bar{A}_l \bar{B}_l^2 - \bar{A}_u \bar{B}_u^2)}{3} + \frac{3(\bar{A}_l \bar{B}_l \bar{C}_l - \bar{A}_u \bar{B}_u \bar{C}_u)}{2} + \frac{4(\bar{B}_l^2 \bar{C}_l - \bar{B}_u^2 \bar{C}_u)}{5} + \frac{2(\bar{A}_l^2 \bar{C}_l - \bar{A}_u^2 \bar{C}_u)}{3} + \frac{2(\bar{C}_l^3 - \bar{C}_u^3)}{7} + \frac{4(\bar{A}_l \bar{C}_l^2 - \bar{A}_u \bar{C}_u^2)}{5}. \quad (46)$$

Za trougaonu (proporcionalnu) raspodelu slučajne rasplinite promenljive su:

For the triangular (proportional) distribution of a random fuzzy variable are:

$$F(\tilde{c}_{ij}) = \frac{\bar{B}_l - \bar{B}_u}{3} + \frac{2(\bar{C}_l - \bar{C}_u)}{2}, \quad (47)$$

$$M_1(\tilde{c}_{ij}) = \frac{\bar{A}_l \bar{B}_l - \bar{A}_u \bar{B}_u}{3} + \frac{\bar{B}_l^2 - \bar{B}_u^2}{4} + \frac{3(\bar{B}_l \bar{C}_l - \bar{B}_u \bar{C}_u)}{5} + \frac{\bar{A}_l \bar{C}_l - \bar{A}_u \bar{C}_u}{2} + \frac{\bar{C}_l^2 - \bar{C}_u^2}{3}, \quad (48)$$

$$M_2(\tilde{c}_{ij}) = \frac{\bar{A}_l^2 \bar{B}_l - \bar{A}_u^2 \bar{B}_u}{3} + \frac{\bar{B}_l^3 - \bar{A}_u^3}{5} + \frac{5(\bar{B}_l \bar{C}_l^2 - \bar{B}_u \bar{C}_u^2)}{7} + \frac{\bar{A}_l \bar{B}_l^2 - \bar{A}_u \bar{B}_u^2}{2} + \frac{6(\bar{A}_l \bar{B}_l \bar{C}_l - \bar{A}_u \bar{B}_u \bar{C}_u)}{5} + \frac{2(\bar{B}_l^2 \bar{C}_l - \bar{B}_u^2 \bar{C}_u)}{3} + \frac{\bar{A}_l^2 \bar{C}_l - \bar{A}_u^2 \bar{C}_u}{2} + \frac{\bar{C}_l^3 - \bar{C}_u^3}{4} + \frac{2(\bar{A}_l \bar{C}_l^2 - \bar{A}_u \bar{C}_u^2)}{3}. \quad (49)$$

U ovim izrazima su:

In these expressions are:

$$\bar{A}_l = a_{ij}^{(l)} w_i^{(l)}, \quad \bar{B}_l = (a_{ij}^{(m)} - a_{ij}^{(l)}) w_i^{(l)} + (w_i^{(m)} - w_i^{(l)}) a_{ij}^{(l)}, \quad \bar{C}_l = (a_{ij}^{(m)} - a_{ij}^{(l)}) (w_i^{(m)} - w_i^{(l)}), \quad (50)$$

$$\bar{A}_u = a_{ij}^{(u)} w_i^{(u)}, \quad \bar{B}_u = (a_{ij}^{(m)} - a_{ij}^{(u)}) w_i^{(u)} + (w_i^{(m)} - w_i^{(u)}) a_{ij}^{(u)}, \quad \bar{C}_u = (a_{ij}^{(m)} - a_{ij}^{(u)}) (w_i^{(m)} - w_i^{(u)}), \quad (51)$$

$$i = 1, 2, \dots, m; \quad j = 1, 2, \dots, n.$$

5.3 Sračunavanje očekivanog idealno pozitivnog i idealno negativnog rešenja

Po kolonama matrice očekivanih vrednosti \mathbf{E} , za svaki kriterijum C_j pronalazi se očekivano pozitivno idealno rešenje e_j^* i negativno idealno rešenje e_j^- po sledećim formulama

$$e_i^* = \{ \max_i e_{ij} : j \in \Omega_b \text{ or } \min_i e_{ij} : j \in \Omega_c \}, \quad (52)$$

$$e_i^- = \{ \min_i e_{ij} : j \in \Omega_b \text{ or } \max_i e_{ij} : j \in \Omega_c \}. \quad (53)$$

Ove vrednosti su elementi vektora očekivanog idealno pozitivnog (EPIS) A_e^* i očekivanog idealno negativnog rešenja (ENIS) A_e^-

$$A^* = [e_1^*, e_2^*, \dots, e_n^*], \quad A^- = [e_1^-, e_2^-, \dots, e_n^-] \quad (54)$$

Varijanse koje odgovaraju očekivanim vrednostima označene su sa v_i^* i v_i^- i one čine vektore

$$V^* = [v_1^*, v_2^*, \dots, v_n^*], \quad V^- = [v_1^-, v_2^-, \dots, v_n^-]. \quad (55)$$

5.4 Određivanje očekivanog Euklidoveg rastojanja i njegove varijanse od EPIS i ENIS

Očekivana Euklidova rastojanja ED_i^* i ED_i^- za svaku alternativu A_j od očekivanog pozitivnog rešenja EPIS A_e^* i očekivanog negativnog idealnog rešenja ENIS A_e^- određuju se prema sledećim formulama

$$ED_i^* = \left[\sum_{j=1}^n (e_{ij} - e_j^*)^2 \right]^{1/2}, \quad i = 1, 2, \dots, m; \quad (56)$$

$$ED_i^- = \left[\sum_{j=1}^n (e_{ij} - e_j^-)^2 \right]^{1/2}, \quad i = 1, 2, \dots, m. \quad (57)$$

Varijanse V_j^* rastojanja alternative A_j od očekivanog pozitivnog idealnog rešenja EPIS A_e^* i varijanse V_j^- od očekivanog negativnog idealnog rešenja ENIS A_e^- , sračunavaju se prema sledećim formulama, uzimajući u obzir pravilo o sabiranju i oduzimanju varijansi međusobno nezavisnih slučajnih vrednosti

$$V_i^* = \sum_{j=1}^n (v_{ij} + v_j^*), \quad V_i^- = \sum_{j=1}^n (v_{ij} + v_j^-), \quad i = 1, 2, \dots, m. \quad (58)$$

5.3 Calculation of the expected ideal positive and ideal negative solutions

For every criterion C_j are found the best expected positive ideal solution e_j^* and the worst negative ideal solution e_j^- in the columns of the matrix of expected values \mathbf{E} by the following formulae

These values are elements of vectors of the expected positive ideal solution (EPIS) A_e^* and expected negative ideal solution (ENIS) A_e^- solution

Variations that correspond to these expected values are denoted as v_i^* and v_i^- and they constitute vectors

5.4 Calculation of the expected Euclidean distances and its variance from EPIS and ENIS.

The expected Euclidean distances ED_i^* i ED_i^- for every alternative A_j from the expected positive ideal solution EPIS A_e^* and from the expected negative ideal solution ENIS A_e^- are calculated by formulas

Variance V_j^* of the distance of alternative A_j from the expected positive ideal solution EPIS A_e^* and variance V_j^- from the expected negative ideal solution ENIS A_e^- , are calculated by the following formulas, taking into account rule for summation and subtraction of variances for the mutually independent random variables

Odgovarajuće standardne devijacije σ_i^* udaljenosti svake alternative A_i od pozitivnog idealnog rešenja A^* i standardne devijacije σ_i^- svake alternative A_i od negativnog idealnog rešenja A^- jesu

$$\sigma_i^* = [V_i^*]^{1/2}, \quad \sigma_i^- = [V_i^-]^{1/2}; \quad i = 1, 2, \dots, m. \quad (59)$$

Dobijena očekivana rastojanja svake alternative A_i od pozitivnog idealnog i negativnog idealnog rešenja, kasnije se koriste za formulisanje pravila za rangiranje alternativa i za izbor najbolje alternative. Očekivana rastojanja od očekivanog pozitivnog idealnog i očekivanog negativnog idealnog rešenja predstavljena su kao rasplinuti brojevi ili kao slučajni (probabilistički) rasplinuti događaji koje opisuju sračunate vrednosti.

5.5 Očekivana relativna bliskost i relativna standardna devijacija do EPIS and ENIS i rangiranje alternativa

Slično kao u TOPSIS metodi s fiksnim podacima, očekivana relativna bliskost svake alternative A_i do očekivanog pozitivno idealnog rešenja ERC_i^* i očekivanog negativnog idealnog rešenja ERC_i^- su bitni indikatori za rangiranje alternativa. Ove vrednosti računaju se prema sledećim formulama

$$ERC_i^* = ED_i^* / (ED_i^* + ED_i^-), \quad i = 1, 2, \dots, m; \quad (60)$$

$$ERC_i^- = ED_i^- / (ED_i^* + ED_i^-), \quad i = 1, 2, \dots, m. \quad (61)$$

Alternativa s manjom vrednošću ERC_i^* i većom vrednošću ERC_i^- bolje je rangirana.

Za rangiranje rasplnutih brojeva, Lee i Li [11] upotrebili su generalisanu srednju vrednost i standardnu devijaciju, koje su zasnovane na merama verovatnoće rasplnutih događaja. Cheng [4] je poboljšao ovaj metod koristeći *koeficijent varijacije* CV , kao relativnu meru varijanse koja povezuje, kako je to poznato iz Statistike, standardnu devijaciju i srednju vrednost. Prema ovom postupku, sračunavaju se koeficijenti varijacije CV_i^* i CV_i^- za distancu alternative A_i ($i = 1, 2, \dots, m$) od očekivanog pozitivnog idealnog rešenja i očekivanog negativnog idealnog rešenja respektivno

$$CV_i^* = \sigma_i^* / ED_i^*, \quad CV_i^- = \sigma_i^- / ED_i^-, \quad i = 1, 2, \dots, m. \quad (62)$$

Alternativa koja ima veću CV_i^* vrednost, a manju CV_i^- ima bolju poziciju na rang-listi. Rangiranje alternativa na ovaj način je jednostavno, ali nekad ima određene nedostatke. Moguć je slučaj poređenja alternativa A_i i A_k koje imaju očekivana rastojanja od

Corresponding standard deviation σ_i^* of the distance of each alternative A_i from the expected ideal positive solution A^* and standard deviation σ_i^- of each alternative A_i from the expected negative ideal solution A^- are

These characteristic values of expected distance of each alternative A_i from the expected positive ideal solution A_e^* and the expected negative ideal solution A_e^- are further used to formulate rules for ranking alternatives and for choice of the best alternative. The expected distances from these solutions are assumed as the random fuzzy numbers or probabilistic fuzzy events described by these values.

5.5 Expected relative closeness and relative standard deviation to EPIS and ENIS and ranking alternatives

Like in the TOPSIS method with crisp data, expected relative closeness ERC_i^* of each alternative A_i to the expected positive ideal solution and expected negative ideal solution ERC_i^- are important indicators for ranking alternatives. These values are calculated by the following formulae

Alternative with smaller ERC_i^* and bigger ERC_i^- are better ranked.

For ranking fuzzy numbers Lee and Li [11] used the generalized mean and standard deviation based on the probability measure of fuzzy events. Cheng [4] improved this method using *coefficient of variation* CV , as a relative measure of the variance that relates, as it is known from Statistics, the standard deviation and the mean value. According to this method coefficients of variation CV_i^* and CV_i^- for the distance of the alternative A_i ($i = 1, 2, \dots, m$) are calculated from the positive expected ideal solution A_e^* and expected negative ideal solution A_e^- , respectively

Alternative with bigger CV_i^* and smaller CV_i^- has the better rank on the rank list. Ranking alternatives in this way are simple, but sometimes has some disadvantages. It is possible when comparing two alternatives A_i and A_k which have expected distances from positive ideal solutions $ED_i^* > ED_k^*$ and

pozitivnog idealnog rešenja $ED_i^* > ED_k^*$ i $CV_i^* < CV_k^*$. Prema ovom pravilu rangiranja, alternativa A_k je bolje rangirana od alternative A_i . Slučaj, alternativu A_k treba bolje rangirati od alternative A_i . Ovaj zaključak neće biti prihvaćen od strane donosioca odluka ako je razlika između CV_i^* i CV_k^* mala. U tom slučaju, naročito kada alternativa A_k ima manju očekivanu relativnu blizinu od alternative A_i , tj. $ERC_k^* < ERC_i^*$. Rangiranje prema očekivanoj relativnoj blizskosti ima prednost u odnosu na druga pravila rangiranja. Međutim, u praksi treba koristiti sva pravila, a potom analizirati dobijene rezultate i donosiocu odluke predložiti alternativu koja maksimalno zadovoljava ova pravila.

6 RASPODELA RASPOLOŽIVE KOLIČINE NOVCA ZA ODRŽAVANJE OBJEKATA

Raspoloživa količina novca Q , opredeljena za održavanje objekata, može se raspodeliti na osnovu dobijene rang-liste, prema sledećim formulama

– za rang-listu prema ERC_i^*

$$Q_{ci} = (KIC)_i Q, \quad i=1,2,\dots,m; \quad (63)$$

– za rang listu prema CV_i^*

$$Q_{vi} = (KIV)_i Q, \quad i=1,2,\dots,m; \quad (64)$$

gde su $(KIC)_i$ i $(KIV)_i$ koeficijenti raspodele količine novca Q , koji se sračunavaju prema sledećim formulama

$$(KIC)_i = \frac{ERC_i^*}{\sum_{i=1}^m ERC_i^*}, \quad (KIV)_i = \frac{CV_i^*}{\sum_{i=1}^m CV_i^*}, \quad i=1,2,\dots,m. \quad (65)$$

Prema izloženoj proceduri, autori su napisali odgovarajući računarski program FUZZY_TOPSIS korišćenjem MATLAB programskog sistema.

7 PRIMER

Ovaj primer, koji je u vezi s procenom rizika mostova, preuzet je iz rada Wang i Ehleng [17],[18], u kome je problem rešen na sasvim drugačiji način.

Prema Britanskoj agenciji za auto-puteve [2], rizik mosta definiše se kao bilo koji događaj ili hazard koji može onemogućiti postizanje poslovnih ciljeva ili ostvarivanja očekivanja zainteresovanih strana (vlasnika, deoničara, korisnika i dr.) i definiše se kao proizvod verovatnoće i posledice ostvarenog događaja.

U primeru je analizirano pet mostovskih konstrukcija BS_1, BS_2, \dots, BS_5 koje su predstavljene kao alternative A_1, A_2, \dots, A_5 . Sve posledice i verovatnoće rizičnih događaja procenjene su na osnovu evidencija i procena tri inženjera eksperta, imajući u vidu četiri kriterijuma: *sigurnost* (C_1), *funkcionalnost* (C_2), *održivost* (C_3) i *okruženje* (C_4). Eksperti su takođe procenili i koeficijenate značaja alternativa. Ove vrednosti izražene su kao lingvističke i numeričke vrednosti, koje su

$CV_i^* < CV_k^*$. According to this ranking rule, alternative A_k is better ranked than alternative A_i . This conclusion will not be accepted by the decision maker if differences between CV_i^* and CV_k^* are small. In such a case alternative A_k will be ranked better than alternative A_i , especially when alternative A_k has smaller expected relative closeness than alternative A_i , i.e.

$ERC_k^* < ERC_i^*$. Ranking according to the expected relative closeness have advantage over other rules. However, in practice all the rules should be applied, then, the obtained results analyzed and the alternative which best satisfies these rules should be proposed to the decision maker.

6 DISTRIBUTION OF AVAILABLE AMOUNT OF MONEY FOR OBJECTS MAINTENANCE

An available amount of money Q , which is assigned for the maintenance of considered objects, should be delivered according to the obtained rank list by the following formulae

– for the rank list according to ERC_i^* ,

– for the rank list according to CV_i^* ,

where $(KIC)_i$ and $(KIV)_i$ coefficients of distribution of the amount of money Q that are calculated according to the following formulas

According to this procedure, the authors have written a corresponding computer program FUZZY_TOPSIS in MATLAB programming system.

7 EXAMPLE

This example, which is related to the bridge risk assessment, is taken from papers written by Wang and Ehleng [17],[18] where this problem is solved in quite different way.

According to British Highway Agency [2] bridge risk is defined as any event or hazard that could hinder the achievement of business goals or the delivery of stakeholder expectations and it is defined as product of the likelihood (probability) and consequence of the occurred event.

In this example five bridge structures BS_1, BS_2, \dots, BS_5 are considered which represent alternatives A_1, A_2, \dots, A_5 . All consequences and probabilities of the risk events are assessed on the base of evidence and engineering judgment by three experts against four criteria: *safety* (C_1), *functionality* (C_2), *sustainability* (C_3) and *environment* (C_4). The significance coefficients of alternatives are also assessed by experts. These values

konačno transformisane u trougaone fuzzy brojeve. Dobile vrednosti su elementi fuzzy matrice odlučivanja $\tilde{F} = (F_l, F_m, F_u)$ i predstavljaju nivo rizika konstrukcije mosta BS_i u odnosu na kriterijum C_j ($i=1,2,\dots,5$; $j=1,2,\dots,4$). Zadatak je odrediti optimalnu shemu (redosled rangiranja) i koeficijente raspodele količine novčanih sredstava Q za održavanje mostova.

are assessed as linguistic and numeric variables that are finally transformed into triangular fuzzy numbers. These values are elements of the fuzzy decision matrix $\tilde{F}=(F_l, F_m, F_u)$ and denotes levels of risk of bridge structure BS_i against criterion C_j ($i=1,2,\dots,5$; $j=1,2,\dots,4$). The task is to determine optimal scheme (rank order) and coefficients of distribution of available amount of money Q for the bridge maintenance.

$$F_l = \begin{bmatrix} 73 & 38 & 62 & 15 \\ 62 & 62 & 38 & 22 \\ 27 & 73 & 10 & 15 \\ 0 & 62 & 62 & 27 \\ 0 & 0 & 62 & 73 \end{bmatrix}, \quad F_m = \begin{bmatrix} 85 & 73 & 85 & 50 \\ 85 & 85 & 73 & 50 \\ 62 & 85 & 38 & 50 \\ 0 & 85 & 85 & 62 \\ 0 & 0 & 85 & 85 \end{bmatrix}, \quad F_u = \begin{bmatrix} 100 & 95 & 100 & 85 \\ 100 & 100 & 95 & 78 \\ 90 & 100 & 73 & 85 \\ 5 & 100 & 100 & 90 \\ 5 & 10 & 100 & 100 \end{bmatrix}.$$

$$w_l = [0.77 \ 0.50 \ 0.30 \ 0.13], \quad w_m = [0.93 \ 0.70 \ 0.50 \ 0.30], \quad w_u = [1.00 \ 0.87 \ 0.70 \ 0.50].$$

Pošto se rangira prema najvećem riziku, podskupovi Ω_b i Ω_c jesu

Since the rank order is calculated according to high level of risk, the subsets Ω_b and Ω_c are

$$\Omega_b = (C_1, C_2, C_3, C_4), \quad \Omega_c = \emptyset.$$

Korišćenjem računarskog programa FUZZY TOPSIS, koji su razvili autori ovog rada, dobijeni su odgovarajući rezultati, sumirani u sledećoj tabeli.

The corresponding results summarized in the following table are obtained by using computer program FUZZY TOPSIS developed by the authors of this paper.

Tabela 1. Sumarni rezultati
Table 1. Summary results

Rang alternative Rank of alternative	Očekivana udaljenost. alter. ED_i^* Expected distance of altern. ED_i^*	Očekivana relat. blisk. altern. ERC_i^* Expect. relat. closen. of altern. ERC_i^*	$(KIC)_i$ %	Koef. varijanse alternative CV_i^* Coeff. of var. of alternat. CV_i^*	$(KIV)_i$ %
1	$A_2=BS_2$ 0.1203	$A_2=BS_2$ 0.1142	28.7	$A_2=BS_2$ 0.9089	28.6
2	$A_1=BS_1$ 0.1402	$A_1=BS_1$ 0.1322	28.1	$A_1=BS_1$ 0.8455	26.5
3	$A_3=BS_3$ 0.3141	$A_3=BS_3$ 0.2846	23.1	$A_3=BS_3$ 0.7510	23.5
4	$A_4=BS_4$ 0.7684	$A_4=BS_4$ 0.5651	14.1	$A_4=BS_4$ 0.4795	15.0
5	$A_5=BS_5$ 0.9584	$A_5=BS_5$ 0.8129	6.0	$A_5=BS_5$ 0.2028	6.4

Na osnovu dobijenih rezultata, datih u ovoj tabeli, može se zaključiti:

According to the obtained results, given in this table, the following may be concluded:

- Konstrukcija mosta BS_2 (alternativa A_2) ima najmanju očekivanu udaljenost od pozitivnog idealnog rešenja, tj. rešenja s najvećim nivoom rizika;
- Konstrukcija mosta BS_1 (alternativa A_1) ima sve karakteristične vrednosti koje su vrlo bliske vrednostima konstrukcije BS_2 , pa tako ove dve konstrukcije imaju praktično isti nivo rizika i zahtevaju iste količine novca za održavanje;
- Konstrukcije mostova BS_4 i BS_5 imaju manje karakteristične vrednosti i manji nivo rizika, pa samim tim zahtevaju manju količinu novca za održavanje od konstrukcija BS_1 i BS_2 ;
- Redosledi na osnovu očekivane relativne bliskosti ERC_i^* i generalizovanog koeficijenta varijacije CV_i^* u ovom slučaju su isti;
- Koeficijenti raspodele investicija $(KIC)_i$ i $(KIV)_i$ u ovom slučaju su vrlo bliske vrednosti za sve konstrukcije mostova.

- Bridge structure BS_2 (alternative A_2) has the smallest value of the expected distance from ideal positive solution, i.e. solution with the highest values of degree of risk;
- Bridge structure BS_1 (alternative A_1) has all characteristic values that are very close to BS_2 , so that these two structures have practically the same degree of risk and require the same amount of money for the maintenance;
- Bridge structures BS_4 and BS_5 have smaller characteristic values and smaller level of risk, so that they require smaller amount of money for the maintenance in comparison with structures BS_1 and BS_2 ;
- Rank list made by the expected relative closeness ERC_i^* and generalized coefficient of variation CV_i^* in this case are the same;
- Coefficients of investment distribution $(KIC)_i$ and $(KIV)_i$ are very close for all bridge structures in this case.

8 ZAKLJUČAK

Rasplinuti TOPSIS metod omogućava kompletnije, fleksibilnije i realnije modeliranje višekriterijumskog odlučivanja od nerasplinutog TOPSIS metoda s fiksnim vrednostima. U rasplinutom TOPSIS metodu moguće je uvesti neprecizne ulazne podatke za matricu odlučivanja i težine kriterijuma. Metod predložen u ovom radu zasnovan je na generalisanoj očekivanoj vrednosti i varijansi proizvoda elemenata matrice odlučivanja i težina kriterijuma. Za ove proizvode izvedene su odgovarajuće formule za njihovo tačno sračunavanje. Stoga, predloženi metod pruža donosiocu odluka tačnije i relevantnije rezultate nego klasični TOPSIS, što je važno za donošenje korisnih odluka. Ovaj metod, uz korišćenje pomenutog računarski programa, je upotrebljen za rangiranje alternativa, odnosno varijanti trase za buduću železničku prugu Pljevlja – Bijelo Polje – granica sa Kosovom i Metohijom, kao i za još neke investicione projekte. Metod može biti korisno upotrebljen za rangiranje alternativa i optimalnu raspodelu investicionih sredstava na projekte, optimalnu procenu rizika različitih tipova objekata, optimalan izbor objekata za rekonstrukciju, izbor najpovoljnijeg izvođača radova na tenderskim procedurama i u mnogim drugim slučajevima višekriterijumskog odlučivanja u građevinarstvu.

ZAHVALNOST

Ovaj rad je deo naučnoistraživačkog projekta "Upravljanje realizacijom velikih investicionih projekata" TR-16011", koji je podržalo Ministarstvo prosvete i nauke Republike Srbije i koji je urađen na Građevinskom fakultetu Univerziteta u Beogradu.

9 LITERATURA REFERENCES

- [1] Adey, B., Hajdin, R., Brühwiler, E. (2003), „Risk-based approach to the determination of optimal interventions for bridges affected by multiple hazards”, *Engineering Structures*, Vol. 25, pp. 903-912.
- [2] British Highway Agency (2004), Value management of the structures renewal programme, Version 2.2.
- [3] Chen, S.-J. and Hwang, C.-L., (1992), „Fuzzy multiple attribute decision making methods and application”, *Lecture Notes in Economics and Mathematical Sciences*, Springer, New York.
- [4] Cheng, C.-H. (1998), „A new approach for ranking fuzzy numbers by distance method”. *Fuzzy sets and systems*, Vol. 95, pp. 307–317.
- [5] Dubois, D. and Prade, H. (1978), „Operations on fuzzy numbers”, *Int. Journal of System Sciences*, Vol. 9, pp 307/317.
- [6] Ertugrud, I. and Karakasogly, N. (2008), „Comparison of fuzzy AHP and TOPSIS methods for facility location”, *International Journal of Advanced Manufacture and Technology*, Vo. 39, pp. 783–795.
- [7] Hwang, C.-L., Yoon, K. (1981), *Multiple Attribute Decision Making an Applications*, Springer-Verlag, New York.
- [8] Folić, R., (editor) (2011), Proc. of VI Conf. „Assessment, Maintenance and Rehabilitation of Structures and Settlements”, Association of Civil Engineers of Serbia, 710 p.
- [9] Folić, R., (editor) (2011), Proc. of VII Conf. „Assessment, Maintenance and Rehabilitation of Structures and Settlements”, Association of Civil Engineers of Serbia, 608 p.
- [10] Folić, R., (editor) (2013), Proc. of VIII Conf. „Assessment, Maintenance and Rehabilitation of Structures and Settlements”, Association of Civil Engineers of Serbia, 638 p.
- [11] Lee, E. S and Li, R. L. (1988), „Comparison of fuzzy numbers based on probability measure of fuzzy events”. *Comput Math Appl*, Vol. 15, pp. 887–896.

8 CONCLUSION

Fuzzy TOPSIS method enables more complete, flexible and realistic modelling of the multiple criteria decision making problems than crisp TOPSIS method with crisp values. In the Fuzzy TOPSIS it is possible to introduce imprecise input data for the decision matrix and weights of criteria. The method proposed in this paper is based on the generalised expected values and variances of products of the decision matrix elements and weights of criteria. Thus, corresponding formulas and their exact calculation are derived for these products. Therefore, proposed method provides more accurate and relevant results for the decision maker in comparison with classic TOPSIS, which is important for useful decision making. This method with corresponding computer program is used for ranking traces of the future railway Pljevlja – Bijelo Polje – Border with Kosovo and Metohija, as for some other investment projects. The method may be used successfully for ranking of alternatives and optimal distribution of investments on the projects, optimal risk assessment of different types of objects, optimal choice of objects for reconstruction, choice of the most acceptable contractor in tender procedures and in many other cases of multicriteria decision making in the Civil Engineering.

ACKNOWLEDGEMENT

This paper is the part of the scientific-research project "Management of realization of large investment projects TR-16011", supported by the Ministry of education and science of the Republic of Serbia and realised at the Faculty of Civil Engineering, University of Belgrade.

- [12] Opricović, S (1998), *Multiple criteria optimization of systems in Civil Engineering* (in Serbian), University of Belgrade, Faculty of Civil Engineering, Belgrade.
- [13] Opricović, S., Tzeng, G-H. (2004), „Compromise solution by MCDM methods: A comparative analysis of VICOR and TOPSIS”, *Europ. J. of Operational Research*, Vol. 156, pp. 445–455.
- [14] Opricović, S.(2007), „A Fuzzy Compromise Solution for Multicriteria Problems”, *Int. J. of Uncertainty, Fuzziness and Knowledge-based Systems*, Vol. 15, No. 3, pp. 363–380.
- [15] Prašćević, Ž., Prašćević, N.,(2011), „Application of Fuzzy TOPSIS Method for Choice of Objects for Reconstruction and Maintenance”, Proc. of VII Conf. „Assessment, Maintenance and Rehabilitation of Structures and Settlements”, edited by R. Folić, Association of Civil Engineers of Serbia, pp 25–33. Prascevic, Ž., Prašćević, N. (2013), „One modification of fuzzy TOPSIS method”, *Journal of Modelling in Management*, Vol. 8, pp.81–102.
- [16] Wang, Y-M. and Elhang, T. M. S. (2006), “Fuzzy TOPSIS method based on alfa level with an application to risk management”, *Expert Systems with Application* Vol. 31, pp. 309-319.
- [17] Wang, Y-M. and Elhang, T. M. S. (2007), „A fuzzy group decision making approach for bridge risk assessment”, *Computers and Industrial Engineering*, Vol. 53, pp. 137–148.
- [18] Zadeh, L. A. „Fuzzy Sets”(1965), *Information and Control*, Vol. 8, pp. 338-353.
- [19] Zadeh, L. A.,(1975), „Probability Measure of Fuzzy Events”, *Journal of Mathematical Analysis and its Applications*, Vol. 23, No 2, pp. 421–428.
- [20] Zimmermann, H-J., „Description and optimization of fuzzy systems”, *Intern. Journal of General Systems*, 1976, Vol. 2, pp. 209–215.

REZIME

PRIMENA MODIFIKOVANOG RASPLINUTOG TOPSIS METODA ZA VIŠEKRITERIJUMSKE ODLUKE U GRAĐEVINARSTVU

Živojin PRAŠĆEVIĆ
Nataša PRAŠĆEVIĆ

U ovom radu predlaže se i primenjuje jedan modifikovani rasplinuti TOPSIS metod za višekriterijumsko rangiranje objekata za rekonstrukciju i održavanje. Na početku se daje kratak osvrt na nastanak i razvoj ovog metoda i opisuje se TOPSIS procedura s fiksnim (nerasplnutim) ulaznim podacima koji sačinjavaju matricu odlučivanja i težinske koeficijente kriterijuma. Ova procedura se ilustruje jednim jednostavnim brojevanim primerom. Objasnjava se neophodnost prikazivanja ovih parametara - kao trougaonih rasplnutih brojeva - zbog nemogućnosti njihovog preciznog određivanja ili procenivanja u praksi. U radu se daju tačni izrazi, koje su autori ranije izveli, za određivanje proizvoda elemenata matrice odlučivanja i težinskih koeficijenata kao trougaonih rasplnutih brojeva. Ovi parametri za svaku alternativu (objekat) tretiraju se kao slučajne rasplnute veličine, za koje se određuju tačne generalisane očekivane vrednosti, varijanse i standardne devijacije. Iz normalizovane matrice očekivanih vrednosti određuju se očekivana idealna pozitivna i očekivana idealna negativna rešenja. Za svaku alternativu određuju se generalisane očekivane distance i relativne bliskosti ovim rešenjima, kao i odgovarajuće varijanse i koeficijenti varijacije. Alternative se rangiraju prema ovim vrednostima. U radu se predlažu izrazi za sračunavanje koeficijenta raspodele investicionih sredstava na (alternative) objekte. Na kraju, dat je jedan primer rangiranja mostovskih konstrukcija u odnosu na rizik i formulisani su odgovarajući zaključci.

Ključne reči: Rasplinuti (fuzzy) TOPSIS, rasplinuti broj, održavanje objekata, raspodela investicionih sredstava, upravljanje rizikom.

SUMMARY

APPLICATION OF MODIFIED FUZZY TOPSIS METHOD FOR MULTICRITERIA DECISIONS IN CIVIL ENGINEERING

Živojin PRASCEVIC
Nataša PRASCEVIC

In this paper is presented and applied one fuzzy TOPSIS method for the multicriteria ranking of objects for reconstruction and maintenance. At the beginning is given short review on the genesis and development of this method and described a TOPSIS procedure with crisp input data that constitute a decision matrix and weights of criteria. This procedure is illustrated by one simple numerical example. The necessity of presentation of these parameters as triangular fuzzy numbers due to impossibility of their precise determination or assessment in the practice. The exact expressions for the determination of these products of the decision matrix and weights coefficients as triangular fuzzy numbers, that authors of this paper are derived earlier, are given in the paper. For every alternative (the object) these parameters are assumed as random fuzzy numbers for which are determined generalised expected values, variances and standard deviations. From the normalised matrix of the expected values are determined expected ideal positive and ideal negative values. For every alternative are determined generalized expected distances and relative closenesses to the ideal positive and ideal negative solution. The ranking of alternatives is performed according to these values. Mathematical expressions for coefficients of investments distribution on the alternatives (objects) are proposed in the work. One example of ranking of the bridge structures according to the risk is given at the end of the work and formulated corresponding conclusions.

Key words: Fuzzy TOPSIS, fuzzy number, maintenance of objects, distribution of investments, risk management.

KARAKTERISTIKE TRANZITNE ZONE BETONA NA BAZI LAKOG AGREGATA

CHARACTERISTICS OF LIGHTWEIGHT AGGREGATE CONCRETE INTERFACIAL TRANSITION ZONE

Vesna MILOVANOVIĆ
Vilma DUCMAN
Miroslava RADEKA

ORIGINALNI NAUČNI RAD
ORIGINAL SCIENTIFIC PAPER
UDK: 691.322

1 UVOD

Proizvodnja konstrukcijskih betona s poboljšanim termoizolacionim svojstvima na bazi kvalitetnog lakog agregata (LA) proizvedenog od otpadnih materijala predstavlja novu, dodatnu vrednost koja utiče na racionalno korišćenje prirodnih resursa i upravljanje otpadom. S lakim agregatom mogu se uspešno proizvoditi betoni za monolitne konstrukcije kao i prefabrikovani elementi. Dobre strane upotrebe lakih agregata proizvedenih na ovaj način jesu:

- zamenjuju prirodne sirovine zbog čega se smanjuje količina otpadnog materijala na deponijama;
- povećavaju uštede u izgradnji i eksploataciji objekata smanjenjem opterećenja na temelje (do 25%), čime se povećava otpornost konstrukcije na dejstvo zemljotresa;
- povećavaju toplotno-izolaciona svojstva elementa konstrukcije.

Kao polazna sirovina za proizvodnju ove vrste agregata najčešće se koristi: zgura visokih peći, leteći pepeo, otpadno staklo, silikatni mulj, papirni mulj, itd. [4], koji po svojim karakteristikama uspešno konkurišu lakim agregatima dobijenim od prirodnih sirovina: vermikulit, perlit i glina.

Vesna Bulatović, asistent, Univerzitet u Novom Sadu, Fakultet tehničkih nauka - Departman za građevinarstvo i geodeziju, Trg Dositeja Obradovića 6, Novi Sad
e-mail: vesnam@uns.ac.rs
Vilma Ducman, Zavod za gradbenistvo, 11001 Ljubljana, Dimičeva 12, Slovenia, e-mail: vilma.ducman@zag.si
Miroslava Radeka, profesor, Univerzitet u Novom Sadu, Fakultet tehničkih nauka - Departman za građevinarstvo i geodeziju, Trg Dositeja Obradovića 6, Novi Sad
e-mail: mirka@uns.ac.rs

1 INTRODUCTION

The production of construction concrete with enhanced thermal insulating characteristics based on quality lightweight aggregate (LWA) produced from waste materials, represents a new, additional quality which influences rational usage of natural resources and waste management [3,4]. Concrete for monolith constructions along with prefabricated elements can be easily produced with lightweight aggregate. Positive sides of the use of lightweight aggregate produced in this way are:

- Natural materials are replaced in this way, which results in reduced amount of waste material deposited in landfills
- There is a reduction in building expenses by reduction of deadweight of the structure (up to 25%) and increase of overall earthquake resistance
- Thermal insulating properties of construction elements are increased

Mostly used raw materials for production of LWA are: blast furnace slag, fly ash, waste glass, silicate sludge, paper sludge [4] etc., all of which successfully can replace LWA made from natural materials: vermiculit, perlite and clay.

VesnaBulatović, asistent, University in Novi Sad, Faculty of Technical sciences-Department of Civil Engineering and Geodesy, TrgDositejaObradovica 6, Novi Sad,
e-mail: vesnam@uns.ac.rs
VilmaDucman, Zavodzagradbenistvo, 11001 Ljubljana, Dimičeva 12, Slovenia, e-mail: vilma.ducman@zag.si
MiroslavaRadeka, professor, University in Novi Sad, Faculty of Technical sciences-Department of Civil Engineering and Geodesy, TrgDositejaObradovica 6, Novi Sad
e-mail: mirka@uns.ac.rs

Beton na bazi lakog agregata ima u svežem i očvrslom stanju osobine drugačije od običnog betona. One su posledica osobina lakog agregata (mala zapreminska masa, dobre termoizolacione karakteristike, sposobnost da upijenu vodu koristi za negu betona u procesu očvršćavanja) [7] po kojim se razlikuje od osobina normalnog agregata. Osobine očvrsllog betona na makronivou, na kom se definišu inženjerska svojstva betona, posmatraju se kao osobine homogenog materijala, dok se na mezonivou smatra da se sastoji od tri faze: 1) agregat 2) cementna pasta i 3) tranzitna zona (TZ) između ove dve faze. Uticaj TZ na čvrstoću i propustljivost betona veoma je velika. Teksturalna i mineraloška svojstva površine lakog agregata utiču na formiranje mikrostrukture u ovoj zoni. Iz ove činjenice je proistekao značaj proučavanja mikrostrukture formirane tranzitne zone, jer je poznato da interakcija zrna agregata s cementnom pastom u velikoj meri modifikuje osobine betona u pogledu čvrstoća, modula elastičnosti i propustljivosti za gasove i tečnosti [2]. Tranzitna zona koja se formira između agregata normalne težine i očvrsllog cementnog kamena je porozna (u betonima normalne težine). Veća poroznost je pripisana „efektu zida“, koji vodi ka smanjenju sadržaja zrna nehidratiranog cementa u poređenju s cementnom matricom, usled čega dolazi do rasta poroznosti [12a]. To znači da za isti vodocementni faktor u tranzitnoj zoni ima manje nehidratiranih zrna nego u cementnoj matrici. Ako je vodocementni faktor u celoj masi 0.4, u cementnoj matrici će biti 0.36 [12b].

Prema literaturnim podacima [10], formiranje tranzitne zone se odvija u nekoliko faza:

- prvo se formira film od vode na površini zrna agregata što dovodi do povećanja vodocementnog faktora;

- kasnije, kao i u cementnoj pasti, dolazi do rastvaranja kalcijum-sulfata i kalcijum-aluminata. Najveći deo zrna cementa sastavljan je od više minerala i na početku prevladavaju reakcije minerala C_3A i C_3S . U prvim momentima hemijske reakcije stvara se amorfni sloj bogat aluminijumom. Iz ovog sloja počinju da se razvijaju kristali etringita (AFt), a kada počne hidratacija tri kalcijum-silikata (C_3S), na kristalima AFt počinje rast kalcijum-siliko-hidrata (CSH) i popunjavanje praznog prostora. Na kraju ove etape formiraju se pore s prečnikom manjim od $1\mu m$. Hidratacija se potom nastavlja rekristalizacijom AFt i formiranjem većih kristala. Uvećanje ovih kristala i kontinuiran rast CSH produkata na kraju dovodi do bolje popunjenosti prostora čvrstom materijom i smanjenjem poroznosti čime se poboljšava gustina i čvrstoća TZ [10];

- zbog većeg vodocementnog faktora u tranzitnoj zoni u odnosu na cementnu matricu, joni formiraju veće kristale i porozniju strukturu.

Proces hidratacije se takođe menja i pod uticajem superplastifikatora. Njihova uloga je da menjaju reološka svojstva svežeg betona [11] u interakciji, pre svega sa C_3A i njegovim produktima hidratacije. Oni takođe usporavaju proces hidratacije alita, a s povećanjem sadržaja C_3A , količina polimera koji se adsorbuje je veća [15].

Concrete based on LWA (LWAC) in its fresh and hard condition has qualities different from ordinary concrete. They come as the consequence of LWA properties (small apparent density, good thermo insulating properties and the ability to use absorbed water for internal curing during hardening process) [7] which makes it different from ordinary concrete. The characteristics of hardened concrete on macro level, which is used to define engineering characteristics of concrete, are seen as the characteristics of homogenous material, whereas it is considered that at mezo level there are three phases: 1) aggregate 2) cement paste (matrix) and 3) an interfacial transition zone (ITZ) which is between these two phases. The influence of ITZ to the strength and permeability of concrete is very high. Textual and mineralogical characteristics of the surface of LWA influence the formation of microstructure in this zone. Thus, it is important to study microstructure of the formed ITZ since it has been recognised that the interaction of aggregate with cement paste to a great extent modifies the characteristics of concrete when it comes to hardness, the module of elasticity and permeability to gases and liquids [2]. ITZ formed between the normal aggregate and hardened cement paste is porous (in ordinary concrete). The higher porosity is due to a "wall effect", leading to lower content of unhydrated cement grains as compared to bulk phase and consequently to an increased porosity [12a]. This means that the volume fraction of unhydrated cement grains is lower in ITZ than in cement matrix for the same water cement ratio. The reduction of water cement ratio in the bulk phase was expected to be about 0.36 compared to overall w/c of 0.4 [12b].

According to the data given in the reference [10] the formation of ITZ takes place through several stages:

- firstly, a water film is being formed on the surface of aggregate grain which leads to the increase of the water/cement ratio in the vicinity of aggregate grain;

- then, as it happens in the cement paste, in the ITZ occurs dissolving of calcium sulphate and calcium aluminate. Most cement grains are multi mineral and early reactions are dominated by C_3A and C_3S reactions. In the first moments of a chemical reaction there comes to the formation of an amorphous layer rich in aluminium. From this layer start the formation of ettringite crystals (AFt), and when the hydration C_3S starts, on crystals AFt start to grow CSH compounds and to fill porous space. At the end of this stage the diameter of the pores that are being formed is less than $1\mu m$. Hydration then continues with recrystallization of AFt and the creation of bigger crystals. The enlargement of these crystals and the continuous growth of CSH compounds eventually bring to a better filling of space with products of hydration and decreased porosity which improve density and strength of ITZ [10];

- due to the higher water/cement ratio in ITZ than in cement matrix, the ions form large crystals and therefore porous structure appears.

The hydration process is also changing in the presence of superplasticizer. They change the rheology [11] of the fresh concrete by adsorbing preferably on the C_3A phase. They also adsorb on C_3A hydration products and retard alite hydration. With the increasing C_3A content of the cement the amount of polymer adsorbed is increasing. [15].

Tranzitna zona lakoagregatnog betona razlikuje se od TZ betona normalne težine, jer je porozan i upija vodu [16a]. Brzina upijanja vode zavisi od veličine i vrste pora, kao i od toga da li agregat formira gustu spoljašnju opnu (zatvorena poroznost) ili ne (otvorena poroznost). Laki agregat sa gustom spoljašnjom opnom formira neporoznu tranzitnu zonu. Može se zaključiti da agregat sa spoljašnjom opnom veće gustine utiče na tranzitnu zonu tako da postaje slična onoj koja se formira kod agregata normalne težine [2]. Kada opna nije velike debljine, cementna pasta može delimično da penetrira u LA kroz otvorene pore i na taj način omogućiti dobre mehaničke osobine između cementne matrice i agregata dok se u tranzitnoj zoni smanjuje vodocementni faktor i poroznost. Kod nekih vrsta lakih agregata s pucolanskim osobinama dolazi i do hemijske reakcije. Kada dolazi do hemijske reakcije, stvara se jaka veza između agregata i cementne matrice [13].

Procena teksturalnih svojstava tranzitne zone veoma je kompleksan proces. Scrivener K. [12a] prvi put je koristila SEM i EDS-a (u *backscatter* opciji). Drugi autori se bave isključivo analizom upijanja i otpuštanja vode zrna lakog agregata [4], a u poslednje vreme se nalaze i radovi vezani za određivanje mikrotvrdoće tranzitne zone.

Analizom teksturalnih svojstava tranzitne zone putem SEM-a, EDS-a i programa za analizu slike, mogu se dobiti informacije o promeni sastava ove zone i poroznosti. Nevolja je što je za izvođenje relevantnih zaključaka potreban veliki broj merenja, a ispitivanja zahtevaju posebnu pripremu uzorka i veoma dugo trajaju.

Merenjem mikrotvrdoće takođe mogu da se prate promene teksturalnih svojstava tranzitne zone u odnosu na ostatak cementne matrice [5,6]. Ovo je jedna od nekoliko metoda za direktno merenje bar nekih mehaničkih svojstava tranzitne zone. U cilju skeniranja TZ kod testa mikrotvrdoće koriste se veoma mala opterećenja s ciljem da se stvore veoma mali otisci, obično s dimenzijama od nekoliko mikrona [2]. Kvalitet informacija u pogledu poroznosti i sastava tranzitne zone pre svega zavisi od dimenzija tela koje utiskujemo u ispitivani uzorak i od kvaliteta pripreme površine u koju se izvodi utiskivanje [7], kao i od heterogenosti strukture na mikronivou. Naime, vrlo često najslabiji deo TZ nije fizička veza na površini između lakog agregata i cementne paste, već 5 do 10 μm unutar cementne paste. Na ovom rastojanju, najslabiji deo mogu biti kristali kalcijum-hidroksida određene orijentacije. Nažalost, ove stvari ponekad otežavaju pravilno tumačenje čvrstoća izmerenih na ovaj način.

U radu su dati rezultati ispitivanja sastava tranzitne zone korišćenjem SEM i EDS analize kao i merenjem mikrotvrdoće s ciljem da se ustanovi kako promena vrste veziva u betonu utiče na kvalitet TZ betona napravljenog od lakog agregata proizvedenog na bazi silikatnog, papirnog mulja i pepela.

Interfacial transition zone of lightweight aggregate is different from the ITZ of the ordinary concrete, since lightweight aggregate is porous and absorbs water [16a]. The rate of water absorption depends on the size and the type of pores, as well as whether aggregate have a thick outer shell (closed porosity) or not (open porosity). Lightweight aggregate with a thick outer shell forms high porosity ITZ zone. It can be concluded that increased density of the outer shell of the lightweight aggregate influences ITZ so that it becomes similar to the one which forms with the aggregates of normal weight [2]. When thick outer shell is not present cement paste can partially penetrate into lightweight aggregate through the open pores and in that way a good mechanical binding between matrix and aggregate can be enabled while water/cement ratio in the ITZ would decrease as well as porosity. In some types of LWA with pozzolanic properties it comes to chemical reactions in this zone. When chemical reaction is present a strong chemical bond between aggregate and cement paste matrix may develop [13].

Evaluation of textural features of ITZ is a very complex process. Scrivener K. [12a] used SEM and EDS (in backscatter option) for the first time. Other authors only carry out analysis of absorption and release of water of LWA [16a, 16b]. Lately there are papers and work related to determination of micro hardness of ITZ.

The analysis of textural features of ITZ with SEM, EDS and a program for analyzing pictures can give information about the change of structure of this zone and porosity. The trouble is that for coming to the relevant conclusions it is necessary to carry out a number of measuring. This type of testing requires a special preparation of a sample, which takes very long time.

The changes of textural features of ITZ compared to the cement paste matrix can be followed as well as by micro hardness measurements [5,6]. This is one of several methods which is able to measure directly at least some mechanical properties of the ITZ. In order to scan across the ITZ with micro hardness tests, very small load are used, in order to create very small indentation, typically with dimensions of a few microns [2]. The quality of information when it comes to porosity and structure of ITZ in the first place depends on the geometry of indenter and upon the surface preparation [7], as well as heterogeneous structure on the interface on a micro scale. Namely, very often the weakest part of the ITZ is not at the physical interface between LWA and cement paste, but rather 5 to 10 μm inside the paste. On that distance the weakest part could be specifically oriented calcium hydroxide crystals. Unfortunately these things sometimes prevent converting micro hardness measurements into meaningful strength values.

The paper gives the results of testing structure of ITZ by using SEM and EDS analysis as well as micro hardness values with the aim of determining how the change of a concrete binder influences the quality of ITZ of concrete made of LWA based on silicate sludge, paper mud and ash.

2 MATERIJALI I METODE

Za spravljanje konstrukcijskog betona korišćene su dve vrste lakog agregata: LA na bazi otpadnih materija (Termit a.d., iz Slovenije) i komercijalni laki agregat Leca-Laterlite (Italy). Najveći udeo u odnosu na ukupnu količinu lakog agregata imao je laki agregat napravljen od silikatnog mulja, mulja iz papirne industrije i pepela [4]. Silikatni mulj je nastao prosejavanjem peska na iskopu. Pre pečenja sirovinna masa je granulirana. Temperatura pečenja je 900°C.

Upijanje vode i zapreminska masa samog zrna lakog agregata određene su na osnovu procedure date u standard SRPS EN 1097-6:2007.

Čvrstoće zrna LA određene su prema proceduri datoj u literaturi [8].

Na bazi ovog agregata i peska napravljene su četiri vrste betona sa sledećim komponentnim materijalima:

Cement: CEM I 42,5R i CEM II/B-M(S-V-L)32,5R (Lafarge-BFC, Srbija), *Leteći pepeo* (Termoelektrana „Nikola Tesla B” Obrenovac), *Metakaolin* („Metamax” – SAD)

Agregat: Sitan: prirodni rečni pesak (0/4 mm) i laki agregat, Leca (2/3 mm), Italija; Krupan: laki agregat (4/8 mm), proizvođač Termit d.d, Slovenija

Hemijski dodatak: Superplastifikator Sika Viscocrete 4000BP

Voda: Gradski vodovod

Sastav betonskih mešavina, zajedno sa oznakama, dat je u Tabeli 1.

2 MATERIALS AND METHODS

Two types of LWAs were used for the preparation of structural concretes: LWA produced from waste materials and commercial one Leca-Laterlite (Italy). The main part of total amount of LWAs was prepared of silica sludge, paper mud and ash [4]. The silica sludge remains after sand screening in quarry (Termit d.d., factory from Slovenia). Before firing the batch was granulated. Firing temperature was 900°C.

Water absorption and apparent density were determined according to the procedure given in standard SRPS EN 1097-6:2007.

Mechanical strength of single LWAs granules was determined according to the procedure defined in [8].

Based on this LWAs and river sand, four types of structural concretes with the following consisting materials were made:

• **Cement:** CEM I 42,5R and CEM II/B-M (S-V-L) 32,5R (Lafarge-BFC, Serbia), Fly ashe (Power plant "Nikola Tesla B" Obrenovac), Metakaolin ("Metamax"-SAD)

• **Aggregate:** small fractions: river sand (0/4mm) and lightweight aggregates: Leca (2/3mm), Italy; large fractions : lightweight aggregate (4/8mm), produced by Termit d.d, Slovenia

• **Admixture:** Superplastifikator Sika Viscocrete 4000BP

• **Water:** tap water

The composition of structural concrete mixtures is given in Table 1.

Tabela 1. Sastav betonskih mešavina, komponente su u kg/m³
Table 1. Composition of structural concrete mixtures, kg/m³

Vrsta betona Type of concrete	LSLL-1	LSLL-2	LSLL-4	LSLL-5
CEM I 42,5R	450	-	400	244
CEM II/B-M(S-V-L)32,5R	-	450	-	-
Voda / Water	180	180	180	183
Dodatna voda / Additional water	119,5	119,5	121,2	119,5
Rečni agregat / River aggregate (0/4mm)	749	749	771	760
Leca-Laterlite / LWA Leca-Laterlite (2/3mm)	90	90	91	90
Lakoagregatni agregat - Termit / LWATERMIT (4/8mm)	327	327	332	327
Leteći pepeo / Fly ash	-	-	-	97,6
Metakaolin / Metakaolin	-	-	-	24,4
Sika VSC 4000BP / Sika VSC 4000BP	2,25	3,15	2,0	2,56

Da bi se sprečila absorpcija vode u većoj meri iz cementne paste, što smanjuje količinu vode koja je neophodna za hidrataciju cementa, LA se pre spravljanja betonske mešavine natapa vodom u trajanju od 30 min (dodatna voda). Količina upijene vode osigurava da LA bude „površinski zasićen” vodom.

Ukupna poroznost i raspodela veličina pora u lakom agregatu Termit proizvedenom u Sloveniji (LWA-Termit), određena je živinom porozimetrijom (MIP). Male kocke, veličine oko 1cm³, sušene su u sušnici 24 h na 105°C i analizirane u uređaju Micromeritics Autopore IV 9500 model. Uzorci su analizirani u opsegu pritisaka od 0 do 414 MPa.

Karakteristike tranzitne zone određene su putem

In order to prevent great absorption of water from the cement paste, which decreases the water amount needed for the cement hydration, LWAs were being pre-wetted with water for 30 minutes (additional water). This amount of absorbed water ensures "surface-saturated" condition prior to mixing.

Total porosity and pore size distribution of lightweight aggregate Termit, produced in Slovenia (LWA-Termit), was determined by means of mercury intrusion porosity (MIP). Small block, approximately 1cm³ in size, were dried in an oven for 24h at 105°C and analysed on a Micromeritics Autopore IV 9500 model. Samples were analysed in the range of 0 to 414 MPa.

The characteristics of ITZ were determined by SEM

SEM i EDS analize u *backscatter* modu, na uređaju JSM-6460HV, JEOL, Tokyo, Japan. Slike poliranih delova uzorka u *backscatter* modu snimljene su za različita uvećanja. Mikrohemijska analiza je bila koncentrisana na određivanja odnosa elemenata u tranzitnoj zoni kao i na odnos elemenata u lakom agregatu u blizini tranzitne zone.

Test tvrdoće po Vickersu (HV 0.3) urađen je na uređaju za određivanje mikrotvrdoće HVS-1000A, uz upotrebu opterećenja od 2.942 N (0.3 kgf) u trajanju od 15 s. Dijagonale otiska nastale aplikacijom Vickersovog dijamantskog utiskivača na površinu merene su preko optičkog uređaja sa uvećanjem od 400× i s tačnošću od ±0.1 μm. Uzorci na kojim je rađeno merenje bili su u obliku kvadratnih ploča s paralelnim površinama ukupnih dimenzija 4 cm × 4 cm × 1 cm. Pored toga, izbegnuta su merenja na bilo kakvim površinskim defektima (kao šupljine). Urađeno je najmanje pet merenja na svakom uzorku. Tvrdoća po Vickersu, HV, dobijena je prema relaciji:

$$HV = \frac{2F \sin\left(\frac{\alpha}{2}\right)}{d^2} = 1.8544 \frac{F}{d^2}$$

gde je F [kgf] opterećenje utiskivača, α je ugao između dijagonala dijamantskog utiskivača u obliku piramide i iznosi 136° i d[mm] jeste aritmetička sredina dužine dve dijagonale kod otiska.

3 REZULTATI I DISKUSIJA

Silikatni mulj sadrži više od 60 mas % veoma finog silikatnog peska, feldspata i gline. Papirni mulj sadrži oko 38 mas % organskih materija kao i kalcit i kaolin. Sagorevanjem organskih materija iz papirnog mulja u prisustvu glinenih minerala formira se porozna struktura. Prisustvo papirnog mulja utiče na formiranje značajne količine otvorene poroznosti u LA-Termit. Potvrda ovoga je vrednost ukupnog upijanja vode (34 mas %) i sposobnost da se skoro celokupna količina vode upije u prvih 5 min absorpcije. Podaci za brzinu upijanja vode kao i za ukupnu količinu upijene vode dati su u Tabeli 2.

and EDS analysis in backscatter mode on the instrument JSM-6460HV, JEOL, Tokyo, Japan. Back-scattered images of polished sections were obtained in diverse magnifications. Micro chemical analysis was focused on chemical composition of ITZ as well as composition of LWA close to ITZ.

Vickers hardness test (HV 0.3) was carried out with a micro-hardness tester HVS-1000A, by applying indentation load of 2.942 N (0.3 kgf) during 15 s dwell time. The indentation diagonals made by Vickers diamond pyramid indenter on the surface were measured optically under the magnification of 400× and by the precision of ±0.1 μm. The samples used for the measurements were shaped as square plates with parallel opposite sides and overall dimensions of 4 cm × 4 cm × 1 cm. Furthermore, during the measurements any large surface defects (like voids) were avoided. At least, five micro-hardness measurements were performed on every sample. The Vickers hardness values, HV, were obtained by the following relation:

where F [kgf] is the indentation load, α is the diamond pyramid indenter diagonal angle, equal to 136°, and d [mm] is the arithmetic mean of two diagonal lengths of the indentation.

3 RESULTS AND DISCUSSION

Silica sludge contains over 60 mass% very fine silica sand, feldspar and clay. Paper mud contains about 38 mass% of organic compounds as well as calcite and kaolinite. Combustion of organic compounds from paper mud in the presence of clay minerals formed porous structure. The presence of paper mud influenced the formation of significant amount of open porosity in LWA-Termit. The indication of it was overall water absorption (34 mass%) and capability to absorb almost all amount of water in the first 5 min of absorption. Data for water absorption rate and total water absorption as well as apparent density of single grain for both LWAs are given in Table 2.

The biggest amount of water was absorbed in the first 5minutes. The water absorption of LWA after 30 minutes is: for LWA-Termit (0/4mm) and for LWA Leca (2/3mm) is respectfully 33.2% and 12.1%, Table 2.

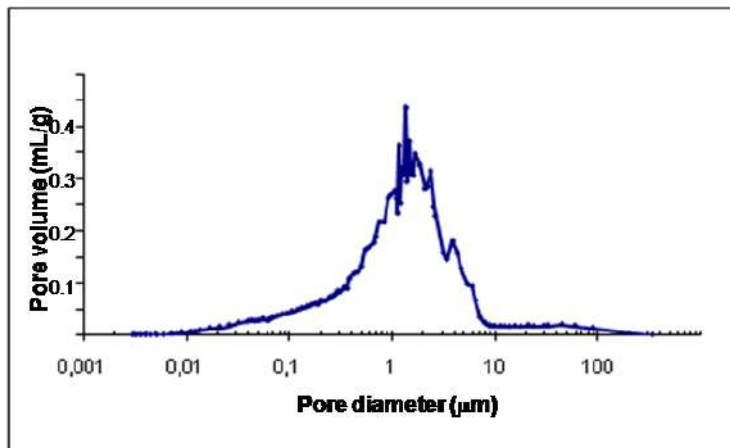
Tabela 2. Upijanje vode, zapreminska masa zrna i čvrstoća zrna
Table 2. Water absorption, apparent density and mechanical strength of LWAs grains

	5 min mas% mass%	15 min mas% mass%	30 min mas% mass%	60 min mas% mass%	120 min mas% mass%	Zap. masa Apparent density kg/m ³	Čvrstoća Strength MPa
LA -Termit (4/8mm) LWA Termit (4/8mm) mass %	32,3	32.8	33.3	33.4	33.9	1300	2.6
Leca Laterlite (2/3mm) Leca Laterlite (2/3mm) mass %	7,6	8,0	8,9	10,1	10,3	630	≥2,5

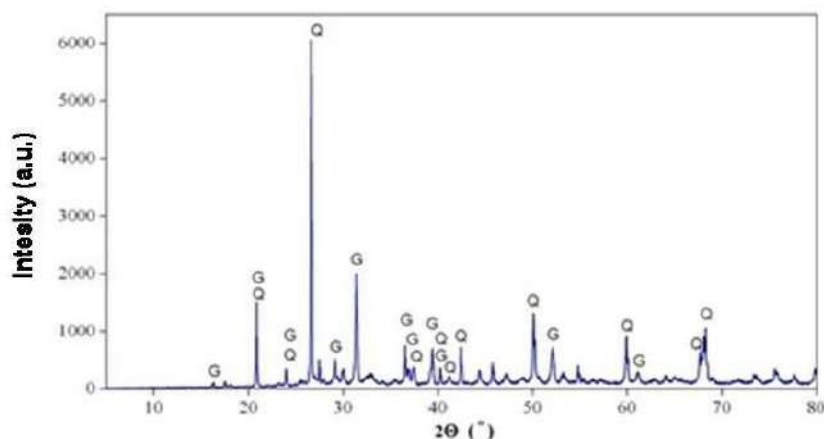
LA – Termit, slika1, ima veoma veliku otvorenu poroznost, Tabela 2. Raspodela veličina pora, slika 2, ukazuje na to da je dominantan prečnik pora oko 1 μ m, dok je ukupna poroznost 46.5 %. Ova veličina pora omogućava dodatnoj vodi da iz ovih i većih pora curi u TZ i učestvuje u procesu hidratacije cementne paste. Na osnovu vrednosti ukupne i otvorene poroznosti utvrđeno je da je zatvorena poroznost oko 12%.



Slika 1. Laki agregat-Termit
Figure 1. Lightweight aggregate-Termit



Slika 2. Raspodela veličina pora u LA-Termit
Figure 2. Pore size distribution in LWA-Termit



Slika 3. Rendgeno-strukturna analiza LA-Termit (Q- kvarc, G-gelenit)
Figure 3. XRD analysis of LWA-Termit (Q- quartz, G-gehlenite)

Mineraloški sastav LA-Termit (slika 3) ukazuje na prisustvo dva dobro iskristalisana minerala: gelenit i kvarc.

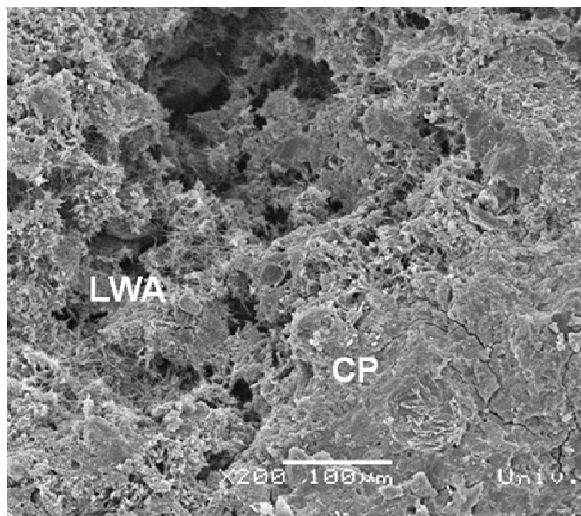
Na slici 4a predstavljeno je zrno LWA-Termit u betonu LSLL1, starosti 14 dana. Zapaža se da ne postoji oštra granica između zrna LA-Termit i cementne paste. Mikrostruktura poprečnog preseka LA-Termit, slika 4a, ukazuje na prisustvo šupljina i pukotina nastalih u toku procesa proizvodnje. Odsustvo guste spoljašnje opne, koja kontroliše absorpciju/desorpciju vode, trebalo bi da omogući dotok vode u cementnu pastu tokom hidratacije u slučaju desorpcije. Na ovaj način, slojevi cementne paste bliži površini LA postaju gušći za kraće vreme. U unutrašnjosti zrna LWA mogu se videti kristalne forme

LWA-Termit, Figure 1, has a very high open porosity, Table 2. Pore size distribution, Figure 2, indicates that dominant pore diameter is 1 μ m, while total porosity is 46.5%. This size of the pores enables additional water from these and bigger pores to take part in the process of hydration of cement paste. Based on the values of total and open porosity it was determined that the closed porosity is around 12%.

Mineralogical composition of LWA-Termit, (Figure 3) shows the presence of two well crystallized minerals: gehlenite and quartz.

Figure 4a shows a grain of LWA-Termit in concrete LSLL1, 14 days old. It is evident that there is no distinct difference between the LWA grain and the cement paste. The microstructure of the LWA-Termit grain cross section, Figure 4a, indicates the presence of voids and fissures formed during the manufacturing process. The lack of outer shell, which controls absorption/ desorption of water, should facilitate supply of cement paste with water in the case of desorption. In that way near-surface layer of the cement paste becomes denser in a shorter period of time. Inside of the LWA grain nano sized

nanoveličine, slika 4b, koje podsećaju na etringit čija identifikacija u ovoj veličini nije laka. Nastale su najverovatnije nakon absorpcije vode u LWA, ali ovu pojavu treba dodatno istražiti.

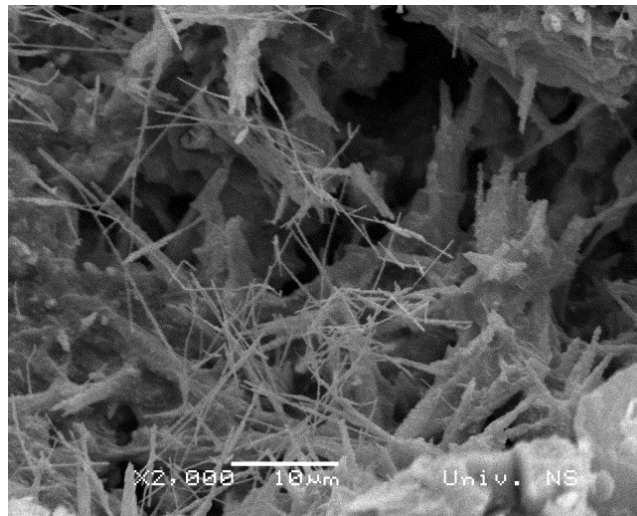


Slika 4a. SEM LA-Termit u betonu LSLL1, starost 14 dana (x200)

LWA-lak agregat, CP- cementna pasta

Figure 4a. SEM of LWA-Termit in LSLL 1 concrete, 14 days old (x200),

LWA-lightweight aggregate, CP-cement paste



Slika 4b. SEM LA-Termit u betonu LSLL1, starost 14 dana (x2000)

Figure 4b. SEM of LWA-Termit in LSLL 1 concrete, 14 days old, (x2000)

Iako na poprečnom preseku LA-Termit nije utvrđeno da postoji gusta spoljašnja opna, razlike u sastavu površine i unutrašnjeg dela zrna jesu moguće. Po rastvaranju neizreagovanih zrna cementa, javlja se koncentracioni gradijent koji može dovesti do difuzije jona iz cementne paste do TZ i unutrašnjih delova LA. Najpokretljiviji joni u portland cementu su Na^+ , K^+ , $\text{Al}(\text{OH})_4$, Ca^{2+} [13].

Na osnovu EDS ispitivanja sadržaja elemenata u tranzitnoj zoni u opsegu od $-10 \mu\text{m}$ (počinje u zrnima lakog agregata) do $\approx 90 \mu\text{m}$ (završava se u cementnoj pasti), i kriterijuma datih u radu [14], određuje se odnos atoma (Ca, Si, Al, Fe, S) i tip hidratisanog produkta prema sledećim formulama:

$$\text{C-S-H: } 0.8 \leq \text{Ca/Si} \leq 2.5,$$

$$\text{CH: } \text{Ca/Si} \geq 10,$$

$$\text{AFm}^1: \text{Ca/Si} \geq 4.0,$$

$$(\text{Al}+\text{Fe})/\text{Ca} \leq 0.2$$

$$(\text{Al}+\text{Fe})/\text{Ca} \leq 0.4, \text{ S/Ca} \leq 0.04$$

$$(\text{Al}+\text{Fe})/\text{Ca} > 0.4, \text{ S/Ca} > 0.15$$

Na osnovu datih kriterijuma utvrđuje se koja jedinjenja preovlađuju u hidratnim formama (CSH, CH, AFm). Ako rezultati pokazuju sastav koji je između ovih granica, smatra se da su formirane hidratne forme mešavina oksida. Ideja je bila da se napravi razlika između hidratnih oblika bogatih C-S-H jedinjenjima, jedinjenjima kalcijum-hidroksida (CH) i monosulfata (AFm) ili etringita (AFt). Primer proračuna je dat u tabelama 3-7 za različite betone starosti sedam dana.

Although the shell structure is not seen in the cross section of LWA grain the differences in oxide composition of surface and inner part of the LWA are possible. After the dissolution of cement anhydrous grains, the appearance of concentrations gradient could induce a transport of ions by diffusion from cement paste to ITZ and inner part of LWA. The most mobile ions are Na^+ , K^+ , $\text{Al}(\text{OH})_4$, Ca^{2+} in ordinary portland cement [13].

EDS examinations of element composition in ITZ ranged between $-10 \mu\text{m}$ (starts in the grain of LWA) to $\approx 90 \mu\text{m}$ (finished in cement paste), and the criteria given in paper [14] determines the ratio of atoms (Ca, Si, Al, Fe, S) and type of hydrated products according to the following formulas:

Based on the given criteria, it is determined which compounds are dominant in hydration forms (CSH, CH, AFm). If the results show structure which is between these values then it is considered that the produced hydration forms are mixtures of oxides. The idea was to make difference between hydrates rich in C-S-H compounds, compositions rich in calcium hydroxide (CH) and monosulphate (AFm) or etringite (AFt). The examples of calculations are given in Tables 3-7.

¹ AFm su u hidratisanom cementu produkti hidratacije C_3A (monosulfat i monokarbonat).

¹ AFm phases in hydrated cements are products of C_3A hydration (monosulfate and monocarbonate)

Na osnovu datih kriterijuma utvrđuje se koja jedinjenja preovlađuju u hidratnim formama (CSH, CH, AFm). Ako rezultati pokažu sastav koji je između ovih granica, smatra se da su formirane hidratne forme mešavina oksida. Ideja je bila da se napravi razlika između hidratnih oblika bogatih C-S-H jedinjenjima, jedinjenjima kalcijum-hidroksida (CH) i monosulfata (AFm) ili etringita (AFt). Primer proračuna je dat u tabelama 3-7 za različite betone starosti sedam dana. U Tabeli 3 je predstavljen hemijski sastav spoljašnje opne zrna LA-Termit, pre ugrađivanje u beton. Struktura LA-Termit u blizini TZ prikazuju tačke 1-3 u Tabeli 4, tačke 3 i 4 u Tabeli 5 i 6, tačke 4-6 u Tabeli 7. Ostale tačke pokazuju sastav tranzitne zone.

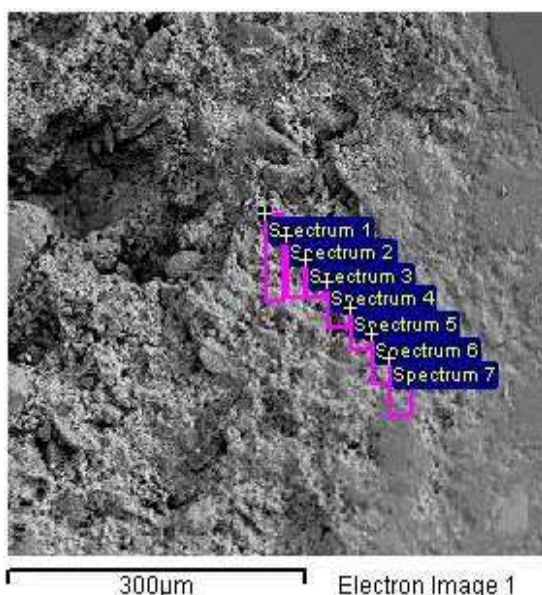
Based on the given criteria, it is determined which compounds are dominant in hydration forms (CSH, CH, AFm). If the results show structure which is between these values then it is considered that the produced hydration forms are mixtures of oxides. The idea was to make difference between hydrates rich in C-S-H compounds, compositions reach in calcium hydroxide (CH) and monosulphate (AFm) or etringite (AFt). The examples of calculations are given in Tables 3-7. Chemical composition of the LWA-Termit grain outer shell before concrete preparation is presented in Table 3; in Table 4 points 1-3 show structure of the grain of LWA-Termit, in Tables 5, 6 these points are 3 and 4 while in Table 7 are 4-6. The rest of the points show the composition of ITZ.

Tabela 3. Rezultati EDS analiza spoljašnje opne zrna LA-Termit, mas%
Table 3. The results of EDS analysis of LWA -Termit grain outer shell, mass%

Spec.	C	O	Mg	Al	Si	K	Ca	Ti	Fe	Ca/Si	(Al+Fe)/Ca	S/Ca	
Range	24.6-45	47.9-50	0.57-0.86	4.43-12.9	0-18	0-0.4	11.2-30.2	0-0.3	0.46-0.74				
Aver.	23.2	32.6	0.68	8.45	9.4	0.2	21.2	0.1	0.61	2.25	0.43	-	mix

Analizom sastava tačaka 1 i 2 (spektri 1 i 2), Tabela 4, koje se nalaze u zrnju LA-Termit vidi se povećanje koncentracije kalijuma i gvožđa u odnosu na vrednosti u Tabeli 3. Odnos Ca/Si raste od tačke 1 do 3. Rast odnosa atoma Ca/Si upućuje na postojanje difuzije jona. Zbog velikih razlika u sastavu zrna LA-Termit, Tabela 3, teško je reći u kom smeru se dominantno odvija difuzija (od cementne paste ka zrnju LA ili obrnuto, ili u oba pravca).

By analyzing the composition of points 1 and 2 (spectrum 1 and 2), Table 4, which are in the LWA-Termit grain, a certain increase of the concentration of potassium and iron can be seen in comparison to values in Table 3. The increase of Ca/Si ratio indicates the diffusion of ions between cementitious paste and LWA-Termit grain. Due to the large differences in the composition of LWA-Termit grain, Table 3, it is difficult to say in which direction the diffusion dominantly takes place (from cement paste to the LWA grain or vice versa, or that it maybe goes in both directions) [16b].



Slika 5. Mesta na kojim je urađena EDS analiza 7 dana starog betona LSSL-1
Figure 5. Spots on which EDS analysis was carried out for 7-day old concrete LSSL-1

Tabela 4. Rezultati EDS analize betona LSLL-1 starog 7 dana
Table 4. The results of EDS analysis of 7-day old concrete LSLL-1

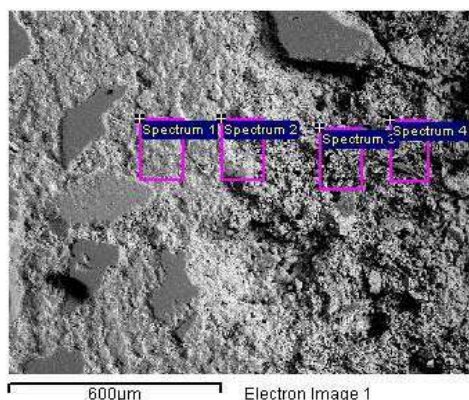
Spec	C	O	Mg	Al	Si	K	Ca	Ti	Fe	Ca/Si	Al+Fe/Ca	
Tačke u LA-Termit Points in LWA-Termit												
Spec 1	0.00	49.40	0.87	6.17	15.29	1.46	25.61		1.21	1.67	0.29	mix
Spec 2	13.81	43.07	0.78	5.44	9.89	0.64	25.22		1.15	2.55	0.26	mix
Spec 3	0.00	50.29	1.37	6.38	9.29	0.57	30.66	0.25	1.20	3.00	0.25	mix
Tačke u TZ Points in ITZ												
Spec 4	25.39	42.75	0.49	3.29	5.43	0.84	21.27		0.55	3.91	0.18	mix
Spec 5	16.78	47.54	0.77	2.43	5.07	1.20	25.92		0.29	5.11	0.10	mix
Spec 6	13.39	44.52	0.89	4.77	7.69	1.22	26.66		0.86	3.47	0.21	mix
Spec 7	14.65	45.36	0.43	4.46	13.79	0.79	19.79		0.73	1.44	0.26	mix

U betonu gde je kao vezivo korišćen CEM I 42,5R (LSLL1), na mestima 1 i 2, koja se nalaze u zrnju LWA-Termit, odnosi Ca/Si i (Al+Fe)/Ca bliski su vrednostima za CSH jedinjenja, Tabela 4. Moguće je da zidovi pora LWA služe kao termodinamički najpovoljnija mesta za formiranje CSH (heterogena nukleacija). U tačkama gde treba da se nalazi TZ (tačke 4-7, Tabela 4) dobijeno je povećanje vrednosti Ca/Si (tačke 4 i 5), a potom smanjenje (tačke 6 i 7). Ovi rezultati su u skladu s pretpostavljenom strukturom sloja TZ najbližeg zrnju agregata, jer ukazuju na povećanje koncentracije portlandita. Naime ovaj deo ITZ trebalo bi da bude u većoj meri sastavljen od kristala portlandita, a potom i od CSH, AFm i Aft jedinjenja.

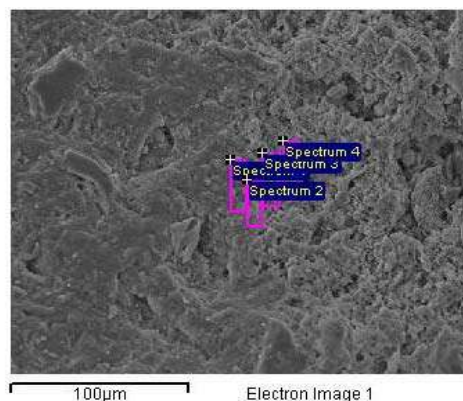
Poređenjem vrednosti udela elemenata, pre svega Ca i Si u betonu LSLL1, sa betonom napravljenim od manje količine istog cementa i većim vodocementnim faktorom (LSLL4-CEM I 42,5R), Tabele 4 i 6, uočava se povećanje koncentracije pomenutih, ali i drugih elemenata (kao Al i Fe) kod betona LSLL 4 (tačke 1 i 2- TZ zona). Prema navodima datim u literaturi [12b] vodocementni faktor ima mali uticaj na mikrostrukturu tranzitne zone. U uslovima povećanog vodocementnog faktora odvija se kontinualno rastvaranje i interakcija vode sa CSH. Posebno su visoke koncentracije elementa Si,

In concrete where CEM I 42,5R (LSLL1) was used as a binder, in points 1 and 2 (Table 4 spectrum 1 and 2), which are in LWA-Termit grain, the ratios Ca/Si and (Al+Fe)/Ca are close to the values for CSH compounds. It is possible that the walls of the LWA pores are used as thermodynamically most favourable places for the formation of CSH (heterogeneous nucleation). In points where there should be ITZ (points 4 - 7), there was an increase in value of Ca/Si (points 4 and 5), and then a decrease (points 6 and 7). These results are in accordance with the assumed structure of the layer closest to the grain of the LWA-Termit indicating the increase of mineral portlandit. Namely, this part of ITZ should be mostly composed of the portlandit crystals and CSH, AFm and Aft phases as well.

When comparing the values of the ratio of elements, first of all Ca and Si in concrete LSLL1, with concrete made from a less amount of cement and greater water cement ratio (LSLL4-CEM I 42,5R), Tables 4 and 6, it can be found that the concentration of the mentioned and other elements (Al and Fe) has increased in concrete LSLL4 (spectrum 1 and 2-ITZ zone). According to reference [12b] water to cement content have a minor influence on the microstructure of the ITZ. In the conditions of the increased water/cement ratio (LSLL 4)



Slika 6. Mesta na kojim je urađena EDS analiza za beton LSLL-2 starosti 7 dana
Figure 6. Spots on which EDS analysis was carried out for 7-day old LSLL-2



Slika 7. Mesta na kojim je urađena EDS analiza za beton LSLL-4 starosti 7 dana
Figure 7. Spots on which EDS analysis was carried out for 7-day old concrete LSLL-4

što može da se odrazi na povećanje mikrotvrdoće [9].

a continuous dissolution and an interaction of water with CSH happens. The Si content is especially high which could increase micro hardness values [9].

Tabela 5. Rezultati EDS analize betona LSLL-2 starog 7 dana
Table 5. The results of EDS analysis of 7-day old concrete LSLL-2

Spec	O	Mg	Al	Si	K	Ca	Fe	Ca/Si	Al+Fe/Ca	S/Ca	
Tačke u TZ Points in ITZ											
Spec 1	41.52	1.64	2.73	10.53	0.45	42.07	1.06	4.00	0.09	-	mix.
Spec 2	43.95	0.75	3.05	16.62	0.72	33.59	1.32	2.02	0.13	-	CSH
Tačke u LA-Termit Points in LWA-Termit											
Spec 3	40.58	0.94	4.95	16.70	0.94	33.78	2.12	2.02	0.209	-	≈CSH
Spec 4	40.53	0.64	4.13	28.42	1.89	22.48	1.91	0.79	0.267	-	mix.

Kod betona gde se kao vezivo koristio cement CEM II/B-M(S-V-L)32,5R, Tabela 5, odnosi elemenata upućuju da se u tranzitnoj zoni (tačka 2) kao i u znu LWA-Termit formiraju CSH strukture (Spektar 4, Tabela 5, Slika 6). Kalcijum-karbonat koji je kao dodatak prisutan u cementu, može da bude veoma efikasan kao nukleus za CSH strukture.

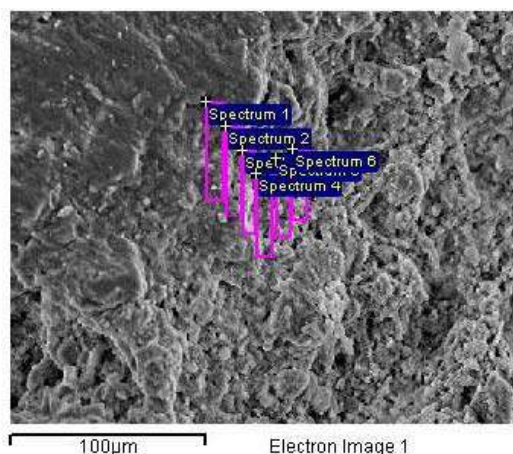
Kod betona LSLL 5 gde je u svojstvu dodatka dodan i metakaolin, dobijeni odnosi su slični rezultatima za prethodno navedene betone. Mnogo veću pažnju privlači smanjenje koncentracije aluminijuma, iako s metakaolinom treba da se poveća sadržaj elementa aluminijuma. U ovom slučaju bi na odvijanje procesa hidratacije mogao veću ulogu da odigra *polycarboxylate-based superplasticator* Sika VSC 4000BP. Absorpcija superplastifikatora na površini C_3A dovodi do usporavanja procesa hidratacije i povećavanja koncentracije elemenata Si i Ca, Tabela 7.

In concrete where cement CEM II/B-M (S-V-L) 32,5R was used as a binder, Table 5, the ratio of elements indicates that in ITZ (spectrum 2), as well as in the LWA-Termit grain, CSH structures are formed (Spectrum 4, Table 5, Figure 6). Calcium carbonate from cement is itself quite effective as a nucleus for C-S-H.

In concrete LSLL5 where metakaolin was used as an addition, the obtained ratios are similar to the results for the previously mentioned concretes. A much greater attention is brought to the decrease in concentration of aluminium, even though with metakaolin the presence of aluminium should be increased. In this case the development of the process of hydration could be influenced much more by *polycarboxylate-based superplasticator* Sika VSC 4000BP. With the absorption on the surface of C_3A compounds the process of the hydration is slower and the concentration of Si and Ca is increased, Table 7.

Tabela 6. Rezultati EDS analize betona LSLL-4 starog 7 dana
Table 6. The results of EDS analysis of 7-day old concrete LSLL-4

Spec	C	O	Mg	Al	Si	K	Ca	Ti	Fe	Ca/Si	(Al+Fe)/Ca	S/Ca	
Tačke u TZ Points in ITZ													
Spec 1		35.13	0.91	7.55	18.92	0.98	34.45		2.05	1.82	0.279		≈CSH
Spec 2		28.89		7.89	13.27	1.55	46.01		2.40	3.47	0.224		mix.
Tačke u LA-Termit Points in LWA-Termit													
Spec 3	0.00	31.46		3.58	7.85	0.61	49.39	3.53	3.59	6.3	0.145		mix.
Spec 4	11.67	35.09	0.62	4.14	14.27	0.48	32.17		1.55	2.25	0.177		CSH



Slika 8. Mesta na kojim je urađena EDS analiza za beton LSLL-5 starosti 7 dana
Figure 8. Spots on which EDS analysis was carried out for 7-day old concrete LSLL-5

Rezultati EDS analize ukazuju:

- da se udeo mešanih produkata hidratacije povećava dok prisustvo kalcijum- hidroksida nije veliko. Njegovo odsustvo kod betona gde se kao vezivo pored cementa koriste dodaci s pucolanskom aktivnošću (zgura, elektrofilterski pepeo, metakaolin) jeste očekivano (betoni LSLL2 i LSLL5) [5]. Međutim, njegovo odsustvo u drugim uzorcima nije očekivano. Takođe je interesantno da nema etringita, s obzirom na to što prisustvo sumpora nije registrovano. Objašnjenje za ovu pojavu može biti interakcija superplastifikatora s rastvornim sulfatnim jonima [15].

The results of EDS analysis show

- the presence of mixed products of hydration, whereas the crystals of calcium hydroxide are not registered in greater amount. The absence/small amount of calcium hydroxide in the samples of concrete where one of the components were pozzolanic materials was expected (concretes LSLL2 and LSLL5) [5]. However, its absence in other samples was unexpected. It is also interesting that there are no AFt considering that the presence of sulphur was not found. The explanation for this could be found in possible interaction of superplastificatos with soluble sulphate ions [15].

Tabela 7. Rezultati EDS analize betona LSLL-5 starog 7 dana
Table 7. The results of EDS analysis of 7-day old concrete LSLL-5

Spec	O	Mg	Al	Si	K	Ca	Ti	Fe	Ca/Si	Al+Fe/Ca	S/Ca	
Tačke u TZ Points in ITZ												
Spec 1	38.95	1.01	3.24	10.19	2.41	42.28		1.92	4.15	0.12	-	mix.
Spec 2	37.34		3.55	10.05	2.84	44.68		1.54	4.45	0.11	-	mix.
Spec 3	35.41		3.54	15.27	2.82	41.07		1.88	2.69	0.13	-	≈CSH
Tačke u LA-Termit Points in LWA-Termit												
Spec 4	45.44		3.46	9.16	2.57	37.75		1.62	4.12	0.135	-	mix.
Spec 5	43.21	1.27	5.15	11.63	1.37	35.74		1.62	3.07	0.189	-	mix.
Spec 6	44.26		4.70	13.59	1.28	33.80	0.77	1.60	2.48	0.186	-	mix.

- Visoke vrednosti za odnos atoma Ca/Si u TZ za betone LSLL 1 i LSLL5 upućuju na slabo prisustvo kalcijum-silikohidrata.

- Promene atomskih odnosa u zrnju LA-Termit u zonama koje su blizu TZ u odnosu na sastav pre ugrađivanja ukazuje na to da postoji difuzija jona između zrna i cementne paste. Osim toga, velika hrapavost površine zrna LWA-Termit olakšava proces kristalizacije produkata hidratacije. Ova pojava je prisutna kod svih analiziranih betona. U zrnju LA-Termit vrednosti odnosa Ca/Si manje su u odnosu na TZ: 1.67 (LSLL-1) i 1.82

- High Ca/Si ratio in ITZ for LSLL-1 and LSLL-5 signifies that the ITZ is relatively poor in calcium silicate hydrates.

- The changes of atomic ratios in the LWA-Termit grain in zones close to ITZ comparing to the composition before the insertion, indicates that there is a diffusion of ions between the grain and the cement paste. Besides, a great roughness of the surface of the LWA-Termit grain makes the process of crystallization of hydration products easier. This occurrence is present in all the analyzed concretes. In LWA-Termit grain the values of

(LSLL-4) što ukazuje na formiranje CSH strukture veće gustine.

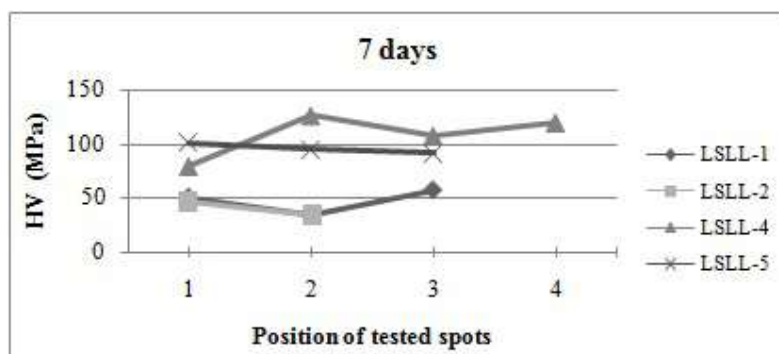
- Visoka vrednost odnosa atoma Ca/Si u TZ kod betona LSLL-1 i LSLL-5 upućuje na relativno mali sadržaj kalcijum-siliko-hidrata.

Na vrednosti mikrotvrdoće tranzitne zone utiče poroznost, vrsta i veličina kristala produkata hidratacije. Srednje vrednosti mikrotvrdoća izmerene u TZ za svaku vrstu betona predstavljene su u odnosu na udaljenost od površine agregata kao tačke 1, 2, 3 i 4. U uslovima merenja čiji rezultati su prikazani u ovom radu, može se smatrati da će vrednosti tvrdoće biti u najvećoj meri rezultat formirane poroznosti (naročito u početnom periodu hidratacije), veličine i vrste zrna kristala produkata hidratacije i veličine čestica neizreagovanog veziva. U tom smislu su interesantna poređenja prikazana na slikama 9 i 10 za sve četiri vrste betona. Na apscisi su sa 1-4 predstavljena ispitna mesta, pri čemu je sa 1 označeno ispitno mesto najbliže zrnu LA-Termit. Ako se uzmu u obzir dimenzije otiska (30-50 μm) i dimenzije TZ (max 100 μm), da se zaključiti da su tačke 3 i 4 već u cementnom kamenu dok na vrednost tvrdoće prve tačke utiče i blizina zrna agregata. Nakon sedam dana, tvrdoća TZ trebalo bi da bude najmanja za betone na bazi Portland cementa (LSLL1 i LSLL4), jer je pakovanje čestica cementa otežano zbog efekta zida. Čestice elektrofilterskog pepela u CEM II (beton LSLL-2) i metakaolina u betonu LSLL5 daleko lakše popunjavaju prostor u TZ što bi trebalo da poveća vrednosti mikrotvrdoće u odnosu na betone na bazi Portland cementa [1]. Međutim, od ovog pretpostavljenog trenda odstupaju vrednosti dobijene za beton LSLL4 (vezivo je bilo čist Portland cement – umanjena količina). Nije moguće dati pouzdano objašnjenje za ove pojave, ali je interesantan podatak da je koncentracija atoma silicijuma u TZ, nakon sedam dana, najveća kod LSLL4 i LSLL5 (tabele 6 i 7, slike 9 i 10). Istovremeno su vrednosti mikrotvrdoće najveće za ove vrste betona stare sedam dana (slike 9 i 10). U drugoj tački vrednosti se mnogo manje razlikuju za različite vrste betona za starost od 28 dana u odnosu na vrednosti dobijene nakon sedam dana. Ovaj podatak ukazuje na to da nestaju početne prednosti u boljem pakovanju čestica veziva u tranzitnoj zoni s procesom hidratacije.

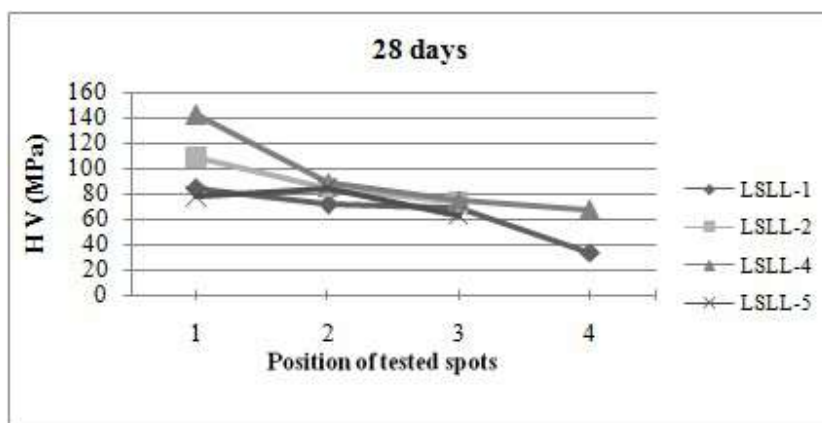
the ratio Ca/Si are smaller in comparison to ITZ: 1.67 (LSLL-1) and 1.82 (LSLL-4), which points to the formation of CSH structures with a greater density.

- High Ca/Si ratio is present in ITZ for LSLL-1 and LSLL-5 signifying that the ITZ is relatively poor in calcium silicate hydrates.

Porosity, type and size of crystals as products of hydration influenced the values of micro hardness of ITZ. The average micro hardness distribution measured in the ITZ of each concrete was plotted versus the distance from aggregate surface presented as points 1, 2, 3 and 4. In the conditions of measuring that gave results from this paper, it can be considered that the values of hardness would be mostly a result of the porosity formed (especially at the beginning of hydration), the size and type of crystal grain produced from hydration and the size of the unhydrated binder particles. Thus, the comparison given in Figures 9 and 10, for all 4 types of concrete is interesting. The x axis shows on tested spots 1-4, where 1 represents tested spot closest to the grain of aggregate. Considering the dimensions of the depth of penetration of indenter (30-50 μm) and dimensions of ITZ (max 100 μm), it brings to the conclusion that points 3 and 4 are already in the cement paste, whereas the value of hardness of the first point is influenced by the closeness of the aggregate grain as well. After 7 days, the hardness of ITZ, as predicted, turned out to be the lowest for the concrete based on Portland cement (LSLL1 and LSLL4), since the packing of particles is harder due to the wall effect. In the same time the particles of fly ashes in CEM II (concrete LSLL-2) and metakaolin in concrete LSLL-5 are far easier to fill in the space in ITZ, which should increase the values of micro hardness in comparison with concrete based on Portland cement [1]. However, this supposed tendency disagrees with the values obtained for concrete LSLL4 (binder was ordinary Portland cement-in a smaller amount than in LSLL1). It is impossible to give a reliable explanation for these occurrences. However, there is an interesting data which shows that the concentration of the atoms of silicon in ITZ, after 7 days, is the highest in LSLL4 and LSLL5, tables 6 and 7. At the same time their micro hardness values are greatest for 7 day old concrete Figures 9 and 10. At the second point the values differ much less for different types of concrete after 28 days, when compared to the values obtained after 7 days. This data implies that initial advantages disappear with the progress of hydration.



Slika 9. Mikrotvrdoća nakon 7 dana
Figure 9. Micro hardness values after 7 days



Slika 10. Mikrotvrdoća nakon 28 dana
Figure 10. Micro hardness values after 28 days

4 ZAKLJUČAK

Istraživanja teksturalnih i mikrostrukturnih promena tranzitne zone korišćenjem SEM i EDS metoda, kao i određivanje mikrotvrdoće, mogu da doprinesu boljem razumevanju veze između vrste formiranih produkata hidratacije i jačine veze između agregata i cementnog kamena. Međutim, uspostavljanje direktne veze između ovih vrednosti i makrosobina betona zahteva i dodatne načine karakterizacije osobina tranzitne zone. Rezultati EDS analize upućuju na to da:

- postoji razmena jona difuzijom između zrna lakog agregata Termit i cementne paste. Osim toga, veliki stepen hrapavosti površine zidova pora pomaže procesu heterogene kristalizacije produkata hidratacije i stvaranja CSH jedinjenja veće gustine;
- vrednosti odnosa Ca/Si velike su za tranzitnu zonu za sve tipove betona, ali su posebno velike za betone LSSL-1 i LSSL-5, što ukazuje na to da je TZ relativno siromašna kalcijum-silikohidratima;
- nije moguće dati pouzdanu vezu između sastava tranzitne zone i vrednosti mikrotvrdoće za različite betone.

ZAHVALNOST

U radu je prikazan deo istraživanja koje je pomoglo Ministarstvo prosvete, nauke i tehnološkog razvoja Republike Srbije u okviru tehnološkog projekta TR 36017 pod nazivom: „Istraživanje mogućnosti primene otpadnih i recikliranih materijala u betonskim kompozitima, sa ocenom uticaja na životnu sredinu, u cilju promocije održivog građevinarstva u Srbiji“.

4 CONCLUSION

The research of textural and micro structural changes of interfacial transition zone, with the use of SEM and EDS methods as well as determination of micro hardness values, can contribute better understanding of relation between the type of hydration products formed and the strength of the connection between the aggregate and the hardened cement paste. However, in order to make a direct connection between these values and the macro characteristics of the concrete additional ways of characterization of ITZ qualities are needed. The results of EDS analysis indicate that:

- There is an exchange of ions through diffusion between the grain of lightweight aggregate Termit and cement paste. Beside that a high level of the roughness of pore walls aids to the process of heterogeneous crystallization of the products of hydration and formation of CSH compounds with a greater density.
- Values of Ca/Si ratio are high interfacial transition zone for all types of concrete, but especially high for LSSL-1 and LSSL-5, signifying that the interfacial transition zone is relatively poor in calcium silicate hydrates
- It is impossible to make a reliable connection between the composition of the interfacial transition zone and the micro hardness values for different concretes.

ACKNOWLEDGEMENTS

The research work reported in this paper is a part of the investigation within the research project TR 36017 "Utilization of by-products and recycled waste materials in concrete composites in the scope of sustainable construction development in Serbia: investigation and environmental assessment of possible applications", supported by the Ministry of Education, Science and Technological Development of the Republic of Serbia. This support is gratefully acknowledged.

5 LITERATURA REFERENCES

- [1] Asbridge, A.H., Page, C.L., Page, M.M: Effects of metakaolin, water/binder ratio and interfacial transition zones on the microhardness of cement mortars, *Cement and Concrete Research* 32, 2002, 1365-1369.
- [2] Bonakdar, A., Mobasher, B., Chawla, N.: Diffusivity and micro-hardness of blended cement materials exposed to external sulfate attack, *Cement & Concrete Composites* 34, 2012, 76-85.
- [3] Chandra, S., Berntsson, L., *Lightweight aggregate concrete, science, technology and applications*, pp 11-19, William Andrew Publishing, Norwich, 2002.
- [4] Ducman, V., Mirtič, B.: Lightweight aggregate processes from waste material, *Advances in Materials Science Research*, 4, Chapter 10, 2011, 307-323.
- [5] Gameiro L.A., Silva S.A., Veiga R. M., Velosa L.A.: Lime-metakaolin hydration products: a microscopy analysis, *Materials and technology* 46, 2012, 145-148.
- [6] Glinicki, A. M., Zielinski, M.: Depth-sensing indentation method for evaluation of efficiency of secondary cementitious materials, *Cement and Concrete Research* 34, 2004, 721-724.
- [7] Internal Curing of Concrete, RILEM Report 41, Eds. K. Kovler and O.M. Jensen, RILEM Publications S.A.R.L., 2007.
- [8] Li, Y., Wu, D., Yhang, J., Chang, L., Wu, D., Fang, Y., Shi, Y.: Measurement and statistics of single pellet mechanical strength of differently shaped catalysts, *Powder Technology*, 113, 2000, 176-184.
- [9] Lo, Y., Gao, F.X., Jeary, P. A.: Microstructure of pre-wetted aggregate on lightweight concrete, *Building and Environment* 34, 1999, 759-764.
- [10] Mehta, P. K., Monteiro, J.M.P.: *Concrete-Microstructure, Properties and Materials*, 3rd Edition, 2006, pp 41-44, Mc-Graw Hill, New York.
- [11] Radonjanin, V., Malešev, M., Lukić, I., Milovanović, V.: Polimer-betonski kompoziti na bazi recikliranog agregata, *Materijali i konstrukcije*, 52, 2009, 1, 91-107.
- [12a] Scrivener, L. K., Crumbie, K.A., Laugesen, P.: The interfacial transition zone (ITZ) between the cement paste and aggregate in concrete. *Interface Sci.* 12, 2004, 411-421.
- [12b] Scrivener, L. K., Characterization of the ITZ and its quantification by test method, in: M. G. Alexander, G. Arlliguie, G. Ballivy, A. Bentur, J. Merchand (eds.), *Engineering and Transport Properties of the Interfacial Transition Zone in Cementitious Composites*, Rilem Report, vol.20, RILEM Publications, 1999, pp 3-14.
- [13] Chandra, S.: Properties of concrete with mineral and chemical admixtures, in: *Structure and Performance of Cements*, Edited by J. Bensted and P. Barnes, 2nd Edition, 2001, pp 140-186, Spon Press, London.
- [14] Trägårdh, J.: Microstructural features and related properties of self compacting concrete, in: A. Skarendahl, O. Peterson (Eds.). *Proceedings of the First International RILEM Symposium on Self Compacting Concrete*. RILEM, Cachan, Cedex, 1999, 175-186.
- [15] Winnefeld, F., Zingg, A., Holzer, L., Pakusch, J., Becker, S.: Interaction of Polycarboxylate-based Superplasticizers and Cements: Influence of Polymer Structure and C₃A-content of Cement, *Cement & Concrete Composites* 31, 2009, 153-162.
- [16a] Zhang, Ming-Hong, Gjörv, Microstructure of the interfacial zone between lightweight aggregate and cement paste, *Cement and Concrete Research*, 20, 1990, 610-618.
- [16b] Zhang, Ming-Hong, Gjörv, Penetration of cement paste into lightweight aggregate Cement and Concrete Research, 22, 1992, 47-55.

REZIME

KARAKTERISTIKE TRANZITNE ZONE BETONA NA BAZI LAKOG AGREGATA

Vesna BULATOVIĆ
Vilma DUCMAN
Miroslava RADEKA

U radu je prikazana karakterizacija tranzitne zone između zrna lakog agregata proizvedenih na bazi otpadnih materijala i vezivnog kamena pomoću metoda SEM, EDS i određivanjem Vickersove tvrdoće. Na bazi SEM i EDS analize, kao i kriterijuma za odnose atoma elemenata koji ulaze u sastav nekih produkata hidratacije, može se dobiti uvid u preovlađujući sastav tranzitne zone. Vrednosti Vickersove tvrdoće za četiri vrste ispitanih betona se nakon sedam dana hidratacije nije moguće povezati sa gustinom pakovanja čestica veziva u tranzitnoj zoni sa velikom sigurnošću, a nakon dvadeset osam dana razlike u vrednostima nisu značajne.

Cljučne reči: laki agregat, otpadni materijal, tranzitna zona

SUMMARY

CHARACTERISTICS OF LIGHTWEIGHT AGGREGATE CONCRETE INTERFACIAL TRANSITION ZONE

Vesna BULATOVIĆ
Vilma DUCMAN
Miroslava RADEKA

The paper presents the characteristics of the interfacial zone between the lightweight aggregate produced on the basis of waste materials and binder matrix with the application of the methods SEM, EDS and the Vickers micro hardness test. On the basis of the SEM and EDS analysis, as well as the criteria for the atomic ratio of elements which compose some products of hydration, we can gain insight into the dominant composition of the interfacial zone. The values of the Vickers micro hardness test for four kinds of tested concrete after seven days of hydration is impossible to correlate with the composition of the interfacial zone in reliable way, whereas after twenty eight days the differences in values are insignificant.

Key words: lightweight aggregate, waste material, interfacial zone.

UPUTSTVO AUTORIMA*

Prihvatanje radova i vrste priloga

U časopisu Materijali i konstrukcije štampaće se neobjavljeni radovi ili članci i konferencijska saopštenja sa određenim dopunama ili bez dopuna, prema odluci Redakcionog odbora, a samo izuzetno uz dozvolu prethodnog izdavača prihvatice se i objavljeni rad. Vrste priloga autora i saradnika koji će se štampati su: originalni naučni radovi, prethodna saopštenja, pregledni radovi, stručni radovi, konferencijska saopštenja (radovi sa naučno-stručnih skupova), kao i ostali prilozi kao što su: prikazi objekata i iskustava - primeri, diskusije povodom objavljenih radova i pisma uredništvu, prikazi knjiga i zbornika radova, kao i obaveštenja o naučno-stručnim skupovima.

Originalni naučni rad je primarni izvor naučnih informacija i novih ideja i saznanja kao rezultat izvornih istraživanja uz primenu adekvatnih naučnih metoda. Dobijeni rezultati se izlažu kratko, jasno i objektivno, ali tako da poznavalac problema može proceniti rezultate eksperimentalnih ili teorijsko numeričkih analiza i tok razmišljanja, tako da se istraživanje može ponoviti i pri tome dobiti iste ili rezultate u okvirima dopuštenih odstupanja, kako se to u radu navodi.

Prethodno saopštenje sadrži prva kratka obaveštenja o rezultatima istraživanja ali bez podrobnih objašnjenja, tj. kraće je od originalnog naučnog rada. U ovu kategoriju spadaju i diskusije o objavljenim radovima ako one sadrže naučne doprinose.

Pregledni rad je naučni rad koji prikazuje stanje nauke u određenoj oblasti kao plod analize, kritike i komentara i zaključaka publikovanih radova o kojima se daju svi neophodni podaci pregledno i kritički uključujući i sopstvene radove. Navode se sve bibliografske jedinice korišćene u obradi tematike, kao i radovi koji mogu doprineti rezultatima daljih istraživanja. Ukoliko su bibliografski podaci metodski sistematizovani, ali ne i analizirani i raspravljani, takvi pregledni radovi se klasifikuju kao stručni pregledni radovi.

Stručni rad predstavlja koristan prilog u kome se iznose poznate spoznaje koje doprinose širenju znanja i prilagođavanja rezultata izvornih istraživanja potrebama teorije i prakse. On sadrži i rezultate razvojnih istraživanja.

Konferencijsko saopštenje ili rad saopšten na naučno-stručnom skupu koji mogu biti objavljeni u izvornom obliku ili ih autor, u dogovoru sa redakcijom, bitno preradi i proširi. To mogu biti naučni radovi, naročito ako su saopštenja po pozivu Organizatora skupa ili sadrže originalne rezultate prvi put objavljene, pa ih je korisno uz određene dopune učiniti dostupnim široj stručnoj javnosti. Štampaće se i stručni radovi za koje Redakcioni odbor oceni da su od šireg interesa.

Ostali prilozi su prikazi objekata, tj. njihove konstrukcije i iskustava-primeri u građenju i primeni različitih materijala, diskusije povodom objavljenih radova i pisma uredništvu, prikazi knjiga i zbornika radova, kao i obaveštenja o naučno-stručnim skupovima.

Autori uz rukopis predlažu kategorizaciju članka. Svi radovi pre objavljivanja se recenziraju, a o prihvatanju za publikovanje o njihovoj kategoriji konačnu odluku donosi Redakcioni odbor.

Da bi se ubrzao postupak prihvatanja radova za publikovanje, potrebno je da autori uvažavaju Uputstva za pripremu radova koja su navedena u daljem tekstu.

Uputstva za pripremu rukopisa

Rukopis otkucati jednostrano na listovima A-4 sa marginama od 31 mm (gore i dole) a 20 mm (levo i desno), u Wordu fontom Arial sa 12 pt. Potrebno je uz jednu kopiju svih delova rada i priloga, dostaviti i elektronsku verziju na navedene E-mail adrese, ili na CD-u. Autor je obavezan da čuva jednu kopiju rukopisa kod sebe zbog eventualnog oštećenja ili gubitka rukopisa.

Od broja 1/2010. prema odluci Upravnog odbora Društva i Redakcionog odbora, radovi sa pozitivnim recenzijama i prihvaćeni za štampu, publikovaće se na srpskom i engleskom jeziku.

Svaka stranica treba da bude numerisana, a optimalni obim članka na jednom jeziku je oko 16 stranica (30000 slovnih mesta) uključujući slike, fotografije, tabele i popis literature. Za radove većeg obima potrebna je saglasnost Redakcionog odbora.

Naslov rada treba sa što manje reči (poželjno osam, a najviše do jedanaeset) da opiše sadržaj članka. U naslovu ne koristiti skraćenice ni formule. U radu se iza naslova daju ime i prezime autora, a titule i zvanja, kao i ime institucije u podnožnoj napomeni. Autor za kontakt daje telefone, faks i adresu elektronske pošte, a za ostale autore poštansku adresu.

Uz sažetak (rezime) od oko 150 do 200 reči, na srpskom i engleskom jeziku daju se ključne reči (do deset). To je jezgrovit prikaz celog članka i čitaocima omogućuje uvid u njegove bitne elemente.

Rukopis se deli na poglavlja i potpoglavlja uz numeraciju, po hijerarhiji, arapskim brojevima. Svaki rad ima uvod, sadržinu rada sa rezultatima, analizom i zaključcima. Na kraju rada se daje popis literature.

Kod svih dimenzionalnih veličina obavezna je primena međunarodnih SI mernih jedinica.

Formule i jednačine treba pisati pažljivo vodeći računa o indeksima i eksponentima. Autori uz izraze u tekstu definišu simbole redom kako se pojavljuju, ali se može dati i posebna lista simbola u prilogu.

Prilozi (tabele, grafikoni, sheme i fotografije) rade se u crno-belom tehničkom, u formatu koji obezbeđuje da pri smanjenju na razmere za štampu, po širini jedan do dva stupca (8cm ili 16.5cm), a po visini najviše 24.5cm, ostanu jasni i čitljivi, tj. da veličine slova i brojeva budu najmanje 1.5mm. Originalni crteži treba da budu kvalitetni i u potpunosti pripremljeni za presnimavanje. Mogu biti i dobre, oštre i kontrastne fotokopije. Koristiti fotografije, u crno-belom tehničkom, na kvalitetnoj hartiji sa oštrim konturama, koje omogućuju jasnu reprodukciju. Skraćenice u prilogima koristiti samo izuzetno uz obaveznu legendu. Prilozi se posebno označavaju arapskim brojevima, prema redosledu navođenja u tekstu. Objašnjenje tabela daje se u tekstu.

Potrebno je dati spisak svih skraćenica korišćenih u tekstu.

U popisu literature na kraju rada daju se samo oni radovi koji se pominju u tekstu. Citirane radove treba prikazati po azbučnom redu prezimena prvog autora. Literaturu u tekstu označiti arapskim brojevima u uglastim zagradama, kako se navodi i u Popisu citirane literature, napr [1]. Svaki citat u tekstu mora se naći u Popisu citirane literature i obrnuto svaki podatak iz Popisa se mora navesti u tekstu.

U Popisu literature se navode prezime i inicijali imena autora, zatim potpuni naslov citiranog članka, iza toga sledi ime časopisa, godina izdavanja i početna i završna stranica (od - do). Za knjige iza naslova upisuje se ime urednika (ako ih ima), broj izdanja, prva i poslednja stranicapoglavlja ili dela knjige, ime izdavača i mesto objavljivanja, ako je navedeno više gradova navodi se samo prvi po redu. Kada autor citirane podatke ne uzima iz izvornog rada, već ih je pronašao u drugom delu, uz citat se dodaje «citirano prema...». Neobjavljeni članci mogu se pominjati u tekstu kao «usmeno saopštenje».

Autori su odgovorni za izneseni sadržaj i moraju sami obezbediti eventualno potrebne saglasnosti za objavljivanje nekih podataka i priloga koji se koriste u radu.

Ukoliko rad bude prihvaćen za štampu, autori su dužni da, po uputstvu Redakcije, unesu sve ispravke i dopune u tekstu i prilogima.

Za detaljnija tehnička uputstva za pripremu rukopisa autori se mogu obratiti Redakcionom odboru časopisa.

Rukopisi i prilozi objavljenih radova se ne vraćaju. Sva eventualna objašnjenja i uputstva mogu se dobiti od Redakcionog odbora.

Radovi se mogu slati i na e-mail: folic@uns.ac.rs ili miram@uns.ac.rs i dimk@ptt.rs

Već sajt Društva i časopisa: www.dimk.rs

* Uputstvo autorima je modifikovano i treba ga u pripremi radova slediti.

Izdavanje časopisa "Građevinski materijali i konstrukcije" finansijski su pomogli:



INŽENJERSKA KOMORA SRBIJE

**MINISTARSTVO ZA NAUKU I TEHNOLOŠKI
RAZVOJ SRBIJE**



**UNIVERZITET U BEOGRADU
GRAĐEVINSKI FAKULTET**



**DEPARTMAN ZA GRAĐEVINARSTVO
FAKULTET TEHNIČKIH NAUKA NOVI SAD**



INSTITUT IMS AD, BEOGRAD



**UNIVERZITET CRNE GORE
GRAĐEVINSKI FAKULTET - PODGORICA**